

On Quantizing Teichmüller and Thurston theories

L. Chekhov^{a)1} and R. C. Penner^{b)2}

^{a)}*Steklov Mathematical Institute,
Gubkina 8, 117966, GSP-1, Moscow, Russia*

^{b)}*Departments of Mathematics and Physics/Astronomy
University of Southern California,
Los Angeles, CA 90089 USA*

Abstract In earlier work, Chekhov and Fock have given a quantization of Teichmüller space as a Poisson manifold, and the current paper first surveys this material adding further mathematical and other detail, including the underlying geometric work by Penner on classical Teichmüller theory. In particular, the earlier quantum ordering solution is found to essentially agree with an “improved” operator ordering given by serially traversing general edge-paths on a graph in the underlying surface. Now, insofar as Thurston’s sphere of projectivized foliations of compact support provides a useful compactification for Teichmüller space in the classical case, it is natural to consider corresponding limits of appropriate operators to provide a framework for studying degenerations of quantum hyperbolic structures. After surveying the required background material on Thurston theory and “train tracks”, the current paper continues to give a quantization of Thurston’s boundary in the special case of the once-punctured torus, where there are already substantial analytical and combinatorial challenges. Indeed, an operatorial version of continued fractions as well as the improved quantum ordering are required to prove existence of these limits. Since Thurston’s boundary for the once-punctured torus is a topological circle, the main new result may be regarded as a quantization of this circle. There is a discussion of quantizing Thurston’s boundary spheres for higher genus surfaces in closing remarks.

1 Introduction

One manifestation of Teichmüller space in contemporary mathematical physics is as the Hilbert space and the algebra of observables for three-dimensional (3D) quantum gravity since E. Verlinde and H. Verlinde [1] have argued that the classical phase space of Einstein gravity in a 3D manifold is the Teichmüller space of its boundary. (Analogously, the classical phase space for 3D Chern–Simons theory is the moduli space of flat connections on the boundary; this theory was quantized in [2, 3].) Teichmüller space possesses its

¹E-mail: chekhov@mi.ras.ru.

²E-mail: rpenner@math.usc.edu.

canonical (Weil–Peterson) Poisson structure, whose symmetry group is the mapping class group of orientation-preserving homeomorphisms modulo isotopy. The algebra of observables is the collection of geodesic length functions of geodesic representatives of homotopy classes of essential closed curves together with its natural mapping class group action.

Given this Poisson structure, one can turn to the problem of quantizing it, thereby obtaining a variant of the quantum 3D gravity description. According to the correspondence principle: (1) the algebra of observables of the corresponding quantum theory is the noncommutative deformation of the $*$ -algebra of functions on it governed by the Poisson structure; (2) the Hilbert spaces of the theory are the representation spaces of these $*$ -algebras; and (3) the symmetry group acts on the algebra of observables by automorphisms. Under the assumption that the quantization of a Poisson manifold exists and is unique, to solve this problem it suffices to construct a family of $*$ -algebras, which depend on the quantization parameter \hbar , and an action of the mapping class group on this family by outer automorphisms, and to show that the algebra and the action thus constructed reproduces the classical algebra, the classical action, and the classical Poisson structure in the limit $\hbar \rightarrow 0$. This program has been successfully performed in [4] and [5], and we describe it in Secs. 2 and 3 of this paper. Actually, the problem that was solved in these papers differs slightly from the original formulation because the methods of [4] are suited for describing only *open* surfaces (surfaces with nonempty boundary, components of which can, however, reduce to a puncture). The corresponding Teichmüller space has a degenerate Weil–Peterson Poisson structure, while the mapping class group acts as symmetry group. We describe the deformation quantization of the corresponding Teichmüller space, the action of the mapping class group by outer automorphisms, the representations of the observable algebra, and the induced action of the mapping class group on the representation space following [4].

As in [1], the representation space of the observable algebra can also be interpreted as the space of conformal blocks of the Liouville conformal field theory. This program is under current development (see [6]). Our construction can be therefore interpreted as the construction of the conformal block spaces and the mapping class group actions for this CFT.

The key point of the quantization procedure is constructing quantum mapping class group transformations that define in a consistent way the morphisms between quantum $*$ -algebras simultaneously preserving the quantum geodesic algebra. The main mathematical ingredient of the construction is a version of the quantum dilogarithm by L. D. Faddeev [13]. We interpret the corresponding five-term relation as the only nontrivial relation in a certain groupoid that has the mapping class group as maximal subgroup. A similar construction has been made independently and simultaneously by R. M. Kashaev [5]. The key difference between these two constructions lies in the dimensions of the Poisson leaves of the two theories: given a graph with v three-valent vertices, e edges, and $f = s$ faces suitably embedded in a surface F_g^s of genus g with s ideal boundary components, the genus is given by Euler’s formula $v - e + f = 2 - 2g$. In Kashaev’s approach, there are $2e$ variables and $v + f$ central elements (at each vertex and at each face), so the Poisson leaf dimension is $2e - v - f = 8g - 8 + 3s$, while in our approach, there are e variables and f central elements, so the Poisson dimension $e - f = 6g - 6 + 2s$ exactly coincides with

the dimension of the Teichmüller space of Riemann surfaces of genus g with s punctures. The approach of [4] is thus appropriate for describing 2D topological theories while that of [5] is suitable for describing Liouville field theory as a lattice theory (for instance, the Liouville field central charge can be calculated, see [14]).

One of the mathematical tools employed in the quantization [4] is the decorated Teichmüller theory [7], and the relevant aspects are briefly reviewed in Section 2. In effect in the classical case, to each edge of a trivalent “fatgraph” Γ (i.e., a graph plus a cyclic ordering of the half-edges about each vertex) embedded as a “spine” (i.e., a deformation retract of the surface) $F = F_g^s$ is assigned a number Z_α , where α here and below indexes the edges of Γ . The tuple (Z_α) gives global coordinates on an appropriate Teichmüller space $\mathcal{T}_H = \mathcal{T}_H(F)$ of F (as first studied by Thurston and later by Fock), where any or all of the “punctures” of F_g^s are permitted to be uniformized instead as circular boundary components (and the subscript H stands for “holes”); the details are given in Section 2.1. The Weil–Petersson Kähler two-form, which is known [9] in the (Z_α) coordinates, pulls back to a degenerate two-form, i.e., to a degenerate Poisson structure on \mathcal{T}_H . Furthermore, the action of the mapping class group $MC = MC(F)$ of F on \mathcal{T}_H , which is again known [9] in the (Z_α) coordinates as well as combinatorially [10], leaves invariant this Poisson structure, and this is the Poisson manifold \mathcal{T}_H with MC -action which has been quantized.

More explicitly still, for each edge α , we may associate a pair of Möbius transformations $R_{Z_\alpha}, L_{Z_\alpha}$ depending upon Z_α with the following property. For any homotopy class γ of geodesic in F with corresponding closed edge-path P on Γ , consider the serial product P_γ of operators $R_{Z_\alpha}, L_{Z_\alpha}$ taken in order as one traverses P in some orientation from some starting point, where one inserts the former (or latter, respectively) if immediately after traversing edge α , then P turns right (or left) in Γ ; thus, the combinatorial geometry of serially traversing edges of Γ as dictated by P determines an ordered product P_γ of matrices depending upon (Z_α) , and the length l_γ of the geodesic representative of γ for the point of \mathcal{T}_H determined by (Z_α) is given by $G_\gamma = 2 \cosh (l_\gamma/2) = |\text{tr } P_\gamma|$. It is the Poisson algebra of these geodesic functions G_γ , the algebra of observables, which has been quantized.

In the quantum case (after passing to a suitable subspace on which the Poisson structure is non-degenerate), standard techniques of deformation quantization produce the appropriate Hilbert space \mathcal{H} of the quantum theory, as well as pairs of operators $R_{Z_\alpha}, L_{Z_\alpha}$ on \mathcal{H}^2 for each edge α of Γ . Again, to the homotopy class of a geodesic γ in F or its corresponding closed edge-path P on Γ , we may assign the ordered product P_γ of these operators as dictated by the combinatorial geometry of P in Γ , whose trace $G_\gamma = \text{tr } P_\gamma$ is the “quantum geodesic operator.” The main point is to prove the invariance under the action of MC , which is intimately connected with functional properties of the quantum dilogarithm as was mentioned before.

In [4] was proved the existence and uniqueness of an appropriate “proper quantum ordering” of operators that enjoy MC -invariance as well as satisfy the standard physical requirements. In Section 3.5, we observe that the natural operatorial ordering given by the combinatorial geometry of edge-paths in Γ can be used to derive this physically correct quantum ordering. The improved ordering is required in the subsequent quantization (discussed below).

In order to explain the further new results in this paper, we must recall aspects of Thurston’s seminal work on surface geometry, topology, and dynamics from the 1970-1980’s, which is surveyed in Section 4. Very briefly, Thurston introduced the space $\mathcal{PF}_0 = \mathcal{PF}_0(F)$ of “projective measured foliations of compact support in F ” as a boundary for the Teichmüller space $\mathcal{T} = \mathcal{T}(F)$, where “Thurston’s compactification” $\overline{\mathcal{T}} = \mathcal{T} \cup \mathcal{PF}_0$ is a closed ball with boundary sphere \mathcal{PF}_0 , where the action of MC on \mathcal{T} extends continuously to the natural action on $\overline{\mathcal{T}}$. Furthermore, the sphere \mathcal{PF}_0 contains the set of all homotopy classes of geodesics in F as a dense subset, i.e., \mathcal{PF}_0 is an appropriate completion of this set. (Unfortunately, the action of MC on \mathcal{PF}_0 has dense orbits, so the beautiful structure of Thurston’s compactification does not descend in any reasonable way, with the current state of understanding, to a useful structure on the level of Riemann’s moduli space.) Thurston also devised an elegant graphical formalism for understanding \mathcal{PF}_0 using “train tracks”, which are graphs embedded in F with the further structure of a “branched one-submanifold” (cf. Section 4.2). In effect, a maximal train track gives a chart on the sphere \mathcal{PF}_0 , and furthermore, the combinatorial expression for inclusion of charts effectively captures the dynamics of the action of diffeomorphisms of F (cf. Section 4.4).

Thus, Thurston theory arises as a natural tool to understand degenerations in Teichmüller space and dynamics on F , and in light of remarks above, its quantization should provide a natural tool for studying degenerations of 3D gravity or Liouville conformal field theory. Many aspects of the survey of classical Thurston surface theory (in Section 4) are required for our subsequent quantization.

In any case, a mathematically natural problem armed with [4] is to “quantize Thurston theory”: assign operators H_γ on \mathcal{H} to each homotopy class γ of geodesic in such a way that as γ converges in \mathcal{PF}_0 to a projectivized measured foliation $[\mathcal{F}, \bar{\mu}]$, then the corresponding operators H_γ converge in an appropriate sense to a well-defined operator $H_{[\mathcal{F}, \bar{\mu}]}$ on \mathcal{H} . Upon choosing a spine $\Gamma \subseteq F$ (i.e., an embedding, up to homotopy, of a graph whose inclusion is a homotopy equivalence), any homotopy class of curve γ may be essentially uniquely realized as an edge-path on Γ . Define the “graph length” $\text{g.l.}(\gamma)$ to be the total number of edges of Γ traversed by this edge-path counted with multiplicities.

In the special case of the torus F_1^1 , we have succeeded here (in Section 5) in showing that the ratio of operators

$$H_\gamma = \text{p.l.}(\gamma)/\text{g.l.}(\gamma)$$

converge weakly to a well-defined operator as γ converges in $\mathcal{PF}_0(F_1^1)$, where the “proper length” is defined by

$$\text{p.l.}(\gamma) = \lim_{n \rightarrow \infty} \frac{1}{n} \text{tr} \log 2T_n\left(\frac{1}{2}P_\gamma\right),$$

with T_n the Chebyshev polynomials. In fact in the classical case, $\text{p.l.}(\gamma)$ agrees with half the length of the geodesic homotopic to γ in the Poincaré metric, and in the quantum case, there is an appropriate operatorial interpretation, both of which are described in Section 5.1. In particular, for several spines whose corresponding charts cover the circle $\mathcal{PF}_0(F_1^1)$, the analysis involves rather intricate estimates. This leads to a natural operatorial quantization (in Section 5.3.4) of the standard simple continued fractions, which are intimately connected with Thurston theory on F_1^1 (as we shall describe in Section 4.5). To complete the basic theory on the torus, one would like an intrinsic operatorial

description of the circle of unbounded operators we have constructed, as well as an an explication of the mapping class group action on it, viz., Thurston’s classification of surface automorphisms.

This paper is organized as follows: Section 2 covers classical Teichmüller theory and Section 3 the Chekhov–Fock quantization; Section 4 surveys classical Thurston theory of surfaces, and Section 5 gives our quantization of Thurston’s boundary for the punctured torus. Excerpts of Sections 2 and 3 are derived from an earlier manuscript of Chekhov–Fock, and we strive to include further mathematical detail. Section 4 surveys aspects of a large literature on Thurston theory and train tracks, explicitly covering only what is required in Section 5. Section 5 should be regarded as work in physics in the sense that some of the formal calculations depend upon manipulations of asymptotic spectral expansions for which there may be remaining mathematical issues. Closing remarks in Section 6 discuss the natural extension of these results to more complicated surfaces as well as other related work. Appendix A includes a novel proof of the required convergence in the classical case for any surface (in a sense, a new proof of the existence of Thurston’s compactification), which may yet be useful in the quantum case. Appendix B contains an analysis of the Casimir operators in the Poisson algebra in the Z -variables and the appropriate diagonalization of Poisson structure.

Acknowledgements We are indebted to L. D. Faddeev, V. V. Fock, M. Lapidus, and F. Bonahon for useful discussions. The work was partially supported by the RFFI Grant No. 01-01-00549 (L.Ch.), by the Program Mathematical Methods in Nonlinear Dynamics (L.Ch.), and by the COBASE Project.

2 Classical Teichmüller spaces

To begin, we shall briefly recall the two related roles played by graphs in Teichmüller theory as both aspects will be required here.

A *fatgraph* or *ribbon graph* is a graph Γ together with a cyclic ordering on the half-edges incident on each vertex, and we canonically associate to Γ a surface $F(\Gamma)$ with boundary obtained by “fattening each edge of the graph into a band” in the natural way; we shall tacitly require all vertices to have valence at least three unless stated otherwise, and we shall call a fatgraph *cubic* if each vertex has valence three. To each homotopy class of homotopy equivalence $\iota : \Gamma \rightarrow F$ for some surface F , where ι respects the orientation, there is a corresponding cell in $\mathcal{T}_g^s \times \mathbb{R}_{>0}^s$ as explained in [11] in the hyperbolic setting [7] and in the conformal setting [21]. Thus, a homotopy class of $\iota : \Gamma \rightarrow F$ is the name of a cell in the canonical cell decomposition. We shall sometimes suppress the mapping $\iota : \Gamma \rightarrow F$ and refer to Γ itself as a *spine* of F , where Γ is identified with $\iota(\Gamma) \subseteq F$. The cell decomposition is invariant under the action of the mapping class group (induced by post-composition of ι with homeomorphisms), and this has been an effective tool for studying Riemann’s moduli space; for instance, we shall recall here the corresponding presentation of the mapping class groups.

The second role of fatgraphs is exclusive to the hyperbolic setting, namely, fatgraphs provide a kind of “basis” for geometrically natural global parameterizations of Teichmüller

space. Specifically, fix a homotopy class $\iota : \Gamma \rightarrow F$ as above, where we now demand that Γ is cubic, and let $E = E(\Gamma)$ denote the set of edges of Γ . In several different contexts, one can naturally identify $\mathbb{R}_{>0}^E$ with a suitable modification of an appropriate Teichmüller space of F .

For instance, for punctured surfaces, recall [7] that the lambda length of a pair of horocycles is $\sqrt{2} e^\delta$, where δ is the signed hyperbolic distance between the horocycles. Lambda lengths give a global real-analytic parametrization of the decorated Teichmüller space as the trivial bundle $\tilde{\mathcal{T}}_g^s = \mathcal{T}_g^s \times \mathbb{R}_{>0}^s$ over Teichmüller space, where the fiber over a point is the space of all s -tuples of horocycles in the surface, one horocycle about each puncture (parameterized by hyperbolic length).

For another example, Thurston’s shear coordinates [16],[18] give global parameters not only on Teichmüller space (cf. Section 2.1.1) but also on the related space of measured foliations (cf. Section 4.6).

On the level of Teichmüller space, the two global coordinate systems (lambda lengths and shear coordinates) are closely related, and we choose to give the exposition here principally in shear coordinates with the parallel lambda length discussion relegated to a series of ongoing remarks. On the other hand, certain proofs of identities involving shear coordinates are easy calculations in lambda lengths.

2.1 Graph description of Teichmüller spaces

2.1.1 Global coordinates on Teichmüller space

In addition to the Teichmüller space \mathcal{T}_g^s and decorated Teichmüller space $\tilde{\mathcal{T}}_g^s$, we shall also require the following modification. Given an open Riemann surface F of finite topological type, a neighborhood of an ideal boundary component is either an annulus or a punctured disk; in the former case, the ideal boundary component will be called a “true” boundary component and in the latter will be called a “puncture.” We shall study the latter as a degeneration of the former with an elaboration

$$\mathcal{T}\text{eich}(F) = \text{Hom}'\left(\pi_1(F), PSL_2(\mathbb{R})\right) / PSL_2(\mathbb{R})$$

of the usual Teichmüller space, where Hom' denotes the space of all discrete faithful representations with no elliptic elements, i.e., $|\text{tr}(\rho(\gamma))| \geq 2$ for all $\gamma \in \pi_1(F)$ for any representation $\rho : \pi_1(F) \rightarrow PSL_2(\mathbb{R})$.

Assume that $\iota : \Gamma \rightarrow F$ is a homotopy class of homotopy equivalence and $\gamma \in \pi_1(F)$ is conjugate in $\pi_1(F)$ to the boundary of a regular neighborhood of an ideal boundary component of $F(\Gamma)$. Thus, the ideal boundary component is a puncture if and only if $\rho(\gamma)$ is a parabolic transformation, i.e., $|\text{tr}(\rho(\gamma))| = 2$. For any $\gamma \in \pi_1(F)$ with $|\text{tr}(\rho(\gamma))| > 2$, the underlying free homotopy class of unbased curves contains a unique hyperbolic geodesic whose length l_γ is given by $G_\gamma = 2\cosh(l_\gamma) = |\text{tr} \rho(\gamma)|$, where G_γ is called the *geodesic operator* and is constant on the conjugacy class of $\gamma \in \pi_1(F)$. Furthermore, by definition,

$$\mathcal{T}_g^s = \{[\rho] \in \mathcal{T}\text{eich}(F) : \forall \gamma \in \pi_1(F) \text{ freely homotopic into the boundary, we have } |\text{tr}(\rho(\gamma))| = 2\}$$

$$\subseteq \mathcal{T}\text{eich}(F)$$

Finally, define the space $\mathcal{T}_H(F)$ to be the 2^s -fold cover of $\mathcal{T}\text{eich}(F)$ branched over \mathcal{T}_g^s , where the fiber is given by the set of all orientations on the boundary components of F .

Theorem 2.1 *Fix any spine $\Gamma \subseteq F$, where Γ is a cubic fatgraph. Then there is a real-analytic homeomorphism $\mathbb{R}^{E(\Gamma)} \rightarrow \mathcal{T}_H(F)$. The hyperbolic length l_γ of a true boundary component γ is given by $l_\gamma = |\sum Z_i|$, where the sum is over the set of all edges traversed by γ counted with multiplicity. Furthermore, $\sum Z_i = 0$ if and only if the corresponding ideal boundary component is a puncture, so $\mathcal{T}_g^s \subseteq \mathcal{T}_H(F)$ is determined by s independent linear constraints.*

The theorem is due to Thurston with a systematic study by Fock. We shall not give a proof here (though there is not a complete proof in the literature so far as we know), but we shall at least give the construction that defines the homeomorphism $\mathbb{R}^{E(\Gamma)} \rightarrow \mathcal{T}_H(F)$.

The basic idea is to associate to each edge of Γ an appropriate cross ratio. To set this up, consider the topological surface $F^+ \subseteq F$ obtained by adjoining a punctured disk to each true boundary component of F . The fatgraph $\iota(\Gamma) \subseteq F \subseteq F^+$ is thus also a spine of F^+ , and its Poincaré dual in F^+ is an ideal triangulation Δ of F^+ (i.e., a decomposition into triangles with vertices among the punctures). In the universal cover of F^+ , each arc of Δ thus separates two complementary triangles which combine to give a topological quadrilateral, and the basic idea is to associate to each edge the cross-ratio of this quadrilateral.

To make this precise and describe the homeomorphism in the theorem, let $\alpha = 1, \dots, E = E(\Gamma)$ index the edges of Γ , and let (Z_α) denote a point of \mathbb{R}^E . We associate the Möbius transformation

$$X_{Z_\alpha} = \begin{pmatrix} 0 & -e^{Z_\alpha/2} \\ e^{-Z_\alpha/2} & 0 \end{pmatrix}. \quad (2.1)$$

to the edge α . To explicate this definition, consider an ideal quadrilateral in the hyperbolic plane triangulated by a diagonal into two ideal triangles T_1, T_2 . We may conjugate in $PSL_2(\mathbb{R})$ to arrange that the vertices of T_1 are $0, -1, \infty$ and the vertices of T_2 are $0, -1, t$, where $0 < t < \infty$, and an appropriate cross ratio of the original quadrilateral is t . Setting $Z_\alpha = \log t$ in the formula above, X_{Z_α} is the Möbius transformation interchanging $0, \infty$ and sending -1 to t , i.e., sending T_1 to T_2 . Notice that $X_{Z_\alpha}^2$ is the identity in $PSL_2(\mathbb{R})$, so X_{Z_α} also sends T_2 to T_1 .

We also introduce the “right” and “left” turn matrices

$$R = \begin{pmatrix} 1 & 1 \\ -1 & 0 \end{pmatrix}, \quad L = R^2 = \begin{pmatrix} 0 & 1 \\ -1 & -1 \end{pmatrix}, \quad (2.2)$$

and define the corresponding operators R_Z and L_Z ,

$$R_Z \equiv R X_Z = \begin{pmatrix} e^{-Z/2} & -e^{Z/2} \\ 0 & e^{Z/2} \end{pmatrix}, \quad (2.3)$$

$$L_Z \equiv LX_Z = \begin{pmatrix} e^{-Z/2} & 0 \\ -e^{-Z/2} & e^{Z/2} \end{pmatrix}. \quad (2.4)$$

Consider a closed oriented edge-path P in Γ , where we assume that P never consecutively traverses an oriented edge followed by its reverse, i.e., there is no “turning back”. Choosing also an initial base point on P , we may imagine the corresponding curve serially traversing the oriented edges of Γ with coordinates Z_1, \dots, Z_n turning left or right from Z_i to Z_{i+1} , for $i = 1, \dots, n$ (with the indices mod n so that $Z_{n+1} = Z_1$). Assign to P the corresponding composition

$$P_{Z_1 \dots Z_n} = L_{Z_n} L_{Z_{n-1}} R_{Z_{n-2}} \dots R_{Z_2} L_{Z_1}, \quad (2.5)$$

where the matrices L_{Z_i} or R_{Z_i} are inserted depending on which turn—left or right—the path takes at the corresponding stage.

Fixing any base point, the assignment $P \mapsto P_{Z_1, \dots, Z_n} \in PSL_2(\mathbb{R})$ gives rise to a representation $\rho \in \mathcal{T}_H(F)$, and this defines the required map $\mathbb{R}^{E(\Gamma)} \rightarrow \mathcal{T}_H(F)$. Furthermore summarizing standard formulas and facts mentioned above, we have

Proposition 2.2 *There is a one-to-one correspondence between the set of conjugacy classes of elements of $\pi_1(F)$ and free homotopy classes of closed oriented geodesics in F . For any spine of F , each free homotopy class is uniquely represented by a cyclically defined closed edge-path P with no turning back, and the length of γ is determined by*

$$G_\gamma \equiv 2 \cosh(l_\gamma/2) = |\operatorname{tr} P_{Z_1 \dots Z_n}|. \quad (2.6)$$

By construction if P corresponds to a boundary component γ of $F(\Gamma)$, then the associated matrix has the form $R_{Z_1} R_{Z_2} \dots R_{Z_n}$, or $L_{Z_1} L_{Z_2} \dots L_{Z_n}$ depending on the orientation. In this case, because all of the matrices R_x (L_x) are upper (lower) triangular, formula (2.6) gives

$$l_\gamma = \left| \sum_{i=1}^n Z_i \right|, \quad (2.7)$$

where the sign of this sum gives the orientation of the boundary component, and $l_\gamma = 0$ corresponds to a puncture. This proves the assertions about boundary lengths.

The Z -coordinates (i.e., log cross ratios) are called (*Thurston*) *shear coordinates* [16],[18] and can alternatively be defined by dropping perpendiculars from each of the two opposite vertices to the diagonal α of a quadrilateral, and measuring the signed hyperbolic distance Z_α along α between these two projections.

Assume that there is an enumeration of the edges of Γ and that edge α has distinct endpoints. Given a spine Γ of F , we may produce another spine Γ_α of F by contracting and expanding edge α of Γ , the edge labelled Z in Figure 1, to produce Γ_α as in the figure; the fattening and embedding of Γ_α in F is determined from that of Γ in the natural way. Furthermore, an enumeration of the edges of Γ induces an enumeration of the edges of Γ_α in the natural way, where the vertical edge labelled Z in Figure 1 corresponds to the horizontal edge labelled $-Z$. We say that Γ_α arises from Γ by a *Whitehead move* along edge α . We shall also write $\Gamma_{\alpha\beta} = (\Gamma_\alpha)_\beta$, for any two indices α, β of edges, to denote the

result of first performing a move along α and then along β ; in particular, $\Gamma_{\alpha\alpha} = \Gamma$ for any index α .

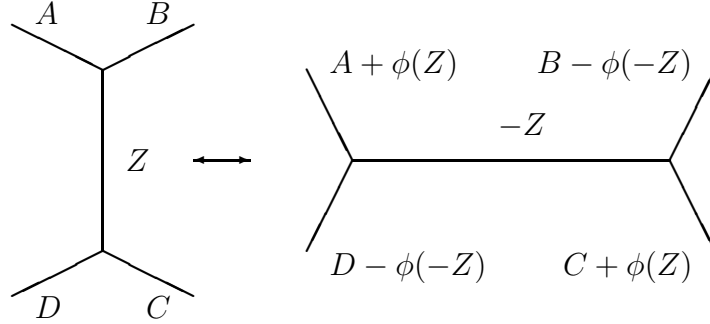


Figure 1-Whitehead move on shear coordinates

Proposition 2.3 [4] *Setting $\phi(Z) = \log(e^Z + 1)$ and adopting the notation of Figure 1 for shear coordinates of nearby edges, the effect of a Whitehead move is illustrated in the figure, viz.,*

$$W_Z : (A, B, C, D, Z) \rightarrow (A + \phi(Z), B - \phi(-Z), C + \phi(Z), D - \phi(-Z), -Z) \quad (2.8)$$

In the various cases where the edges are not distinct and identifying an edge with its shear coordinate in the obvious notation we have: if $A = C$, then $A' = A + 2\phi(Z)$; if $B = D$, then $B' = B - 2\phi(-Z)$; if $A = B$ (or $C = D$), then $A' = A + Z$ (or $C' = C + Z$); if $A = D$ (or $B = C$), then $A' = A + Z$ (or $B' = B + Z$).

Sketch of proof Assume that e is the diagonal of a quadrilateral with consecutive sides a, b, c, d , where e separates a, b from c, d . Identifying an edge with its lambda length, the shear coordinate is given by $Z = \log \frac{bd}{ac}$, i.e., $\frac{bd}{ac}$ is the required cross-ratio [7]. Furthermore, if f is the lambda length of the other diagonal, then the lambda lengths satisfy Ptolemy's relation $ef = ac + bd$ [7], and the transformation laws for shear coordinates in the proposition are readily derived from this either in the surface for (2.8) or in the universal cover of the surface in the various cases. *q.e.d.*

Insofar as hyperbolic lengths of geodesics are well-defined invariants of homotopy classes of curves in F , these lengths must be invariant under Whitehead moves, so we have the following

Lemma 2.4 *Transformation (2.8) preserves the traces of products over paths (2.6).*

2.1.2 Weil–Petersson form

$\mathcal{T}_H(F)$ supports its canonical Weil–Petersson Poisson structure, which has a very simple form in shear coordinates.

Theorem 2.5 [22] *In the coordinates (Z_α) on any fixed spine, the Weil–Petersson bracket B_{WP} is given by*

$$B_{WP} = \sum_v \sum_{i=1}^3 \frac{\partial}{\partial Z_{v_i}} \wedge \frac{\partial}{\partial Z_{v_{i+1}}}, \quad (2.9)$$

where the sum is taken over all vertices v and v_i , $i = 1, 2, 3 \pmod 3$, are the labels of the cyclically ordered half-edges incident on this vertex.

The proof [22] relies on the independence of this form under Whitehead moves as in [10]. Indeed, the equivalent expression for the Weil–Petersson Kähler two-form in the punctured case was first given in lambda length coordinates in [9] starting from Wolpert’s formula [37], and the formula in shear coordinates follows from direct calculation using the expression $Z = \log \frac{bd}{ac}$. (There is more to this geometrically, however, and one must show [19] that the same expression is the Weil–Petersson form for surfaces with boundary.)

The set of Casimir functions is described by the following proposition, whose proof is given in Appendix B.

Proposition 2.6 *The center of the Poisson algebra (2.9) is generated by elements of the form $\sum Z_\alpha$, where the sum is over all edges of Γ in a boundary component of $F(\Gamma)$ and the sum is taken with multiplicity.*

2.1.3 Mapping class group description using graphs.

Recall that the mapping class group $MC(F)$ of an open surface F is the group of homotopy classes of orientation-preserving homeomorphisms of F . No special constraints are imposed by the circle boundary components, i.e., a homeomorphism must fix each boundary component only setwise, and the homotopies must likewise fix each boundary component only setwise. Thus, if F has b boundary component circles, p punctures, and genus g , then $MC(F) \approx MC(F_g^{b+p})$, so we generally write $MC_g^s = MC(F)$ for any surface of genus g with s boundary components. In this section, we establish the combinatorial presentation of MC_g^s associated with the cell decomposition of decorated Teichmüller space.

Recall that a cell in the decomposition of $\widetilde{\mathcal{T}}_g^s$ is described by the homotopy classes of an embedding $\iota : \Gamma \rightarrow F$ of a fatgraph Γ as a spine of F . MC_g^s acts on the set of homotopy classes of such embeddings by post-composition, and the cell decomposition of decorated Teichmüller space $\widetilde{\mathcal{T}}_g^s$ descends to an orbifold cell decomposition of $\widetilde{\mathcal{M}}_g^s = \widetilde{\mathcal{T}}_g^s / MC(F)$.

The *modular groupoid* $MG_g^s = MG(F)$ is the fundamental path groupoid of $\widetilde{\mathcal{M}}_g^s$, and MC_g^s arises as the subgroup of paths based at any point. Specifically, consider the dual graph $\mathcal{G}_g^s = \mathcal{G}(F)$ of the codimension-two skeleton of this decomposition of $\widetilde{\mathcal{M}}_g^s$ (where there is one vertex for each top-dimensional cell, edges correspond to Whitehead moves, and two-dimensional cells correspond to pairs of homotopic paths in the one-skeleton which are homotopic to real endpoints in $\widetilde{\mathcal{M}}_g^s$.) The fundamental path groupoid of \mathcal{G}_g^s is the modular groupoid, and in particular, MC_g^s is the stabilizer in MG_g^s of any vertex of \mathcal{G}_g^s .

We may think of a Whitehead move along edge α of fatgraph Γ producing another fatgraph Γ_α as an ordered pair (Γ, Γ_α) , i.e., an oriented edge of \mathcal{G}_g^s . Letting $[\Gamma_1, \Gamma_2]$ denote the MC_g^s -orbit of a pair (Γ_1, Γ_2) by the diagonal action of the mapping class group, the natural composition descends to a well-defined product

$$[\Gamma_1, \Gamma_3] = [\Gamma_1, \Gamma_2][\Gamma_2, \Gamma_3].$$

Theorem 2.7 [10],[9] *The modular groupoid MG_g^s is generated by Whitehead moves and relabelings by fatgraph symmetries. A complete list of relations in MG_g^s is given by relabelings under fatgraph symmetries together with the two following relations.*

Commutativity *If α and β are two edges with no common endpoints, then*

$$[\Gamma_{\alpha\beta}, \Gamma_\alpha][\Gamma_\alpha, \Gamma] = [\Gamma_{\alpha\beta}, \Gamma_\beta][\Gamma_\beta, \Gamma].$$

Pentagon *If α and β share exactly one common endpoint, then (see Figure 2 drawn for the dual graph)*

$$[\Gamma, \Gamma_\alpha][\Gamma_\alpha, \Gamma_{\beta\alpha}][\Gamma_{\beta\alpha}, \Gamma_{\alpha\beta}][\Gamma_{\alpha\beta}, \Gamma_\beta][\Gamma_\beta, \Gamma] = 1.$$

Furthermore, the expression in Theorem 2.5 for the Weil–Petersson form is invariant under Whitehead moves.

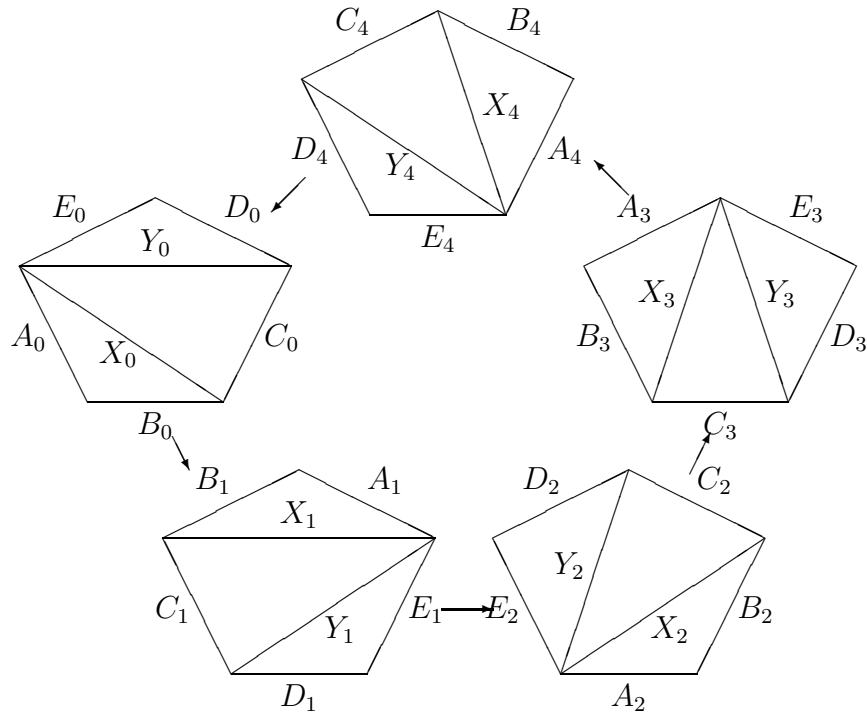


Figure 2-pentagon identity

Proof of Theorem The first parts are immediate consequences of the cell decomposition. Specifically, by connectivity of $\tilde{\mathcal{T}}_g^s$, any two points can be joined by a smooth path, which we may put into general position with respect to the codimension-one faces; this proves the first part. For the second part, a homotopy between edge-paths in $\tilde{\mathcal{M}}_g^s$ can likewise be put into general position with respect to the codimension-two faces; there are two possibilities for a pair of edges depending upon whether their vertices are disjoint or not, corresponding respectively to the commutativity and pentagon relations, proving the second part. The invariance of the expression for the Weil–Petersson form under Whitehead moves is a direct calculation in lambda lengths [11] or shear coordinates using (2.8). *q.e.d.*

2.2 Poisson algebras of geodesic functions

The algebra generated (with multiplication and with the Weil–Petersson Poisson bracket) by the functions $\{G_\gamma\}$ (2.6) was first studied by W. Goldman [23].

2.2.1 Multicurves

In the sequel, disjointly embedded families of geodesics will play a special role as they constitute a basis for the algebra of observables in both the classical case considered here and the quantum case discussed in Section 3. The homotopy class of such a family is called a *multiple curve*. A *multicurve* is multiset based on the set of curves in a multiple curve.

Definition 2.1 Consider the homotopy class of a finite collection $C = \{\gamma_1, \dots, \gamma_n\}$ of disjointly embedded (unoriented) simple closed curves γ_i in a topological surface F , where C need *not* be a multiple curve. A *generalized multicurve* (GMC) \hat{C} in F is a multiset based on C ; one thus imagines $s_i \geq 1$ parallel copies of components of C , or in other words, positive integral weights s_i on each component of C , where s_i is the multiplicity of γ_i in \hat{C} . Further, given a hyperbolic structure on F , we associate to \hat{C} the product $G_{\hat{C}} = G_{\gamma_1}^{s_1} \dots G_{\gamma_n}^{s_n}$ of geodesic operators (2.6) of all geodesics constituting a GMC; these operators Poisson commute in the classical case since the components of C are disjoint. In particular, a GMC containing a contractible component (of length zero) is twice the GMC with this curve removed.

An edge-path on a spine $\Gamma \subseteq F$ or its corresponding geodesic γ in F is said to be *graph simple* with respect to Γ if it does not pass more than once through any edge of Γ . Obviously, the set of graph simple geodesics depends upon Γ and is *not* invariant under Whitehead moves. Nevertheless, this notion will be useful in what follows.

2.2.2 Classical skein relation

The trace relation $\text{tr}(AB) + \text{tr}(AB^{-1}) - \text{tr} A \cdot \text{tr} B = 0$ for arbitrary 2×2 matrices A and B with unit determinant allows one to “disentangle” any product of geodesic functions, i.e., express it uniquely as a finite linear combination of GMCs. Introducing the additional factor $\#G$ to be the total number of components in a GMC, we can then uniformly present the classical skein relation as

$$(-1)^{\#G} \begin{array}{c} \diagup \quad \diagdown \\ \diagdown \quad \diagup \end{array} + (-1)^{\#G} \begin{array}{c} \text{) (} \\ \text{()} \end{array} + (-1)^{\#G} \begin{array}{c} \text{) (} \\ \text{) (} \end{array} = 0, \quad (2.10)$$

2.2.3 Poisson brackets for geodesic functions.

Turning attention now to the Poisson structure, two geodesic functions Poisson commute if the underlying geodesics are disjointly embedded. By the Leibnitz rule for the Poisson bracket, it suffices to consider only “simple” intersections of pairs of geodesics with

respective geodesic functions G_1 and G_2 of the form

$$G_1 = \text{tr}^1 \dots X_C^1 R^1 X_Z^1 L^1 X_A^1 \dots, \quad (2.11)$$

$$G_2 = \text{tr}^2 \dots X_B^2 L^2 X_Z^2 R^2 X_D^2 \dots, \quad (2.12)$$

where the superscripts 1 and 2 pertain to operators and traces in two different matrix spaces.

The bracket between X_C^1 and X_B^2 possesses a simple r -matrix structure

$$\{X_C^1, X_B^2\} = \frac{1}{4}(-1)^{i+j}(e_{ii}^1 \otimes e_{jj}^2)X_C^1 \otimes X_B^2, \quad (2.13)$$

where the “elementary” matrix e_{ij} has entry unity in its i th row and j th column and zero otherwise. Direct calculations then give

$$\{G_1, G_2\} = \frac{1}{2}(G_H - G_1), \quad (2.14)$$

where G_1 corresponds to the geodesic that is obtained by erasing the edge Z and joining together the edges “ A ” and “ D ” as well as “ B ” and “ C ” in a natural way as illustrated in the middle diagram in (2.10); G_H corresponds to the geodesic that passes over the edge Z twice, so it has the form $\text{tr} \dots X_C R_Z R_D \dots \dots X_B L_Z L_A \dots$ as illustrated in the rightmost diagram in (2.10). These relations were first obtained in [23] in the continuous parametrization (the classical Turaev–Viro algebra).

Torus Example For the torus, $\mathcal{T}_H(F_1^1)$ has three generators X, Y, Z , where

$$\{X, Y\} = \{Y, Z\} = \{Z, X\} = 2,$$

corresponding to the combinatorially unique cubic spine and the Casimir element is $X + Y + Z$. The geodesic functions for the three graph simple geodesics are

$$\begin{aligned} G_X &= \text{tr} L X_Y R X_Z = e^{-Y/2-Z/2} + e^{-Y/2+Z/2} + e^{Y/2+Z/2}, \\ G_Y &= \text{tr} R X_X L X_Z = e^{-Z/2-X/2} + e^{-Z/2+X/2} + e^{Z/2+X/2}, \\ G_Z &= \text{tr} R X_Y L X_X = e^{-X/2-Y/2} + e^{-X/2+Y/2} + e^{X/2+Y/2}. \end{aligned} \quad (2.15)$$

Introducing the geodesic function

$$\widetilde{G}_Z = \text{tr} L_Y R_Z R_X L_Z = e^{-X/2-Y/2-Z} + e^{X/2-Y/2}(e^{-Z} + e^Z + 2) + e^{X/2+Y/2+Z},$$

obtained from G_Z by a Whitehead move, we find that $\{G_X, G_Y\} = \widetilde{G}_Z/2 - G_Z/2$, and because relation (2.10) implies that $G_X G_Y = G_Z + \widetilde{G}_Z$, we have

$$\{G_X, G_Y\} = \frac{1}{2}G_X G_Y - G_Z, \quad (2.16)$$

plus the cyclic permutations in X, Y, Z , i.e., the classical Poisson algebra closes in the algebraic span of the geodesic functions $\{G_X, G_Y, G_Z\}$.

2.2.4 Poisson geodesic algebras for higher genera

In order to generalize the torus example, we must find a graph on which graph simple geodesics constitute a convenient algebraic basis. Such a graph is illustrated in Figure 3, where m edges pairwise connect two horizontal line segments. Graph simple closed geodesics in this picture are those and only those that pass through exactly two different “vertical” edges, and they are therefore enumerated by ordered pairs of edges; we denote the corresponding geodesic functions \mathcal{G}_{ij} where $i < j$. The Poisson algebra for the functions \mathcal{G}_{ij} is described by

$$\{\mathcal{G}_{ij}, \mathcal{G}_{kl}\} = \begin{cases} 0, & j < k, \\ 0, & k < i, j < l, \\ \mathcal{G}_{ik}\mathcal{G}_{jl} - \mathcal{G}_{kj}\mathcal{G}_{il}, & i < k < j < l, \\ \frac{1}{2}\mathcal{G}_{ij}\mathcal{G}_{jl} - \mathcal{G}_{il}, & j = k, \\ \mathcal{G}_{il} - \frac{1}{2}\mathcal{G}_{ij}\mathcal{G}_{il}, & i = k, j < l \\ \mathcal{G}_{ik} - \frac{1}{2}\mathcal{G}_{ij}\mathcal{G}_{kj}, & j = l, i < k. \end{cases} \quad (2.17)$$

The graph in Figure 3 has genus $\frac{m}{2} - 1$ and two faces (holes) if m is even and genus $(m-1)/2$ and one face (hole) if m is odd. Such geodesic bases for m even were considered in [24]. The Poisson algebras of geodesics obtained there *coincide exactly* with (2.17). These are the so-called $so_q(m)$ algebras whose representations were constructed in [25].

In the mathematical literature, this algebra has also appeared as the Poisson algebra of the monodromy data (Stokes matrices) of certain matrix differential equations [26] and on the symplectic groupoid of upper-triangular matrices \mathcal{G} [27]. These matrices have entries given by unity on the main diagonal (i.e., we set $\mathcal{G}_{ii} \equiv 1$) and the entries \mathcal{G}_{ij} above it. For $m \times m$ -matrices, there are $\lfloor \frac{m}{2} \rfloor$ central elements of this algebra generated by the polynomial invariants $f_{\mathcal{G}}(\lambda) \equiv \det(\mathcal{G} + \lambda \mathcal{G}^T) = \sum f_i(\mathcal{G})\lambda^i$. The total Poisson dimension d of algebra (2.17) is $\frac{m(m-1)}{2} - \lfloor \frac{m}{2} \rfloor$, and for $m = 3, 4, 5, 6, \dots$ we have $d = 2, 4, 8, 12, \dots$. The dimensions of the corresponding Teichmüller spaces are $D = 2, 4, 8, 10, \dots$, so we see that the Teichmüller spaces are embedded as the Poisson leaves in the algebra (2.17).

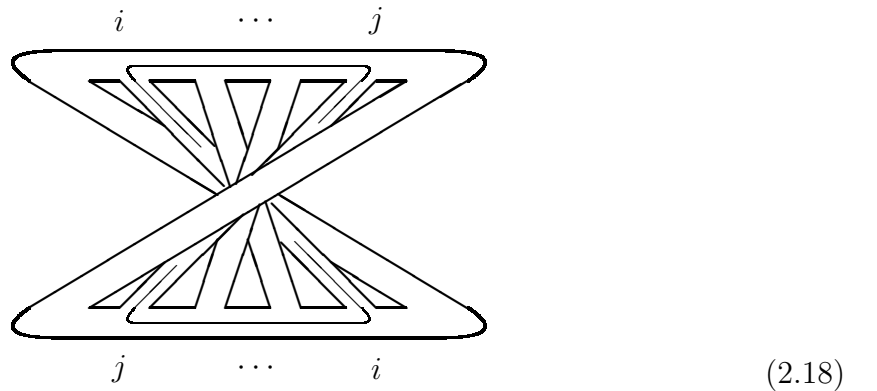


Figure 3-the special spine for higher genera

3 Quantization

A quantization of a Poisson manifold, which is equivariant under the action of a discrete group \mathcal{D} , is a family of $*$ -algebras \mathcal{A}^{\hbar} depending on a positive real parameter \hbar with \mathcal{D} acting by outer automorphisms and having the following properties:

1. (Flatness.) All algebras are isomorphic (noncanonically) as linear spaces.
2. (Correspondence.) For $\hbar = 0$, the algebra is isomorphic as a \mathcal{D} -module to the $*$ -algebra of complex-valued functions on the Poisson manifold.
3. (Classical Limit.) The Poisson bracket on \mathcal{A}^0 given by $\{a_1, a_2\} = \lim_{\hbar \rightarrow 0} \frac{[a_1, a_2]}{\hbar}$ coincides with the Poisson bracket given by the Poisson structure of the manifold.

3.1 Quantizing Teichmüller spaces

Here we construct a quantization $\mathcal{T}^{\hbar}(F)$ of the Teichmüller space $\mathcal{T}_H(F)$ that is equivariant with respect to the action of the mapping class group $\mathcal{D} = MC(F)$.

Fix a cubic fatgraph Γ as spine of F , and let $\mathcal{T}^{\hbar} = \mathcal{T}^{\hbar}(\Gamma)$ be the algebra generated by Z_{α}^{\hbar} , one generator for each unoriented edge α of Γ , with relations

$$[Z_{\alpha}^{\hbar}, Z_{\beta}^{\hbar}] = 2\pi i \hbar \{z_{\alpha}, z_{\beta}\} \quad (3.1)$$

(cf. (2.9)) and the $*$ -structure

$$(Z_{\alpha}^{\hbar})^* = Z_{\alpha}^{\hbar}, \quad (3.2)$$

where z_{α} and $\{\cdot, \cdot\}$ denotes the respective coordinate functions and the Poisson bracket on the classical Teichmüller space. Because of (2.9), the righthand side of (3.1) is a constant taking only five values 0 , $\pm 2\pi i \hbar$, and $\pm 4\pi i \hbar$ depending upon the coincidences of endpoints of edges labelled α and β .

Lemma 3.1 *The center \mathcal{Z}^{\hbar} of the algebra \mathcal{T}^{\hbar} is generated by the sums $\sum_{\alpha \in I} Z_{\alpha}^{\hbar}$ over all edges $\alpha \in I$ surrounding a given boundary component, and the Poisson structure is non-degenerate on the quotient $\mathcal{T}^{\hbar}/\mathcal{Z}^{\hbar}$.*

A standard Darboux-type theorem for non-degenerate Poisson structures then gives the following result.

Corollary 3.2 *There is a basis for $\mathcal{T}^{\hbar}/\mathcal{Z}^{\hbar}$ given by operators p_i, q_i , for $i = 1, \dots, 6g - 6 + 2s$ satisfying the standard commutation relations $[p_i, q_j] = 2\pi i \hbar \delta_{ij}$, $i, j = 1, \dots, 3g - 3 + s$.*

Not only is the proof of Lemma 3.1 given in Appendix B, but also an algorithm for diagonalizing this Poisson structure is described there.

Now, define the Hilbert space \mathcal{H} to be the set of all L^2 functions in the q -variables and let each q -variable act by multiplication and each corresponding p variable act by differentiation, $p_i = 2\pi i \hbar \frac{\partial}{\partial p_i}$. For different choices of diagonalization of non-degenerate Poisson structures, these Hilbert spaces are canonically isomorphic.

Torus Example In the case of the bordered torus, we have three generators, X^{\hbar} , Y^{\hbar} , and Z^{\hbar} , the commutation relations (3.1) have the form $[X^{\hbar}, Y^{\hbar}] = [Y^{\hbar}, Z^{\hbar}] = [Z^{\hbar}, X^{\hbar}] = 4\pi i\hbar$, and the single central element is $X^{\hbar} + Y^{\hbar} + Z^{\hbar}$. In the Darboux-type representation, we can identify, e.g., $(X^{\hbar} + Y^{\hbar})/2$ with q and $(-X^{\hbar} + Y^{\hbar})/2$ with $(-2\pi i\hbar)\partial/\partial q$.

On the level of the modular groupoid as a category where all morphisms are invertible and any two objects are related by a morphism, we have constructed one $*$ -algebra per object. In order to describe the \mathcal{D} -equivariance we must associate a homomorphism of the corresponding $*$ -algebras to any morphism in the modular groupoid. For this, we associate a morphism of algebras to any Whitehead move and must verify that the relations in Theorem 2.7 are satisfied.

We now define the *quantum Whitehead move* or *flip* along an edge of Γ by Eq. (2.8) using the (quantum) function

$$\phi(z) \equiv \phi^{\hbar}(z) = -\frac{\pi\hbar}{2} \int_{\Omega} \frac{e^{-ipz}}{\sinh(\pi p) \sinh(\pi\hbar p)} dp, \quad (3.3)$$

where the contour Ω goes along the real axis bypassing the origin from above. The function (3.3) is Faddeev's generalization [13] of the quantum dilogarithm.

Proposition 3.3 *For each unbounded self-adjoint operator Z on \mathcal{H} , $\phi(Z)$ is a well-defined unbounded self-adjoint operator on \mathcal{H} .*

Proof The function $\phi^{\hbar}(Z)$ satisfies the relations (see [4])

$$\begin{aligned} \phi^{\hbar}(Z) - \phi^{\hbar}(-Z) &= Z, \\ \phi^{\hbar}(Z + i\pi\hbar) - \phi^{\hbar}(Z - i\pi\hbar) &= \frac{2\pi i\hbar}{1 + e^{-Z}}, \\ \phi^{\hbar}(Z + i\pi) - \phi^{\hbar}(Z - i\pi) &= \frac{2\pi i}{1 + e^{-Z/\hbar}} \end{aligned}$$

and is meromorphic in the complex plane with the poles at the points $\{\pi i(m + n\hbar), m, n \in \mathbb{Z}_+\}$ and $\{-\pi i(m + n\hbar), m, n \in \mathbb{Z}_+\}$.

The function $\phi^{\hbar}(Z)$ is therefore holomorphic in the strip $|\operatorname{Im} Z| < \pi \min(1, \operatorname{Re} \hbar) - \epsilon$ for any $\epsilon > 0$, so we need only its asymptotic behavior as $Z \in \mathbb{R}$ and $|Z| \rightarrow \infty$, for which we have (see, e.g., [28])

$$\phi^{\hbar}(Z) \Big|_{|Z| \rightarrow \infty} = (Z + |Z|)/2 + O(1/|Z|). \quad (3.4)$$

Therefore, the function $\phi^{\hbar}(Z)$ increases as $|Z|$ at infinity and represents an operator in \mathcal{H} by the functional calculus [39]. *q.e.d.*

Theorem 3.4 *The family of algebras $\mathcal{T}^{\hbar} = \mathcal{T}^{\hbar}(\Gamma)$ is a quantization of $\mathcal{T}_H(F)$ for any cubic fatgraph spine Γ of F , that is:*

1. *In the limit $\hbar \mapsto 0$, morphism (2.8) using (3.3) coincides with the classical morphism (2.8) where $\phi(Z) = \log(1 + e^Z)$;*

2. Morphism (2.8) using (3.3) is indeed a morphism of $*$ -algebras;
3. A flip W_Z satisfies $W_Z^2 = I$, cf. (2.8), and flips satisfy the commutativity relation;
4. Flips satisfy the pentagon relation.¹

Furthermore,

5. The morphisms $\mathcal{T}^{\hbar}(\Gamma) \rightarrow \mathcal{T}^{1/\hbar}(\Gamma)$ given by $Z_{\alpha}^{\hbar} \mapsto Z_{\alpha}^{1/\hbar}$ commute with morphisms (2.8).

Sketch of the proof Property 1 follows since $\lim_{\hbar \rightarrow 0} \phi^{\hbar}(z) = \log(e^z + 1)$, and Property 3 is obvious.

In order to prove Property 2, we must first verify that $[A + \phi^{\hbar}(Z), B - \phi^{\hbar}(-Z)] = 0$ and $[A + \phi^{\hbar}(Z), D - \phi^{\hbar}(-Z)] = -2\pi i \hbar$ (since the other relations are obviously satisfied), which follows from the identity $\phi^{\hbar}(z) - \phi^{\hbar}(-z) = z$.

For Property 5, we must verify that the morphism $\mathcal{T}^{\hbar}(\Gamma) \rightarrow \mathcal{T}^{1/\hbar}(\Gamma)$ commutes with a flip, that is, $(A + \phi^{\hbar}(Z))/\hbar = A/\hbar + \phi^{\hbar}(Z/\hbar)$, $(B - \phi^{\hbar}(-Z))/\hbar = B/\hbar - \phi^{\hbar}(-Z/\hbar)$, etc., which follows from $\phi^{\hbar}(z)/\hbar = \phi^{1/\hbar}(z/\hbar)$.

Turning finally to the most nontrivial Property 4, we may reformulate it as follows. There are seven generators involved in the sequence of flips depicted in Figure 2 for the dual cell decomposition, which are denoted A, B, C, D, E, X, Y as in the figure. As a result of a flip, the piece of graph shown in Figure 1 just gets cyclically rotated. Denote by $A_i, B_i, C_i, D_i, E_i, X_i$, and Y_i the algebra elements associated to the edges of this piece of graph after i flips are performed. From (2.8), (3.3), these elements evolve as follows:

$$\begin{pmatrix} X_{i+1} \\ Y_{i+1} \\ A_{i+1} \\ B_{i+1} \\ C_{i+1} \\ D_{i+1} \\ E_{i+1} \end{pmatrix} \rightarrow \begin{pmatrix} Y_i - \phi^{\hbar}(-X_i) \\ -X_i \\ D_i \\ E_i \\ A_i + \phi^{\hbar}(X_i) \\ B_i - \phi^{\hbar}(-X_i) \\ C_i + \phi^{\hbar}(X_i) \end{pmatrix} \quad (3.5)$$

We must prove that this operator is periodic with period five.

Assume for a moment that this five-periodicity of X_i has been established. Then five-periodicity of Y_i and other variables follow from simple calculations.

It suffices to prove this five-periodicity for the X_i since the five-periodicity of the other operators such as Y_i then follows from elementary calculations. As to the five-periodicity of X_i , let us “take logarithms” and introduce four new algebra elements

$$U_i = e^{X_i}; \quad V_i = e^{Y_i}; \quad \tilde{U}_i = e^{X_i/\hbar}; \quad \tilde{V}_i = e^{Y_i/\hbar},$$

which satisfy the following commutation relations

$$\begin{aligned} U_i V_i &= q^{-2} V_i U_i, & \tilde{U}_i \tilde{V}_i &= \tilde{q}^{-2} \tilde{V}_i \tilde{U}_i, \\ U_i \tilde{V}_i &= \tilde{V}_i U_i, & V_i \tilde{U}_i &= \tilde{U}_i V_i, \end{aligned} \quad (3.6)$$

¹This result was independently obtained by R. M. Kashaev [5].

where

$$q = e^{-\pi i \hbar}, \quad \tilde{q} = e^{-\pi i / \hbar}.$$

Under the flip, these variables are transformed in an especially simple way,

$$U_{i-1} = V_i^{-1} \tag{3.7}$$

$$V_{i-1} = U_i(1 + qV_i) \tag{3.8}$$

$$\tilde{U}_{i-1} = \tilde{V}_i^{-1} \tag{3.9}$$

$$\tilde{V}_{i-1} = V_i(1 + \tilde{q}\tilde{V}_i). \tag{3.10}$$

As the first step of the proof, we consider the inverse transformation laws for X_i and Y_i :

$$X_{i-1} = -Y_i; \quad Y_{i-1} = X_i + \phi^{\hbar}(Y_i).$$

Equations (3.7) and (3.9) are obvious. Using the standard formula

$$e^{A+F(B)} = e^{\frac{1}{[A,B]} \int_B^{B+[A,B]} F(z) dz} e^A,$$

we obtain

$$\begin{aligned} V_{i-1} &= e^{Y_{i-1}} = e^{X_i + \phi^{\hbar}(Y_i)} = e^{X_i} e^{\int_Y^{Y+2\pi i \hbar} \phi^{\hbar}(z) dz} \\ &= U_i \exp \left(-\frac{\pi \hbar}{2} \int_{\Omega} \frac{e^{-ipz}(e^{-2p\pi \hbar} - 1)}{(-ip) \sinh(\pi p) \sinh(\pi \hbar p)} dp \right) = U_i \exp \left(\frac{\pi \hbar}{i} \int_{\Omega} \frac{e^{-ip(z-\pi i \hbar)}}{p \sinh(\pi p)} dp \right) \\ &= U_i(1 + q^{-2}V_i). \end{aligned}$$

The proof of (3.10) is analogous.

Now, in order to finally prove that X_i is five-periodic, it suffices to verify that both U_i and \tilde{U}_i are five-periodic. Indeed, if only the operator U_i is five-periodic, it does not suffice because the logarithm of an operator is ambiguously defined. However, if we have two families of operators U and \tilde{U} , which depend continuously on \hbar , then, assuming the existence of an operator X (depending continuously on \hbar) such that $U = e^X$ and $\tilde{U} = e^{X/\hbar}$, then this operator is evidently unique. (It can be found as $\lim_{(m+n/\hbar) \rightarrow 0} (U^m \tilde{U}^n) / (m+n/\hbar)$ for any irrational value of \hbar .) The five-periodicity of sequence (3.8) (and (3.10)) is a direct calculation using (3.6).

The only subtlety remaining is the possibility that some of the edges A, B, C, D, E coincide. (Note, however, that X and Y must have exactly one common vertex.) If, say, edges A and C coincide, then the value of the commutator $[A, X]$ is doubled by definition, and we can then fictitiously *split* the edge $A = C$ into two half-edges with the matrices $X_{A/2}$ assigned to each half-edge using the formula

$$X_A = X_{A/2} \begin{pmatrix} 0 & 1 \\ -1 & 0 \end{pmatrix} X_{A/2}. \tag{3.11}$$

The quantities $A/2 = C/2$ have the same commutation relations with the rest of variables as well as the same transformation laws as the quantities A and C before, so the earlier

formulas remain valid if we simply replace there A' by $A'/2$ and A by $A/2$. The net effect is that commutators with $A = C$ are doubled.

If edges A and B coincide, then we must correct formulas (3.4) using a splitting as above but demanding $A'/2 = A/2 + X/2$. Obviously, $[A, X] = 0$ in this case (in which formulas for the quantum ordering below must be also corrected, see Section 3.5).

The formulas in Proposition 2.3 can thus be realized for exponentiated quantities, although in the current quantum case there will be corrections. For instance, formulas (3.8) and (3.9) will be different; indeed, letting $A = C = X$, we calculate that $e^{X/2} \mapsto e^{X/2+\phi^{\hbar}(Z)} =: e^{X/2}(1 + e^Z) \equiv e^{X/2} + e^{X/2+Z} = e^{X/2}(1 + e^{-i\pi\hbar}e^Z)$ since the commutator of X and Z is doubled, where the normal ordering (the Weyl ordering) $:\cdot:$ is explained in the next section. The transformation for e^X itself becomes more complicated when $A = C$, namely, $e^X = (e^{X/2})^2 \mapsto e^X(1 + q^3e^Z)(1 + qe^Z)$. *q.e.d.*

Corollary 3.5 1. *Let K be an operator acting in the Hilbert space $L^2(\mathbb{R})$ and having the integral kernel*

$$K(x, z) = F^{\hbar}(z)e^{-\frac{zx}{2\pi i\hbar}}, \quad (3.12)$$

where

$$F^{\hbar}(z) = \exp\left(-\frac{1}{4}\int_{\Omega}\frac{e^{-ipz}}{p\sinh(\pi p)\sinh(\pi\hbar p)}dp\right) \quad (3.13)$$

Then the operator K is unitary up to a multiplicative constant and satisfies the identity

$$K^5 = \text{const.} \quad (3.14)$$

2. *Let $\hbar = m/n$ be a rational number and assume that both m and n are odd. Introduce a linear operator $L(u)$ acting in the space \mathbb{C}^n and depending on one positive real parameter u through its matrix*

$$L(u)_j^i = F^{\hbar}(j, u)q^{-4ij}, \quad (3.15)$$

where

$$F^{\hbar}(j, u) = (1 + u)^{j/n}\prod_{k=0}^{j-1}(1 + q^{-4k+2}u^{1/n})^{-1}.$$

Then the following identity holds:

$$L(u)L(v + uv)L(v + vu^{-1} + u^{-1})L(u^{-1}v^{-1} + u^{-1})L(v^{-1}) = 1. \quad (3.16)$$

Using this construction, Kashaev [28] constructed the set of eigenfunctions of the quantum Dehn twist transformation. Namely, Kashaev's dilogarithm function $e_b(z)$ is $1/F^{\hbar}(2z)$ from (3.13). We return to this discussion when considering sets of quantum Dehn twists for the torus in Section 5.

3.2 Geodesic length operators

We next embed the algebra of geodesics (2.6) into a suitable completion of the constructed algebra \mathcal{T}^{\hbar} . For any γ , the geodesic function G_{γ} (2.6) can be expressed in terms of shear

coordinates on \mathcal{T}_H :

$$G_\gamma \equiv \text{tr } P_{Z_1 \dots Z_n} = \sum_{j \in J} \exp \left\{ \frac{1}{2} \sum_{\alpha \in E(\Gamma)} m_j(\gamma, \alpha) z_\alpha \right\}, \quad (3.17)$$

where $m_j(\gamma, \alpha)$ are integers and J is a finite set of indices. In order to find the quantum analogues of these functions, we denote by $\widehat{\mathcal{T}}^\hbar$ a completion of the algebra \mathcal{T}^\hbar containing e^{xZ_α} for any real x .

For any closed path γ on F , define the *quantum geodesic* operator $G_\gamma^\hbar \in \widehat{\mathcal{T}}^\hbar$ to be

$$G_\gamma^\hbar \equiv \times \text{tr } P_{Z_1 \dots Z_n} \times \equiv \sum_{\substack{j \in J \\ \kappa \in \{j\}}} \exp \left\{ \frac{1}{2} \sum_{\alpha \in E(\Gamma)} (m_j(\gamma, \alpha) Z_\alpha^\hbar + 2\pi i \hbar c_j^\kappa(\gamma, \alpha)) \right\}, \quad (3.18)$$

where the *quantum ordering* $\times \cdot \times$ implies that we vary the classical expression (3.17) by introducing additional integer coefficients $c_j^\kappa(\gamma, \alpha)$, which must be determined from the conditions below. Notice that the operators $\{G_\gamma^{\frac{1}{\hbar}}\}$ themselves can be considered as belonging to the algebra $\widehat{\mathcal{T}}^\hbar$ insofar as

$$G_\gamma^{\frac{1}{\hbar}} = \sum_{j \in J} \exp \left\{ \frac{1}{2\hbar} \sum_{\alpha \in E(\Gamma)} (m_j(\gamma, \alpha) Z_\alpha^\hbar + 2\pi i c_j^\kappa(\gamma, \alpha)) \right\}. \quad (3.19)$$

In what follows for the notational simplicity, we shall sometimes omit the superscript \hbar from G^\hbar and write it merely G assuming that G is either an operator or a classical geodesic function depending on the context. In this paper, we shall concentrate on the case of quantum functions of the G^\hbar -type; the consideration of the sector $G^{1/\hbar}$ is analogous and does not lead to new effects (at least at the present stage of understanding), so we omit it. We also call a quantum geodesic function merely a quantum geodesic (since implicitly quantum objects admit only functional, not geometrical, descriptions).

We wish to associate an operatorial *quantum multicurve* QMC to a multiset \hat{C} of quantum geodesics corresponding to disjointly embedded families of nonnegative integrally weighted geodesics. One ansatz will be that operators corresponding to disjoint underlying geodesics must commute; this implies that the ordering in which the quantum geodesics enter the product QMC is immaterial, where the product is defined as for GMCs. We next formulate the defining properties of quantum geodesics.

1. If closed paths γ and γ' do not intersect, then the operators G_γ^\hbar and $G_{\gamma'}^\hbar$ commute.
2. *Naturality.* The mapping class group $MC(F)$ (2.8) acts naturally, i.e., for any $\{G_\gamma^\hbar\}$, $\delta \in MC(F)$ and closed path γ in a spine Γ of F , we have $\delta(G_\gamma^\hbar) = G_{\delta\gamma}^\hbar$.
3. *Geodesic algebra.* The product of two quantum geodesics is a linear combination of QMC's governed by the (quantum) skein relation [29].
4. *Orientation invariance.* Quantum traces of direct and inverse geodesic operators coincide.

5. Exponents of geodesics. A quantum geodesic $G_{n\gamma}$ corresponding to the n -fold concatenation of γ is expressed via G_γ exactly as in the classical case, namely,

$$G_{n\gamma} = 2T_n(G_\gamma/2), \quad (3.20)$$

where $T_n(x)$ are Chebyshev's polynomials.

6. Duality. For any γ and γ' , the operators G_γ^{\hbar} and $G_{\gamma'}^{\frac{1}{\hbar}}$ commute.

We shall let the standard normal ordering symbol $:e^{a_1} e^{a_2} \cdots e^{a_n}$: denote the *Weyl ordering* $e^{a_1+\cdots+a_n}$, i.e.,

$$:e^{a_1} e^{a_2} \cdots e^{a_n}: = 1 + (a_1 + \cdots + a_n) + \frac{1}{2!} (a_1 + \cdots + a_n)(a_1 + \cdots + a_n) + \cdots \quad (3.21)$$

for any set of exponents with $a_i \neq -a_j$ for $i \neq j$. In particular, the Weyl ordering implies total symmetrization in the subscripts.

Proposition 3.6 *For any graph simple geodesic G with respect to any spine Γ , the coefficients $c_j^k(\gamma, \alpha)$ in (3.18) are identically zero.*

Proof Consider term-by-term the trace of the matrix product for the quantum graph simple geodesic and expand it in Laurent monomials in $e^{Z_i/2}$. It is easy to see that each term $e^{Z_i/2}$ comes either in power $+1$, or -1 in the corresponding monomial and there are no equivalent monomials in the sum. This means that in order to have a Hermitian operator, we must apply the Weyl ordering with no additional q -factors (by the correspondence principle, each such factor must be again a Laurent monomial in q standing by the corresponding term, which breaks the self-adjointness unless all such monomials are unity). Since quantum Whitehead moves must preserve the property of being Hermitian, if a graph-simple geodesic transforms to another graph-simple geodesic, then a Weyl-ordered expression transforms to a Weyl-ordered expression, and only these expressions are self-adjoint. *q.e.d.*

Torus Example For the torus with one hole, there are three graph simple quantum geodesics for any spine, which are exactly (2.15) in the Weyl-ordered form. The quantum geodesics \tilde{G}_Z obtained from G_Z by the flip transformation is

$$\tilde{G}_Z = e^{-X/2-Y/2-Z} + e^{X/2-Y/2-Z} + e^{X/2-Y/2} \cdot 2 \cos(\pi\hbar) + e^{X/2-Y/2+Z} + e^{X/2+Y/2+Z}. \quad (3.22)$$

The product of two graph simple quantum geodesics is

$$G_X G_Y = e^{i\pi\hbar/2} \tilde{G}_Z + e^{-i\pi\hbar/2} G_Z. \quad (3.23)$$

Denoting $q \equiv e^{-i\pi\hbar}$, $[A, B]_q \equiv q^{1/2}AB - q^{-1/2}BA$, and $\xi = q - q^{-1}$, we obtain from (3.23)

$$[G_X, G_Y]_q = \xi G_Z, \quad [G_Y, G_Z]_q = \xi G_X, \quad [G_Z, G_X]_q = \xi G_Y. \quad (3.24)$$

This algebra is exactly the $so_q(3)$ quantum algebra studied in [25]. There is a unique central element, the quantum Markov relation

$$\mathcal{M} = G_X G_Y G_Z - q^{1/2}(G_X^2 + q^{-2}G_Y^2 + G_Z^2). \quad (3.25)$$

3.3 Algebra of quantum geodesics

Let G_1 and G_2 correspond to the respective graph simple geodesics with respect to the same spine having one nontrivial intersection. For G_1 and G_2 , formula (3.18) implies, by virtue of Proposition 3.6, the mere Weyl ordering.

After some algebra, we obtain (cf. (2.14))

$$G_1 G_2 = e^{-i\pi\hbar/2} G_Z + e^{i\pi\hbar/2} \tilde{G}_Z, \quad (3.26)$$

where G_Z coincides with the Weyl-ordered G_1 in the classical case (cf. (2.14)) while \tilde{G}_Z contains the quantum correction term

$$\begin{aligned} \tilde{G}_Z &= \times \text{tr}^1 \text{tr}^2 \dots (e_{ij}^1 \otimes e_{ji}^2) [X_Z^1 \otimes X_Z^2] \dots \times \\ &= : \text{tr}^1 \text{tr}^2 \dots (e_{ij}^1 \otimes e_{ji}^2) [X_Z^1 \otimes X_Z^2 + 2(1 - \cos \pi\hbar) e_{11}^1 \otimes e_{22}^2] \dots : . \end{aligned}$$

Here $e_{ij}^1 \otimes e_{ji}^2$ is the standard r -matrix that permutes the spaces “1” and “2,” and as a result, the “skein” relation of form (2.14) appears. Locally, this relation has exactly the form proposed by Turaev [29], i.e., for two graph simple geodesics intersecting at a single point, we have the defining relation

$$\begin{array}{c} G_1 \\ \diagdown \\ G_2 \end{array} \quad = \quad e^{-i\pi\hbar/2} \begin{array}{c} \text{) } \\ \text{(} \end{array} \quad + \quad e^{i\pi\hbar/2} \begin{array}{c} \tilde{G}_Z \\ \text{) } \\ \text{(} \end{array} \quad (3.27)$$

(The order of crossing lines corresponding to G_1 and G_2 depends on which quantum geodesic occupies the first place in the product; the rest of the graph remains unchanged for all items in (3.27)). Note, however, that if the quantum geodesics G_1 and G_2 correspond to graph simple geodesics, we may turn the geodesic \tilde{G}_Z again into the graph simple geodesic \tilde{G}'_Z by performing the quantum flip with respect to the edge Z .

If we now compare two unambiguously determined expressions: \tilde{G}'_Z , which must be Weyl ordered, and \tilde{G}_Z obtained from the geodesic algebra, we find that $\tilde{G}_Z = \tilde{G}'_Z$. This enables us to formulate the main assertion.

Lemma 3.7 [4] *There exists a unique quantum ordering $\times \dots \times$ (3.18), which is generated by the quantum geodesic algebra (3.27) and consistent with the quantum mapping class groupoid transformations (2.8), i.e., so that the quantum geodesic algebra is invariant under the action of the quantum mapping class groupoid.*

We can now relax the constraints of graph simplicity of curves: as the quantum geodesic algebra is quantum mapping class group invariant, having two *arbitrary* embedded geodesics with a single intersection, we can transform them using quantum morphisms to a canonical form of graph simple geodesics and employ the Weyl order. Relation (3.27) remains valid in both cases.

Let us now address the problem of multiple intersections. Here, we have the following lemma.

Lemma 3.8 [4] *If more than one intersection of two QMCs occurs, then the quantum skein relations (3.27) must be applied simultaneously at all intersection points.*

This lemma implies the standard Reidemeister moves for curves on a graph, where the empty loop gives rise to a factor $-e^{-i\pi\hbar} - e^{i\pi\hbar}$; that is, for geodesics intersecting generically, apply (3.27) simultaneously at all intersection points to obtain the Reidemeister moves.

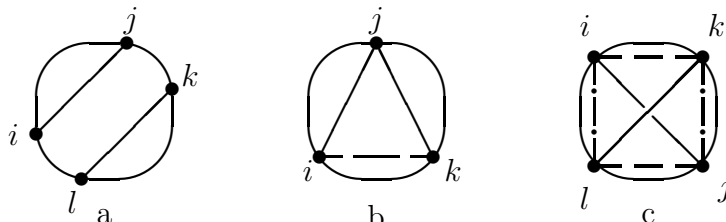
Remark 3.1 The quantum algebra \mathcal{M}_1^2 was studied in [4], where the exact correspondence with Kauffman bracket skein quantization of the corresponding Poisson algebra of geodesics (see [30]) was observed. In [27], this algebra arises as the quantum deformation algebra of the classical groupoid Poisson relations for the group $SL(4)$. This algebra is however only one among many quantum Nelson–Regge algebras corresponding to Riemann surfaces of higher genera which are described in the next section.

3.4 Quantizing the Nelson–Regge algebras

The algebra (2.17) was quantized by the deformation quantization method in [24, 31]. We now explicitly implement the quantization conditions (3.1). It is convenient to represent the (classical or quantum) elements \mathcal{G}_{ij} as chords connecting the points of the cyclically ordered set of indices i, j . There is then a trichotomy: if two chords do not intersect, then the corresponding geodesics do not intersect either, and the quantum geodesics commute (Figure 4a); if two chords have a common endpoint, then the corresponding geodesics intersect at one point, and the three quantum geodesics $\mathcal{G}_{ij}^h, \mathcal{G}_{jk}^h, \mathcal{G}_{ki}^h$ (as depicted in Figure 4b) constitute the quantum subalgebra $so_q(3)$; if two chords intersect at an interior point (as depicted in Figure 4c), then the corresponding geodesics intersect in two points, and the corresponding quantum geodesics \mathcal{G}_{ij}^h and $\mathcal{G}_{kl}^h, i < k < j < l$, satisfy the commutation relation

$$[\mathcal{G}_{ij}^h, \mathcal{G}_{kl}^h] = \xi(\mathcal{G}_{ik}^h \mathcal{G}_{jl}^h - \mathcal{G}_{il}^h \mathcal{G}_{jk}^h) \quad (3.28)$$

with the usual commutator (not the q -commutator) and where again $\xi = q - q^{-1}$.



(3.29)

Figure 4—picture of Nelson–Regge quantum relations

3.5 Improving the quantum ordering

We now extend the construction of QMCs by taking the products of operatorial matrices X_Z, L , and R along oriented geodesics as before, but we do not apply the trace operation as in the definition of the geodesic operators.

For the three cases of oriented curves depicted in Figure 5 below, we may apply the indicated quantum Whitehead move and calculate as follows:

For curve 1, we obtain

$$\begin{aligned}
X_{B'}LX_{-Z}LX_{A'} &= \begin{pmatrix} e^{-B'/2}e^{-Z/2}e^{A'/2} + e^{-B'/2}e^{Z/2}e^{A'/2} & -e^{-B'/2}e^{Z/2}e^{-A'/2} \\ e^{B'/2}e^{-Z/2}e^{A'/2} & 0 \end{pmatrix} \\
&= \begin{pmatrix} e^{A/2-B/2} & -e^{-A/2-B/2-\frac{1}{4}[A,B]} \\ e^{A/2+B/2-\frac{1}{4}[A,B]} & 0 \end{pmatrix} \text{ for } B' \neq A' \\
&= e^{-\frac{1}{8}[A,B]} \begin{pmatrix} e^{-B/2}e^{A/2} & -e^{-B/2}e^{-A/2} \\ e^{B/2}e^{A/2} & 0 \end{pmatrix} \text{ for } B' \neq A' \\
&= \begin{cases} e^{-\frac{1}{8}[A,B]}X_BLX_A & \text{for } A \neq B, \\ X_BLX_A & \text{for } A = B. \end{cases} \tag{3.30}
\end{aligned}$$

For curve 2, we obtain

$$\begin{aligned}
X_{C'}RX_{-Z}LX_{A'} &= \begin{pmatrix} e^{-C'/2}e^{Z/2}e^{A'/2} & -e^{-C'/2}e^{Z/2}e^{-A'/2} \\ e^{C'/2}e^{Z/2}e^{A'/2} + e^{C'/2}e^{-Z/2}e^{A'/2} & -e^{C'/2}e^{Z/2}e^{-A'/2} \end{pmatrix} \\
&= \begin{pmatrix} e^{A/2-C/2+Z/2+\frac{1}{4}[A,B]} & -e^{-A/2-C/2+Z/2} - e^{-A/2-C/2-Z/2} \\ e^{A/2+C/2+Z/2} & -e^{-A/2+C/2+Z/2-\frac{1}{4}[A,B]} \end{pmatrix} \\
&= \begin{pmatrix} e^{-C/2}e^{Z/2}e^{A/2} & -e^{-C/2}e^{Z/2}e^{-A/2} - e^{-C/2}e^{-Z/2}e^{-A/2} \\ e^{C/2}e^{Z/2}e^{A/2} & -e^{C/2}e^{Z/2}e^{-A/2} \end{pmatrix} \\
&= X_CLX_ZRX_A, \tag{3.31}
\end{aligned}$$

and if edges A and C coincide, we merely use the same splitting as in (3.11); no additional factors arise.

For curve 3, we obtain

$$\begin{aligned}
X_{C'}RX_{-Z}RX_{D'} &= \begin{pmatrix} 0 & -e^{-C'/2}e^{Z/2}e^{-D'/2} \\ e^{C'/2}e^{-Z/2}e^{D'/2} & -e^{C'/2}e^{Z/2}e^{-D'/2} - e^{-C'/2}e^{-Z/2}e^{-D'/2} \end{pmatrix} \\
&= \begin{pmatrix} 0 & -e^{-C/2-D/2+\frac{1}{4}[A,B]} \\ e^{C/2+D/2+\frac{1}{4}[A,B]} & -e^{C/2-D/2} \end{pmatrix} \text{ for } C' \neq D' \\
&= e^{\frac{1}{8}[A,B]} \begin{pmatrix} 0 & -e^{-C/2}e^{-D/2} \\ e^{C/2}e^{D/2} & -e^{C/2}e^{-D/2} \end{pmatrix} \text{ for } C' \neq D' \\
&= \begin{cases} e^{\frac{1}{8}[A,B]}X_CRX_D. & \text{for } C \neq D, \\ X_CRX_D & \text{for } C = D. \end{cases} \tag{3.32}
\end{aligned}$$

In these formulas, we have used the identities

$$e^{A'/2+C'/2+Z/2} + e^{A'/2+C'/2-Z/2} = : e^{A/2+C/2} \frac{1}{1+e^{-Z}} (e^{Z/2} + e^{-Z/2}) :$$

$$= e^{A/2+C/2+Z/2} \quad (3.33)$$

and

$$\begin{aligned} e^{-A'/2-C'/2+Z/2} &= : e^{-A/2-C/2}(1 + e^{-Z}) e^{Z/2} : \\ &= e^{-A/2-C/2+Z/2} + e^{-A/2-C/2-Z/2}, \end{aligned} \quad (3.34)$$

where vertical dots denote the Weyl ordering (3.21) as before implying total symmetrization with respect to all the variables $\{A, B, C, D, Z\}$.

As we have just observed and amazingly enough, the only thing that changes under a quantum Whitehead move is the overall factor standing by the product of matrices, and even this factor can easily be taken into account if included with each left-turn matrix L is an overall factor $e^{-\frac{1}{8}[A,B]}$, and included with each right-turn matrix R is an overall factor $e^{\frac{1}{8}[A,B]}$.

The subtlety of potentially multiple intersections between curves corresponds to the possibility that edges of the graph may coincide. As in the previously useful convenient fiction of splitting such an edge into two half-edges, the formulas (3.30), (3.31), and (3.32) remain valid if we replace there $A'/2$ by $A'/4$ and $A/2$ by $A/4$ in case $A = C$ for instance.

We thus have the quantum analogue of Lemma 2.4.

Lemma 3.9 *For any oriented non boundary-parallel geodesic γ , taking the finite (periodic) sequence of matrices with quantum entries in X_{Z_i} as before but making the replacement*

$$\tilde{L} = q^{-1/4}L, \quad \tilde{R} = q^{1/4}R, \quad (3.35)$$

where $q = e^{-i\pi\hbar}$, the resulting product of matrices

$$P_\gamma = (X_{Z_n} \tilde{L} X_{Z_{n-1}} \tilde{R} \dots X_{Z_3} \tilde{L} X_{Z_2} \tilde{R} X_{Z_1} \tilde{R}) \quad (3.36)$$

is invariant under quantum Whitehead moves.

Remark 3.2 In the case of a boundary-parallel curve, where a sub-word of the form $X_{D'} \tilde{R} X_{-Z} \tilde{R}$ transforms to a sub-word of the form $X_D \tilde{\tilde{R}}$, we must set the resulting turn matrices to be

$$\tilde{\tilde{L}} = q^{-1/2}L, \quad \tilde{\tilde{R}} = q^{1/2}R,$$

i.e., they have quantum factors doubled in comparison with \tilde{L} and \tilde{R} .

We now address the question of the proper quantum ordering. Using MCG transformations, we can reduce any simple curve either to the form of a graph simple curve with exactly one left and one right turn (c.f. formulas (2.15) and Figure 5) if this curve is not boundary-parallel, or to the form $X_D \tilde{\tilde{R}}$ or $X_D \tilde{\tilde{L}}$ for a boundary-parallel curve. In both cases, each term in the corresponding Laurent polynomial must be self-adjoint, which immediately results in the Weyl ordering by Proposition 3.6.

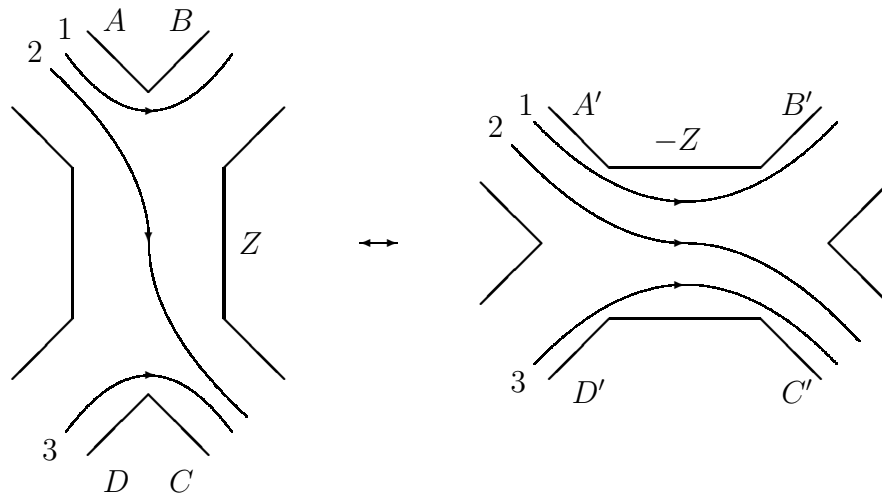


Figure 5-three cases of flips for geodesics

This observation does not suffice to derive the proper quantum ordering in our quantization of Thurston theory since we cannot consider in a consistent way an infinite product of matrices corresponding to infinite leaves of a measured foliation. Our tools for analyzing the Thurston theory in this case will devolve to naturality of the MCG action on the QMC algebra and an operatorial version of infinite continued fractions in Section 5.3.4. On the other hand, the improved quantum ordering is used in our analysis of closed geodesics on the torus, i.e., of operatorial finite continued fraction expansions in Section 5.3.1.

4 Classical Thurston Theory of Surfaces

Let F_g^s denote an oriented smooth surface with $s \geq 0$ punctures (so F_g^s may be closed without boundary in this section), with genus $g \geq 0$, and with negative Euler characteristic $2 - 2g - s < 0$.

4.1 Measured foliations and Thurston's boundary

Define a *measured foliation* on $F = F_g^s$ to be a one-dimensional topological foliation \mathcal{F} of F , where in a neighborhood of any $p \in F$, \mathcal{F} must restrict (in an appropriate chart) to the horizontal foliation as in Figure 6a or it must restrict to a foliation with one n -pronged singularity at p , for $n \geq 3$, as illustrated in Figure 6b.



Figure 6-pictures of foliations

Furthermore, \mathcal{F} comes equipped with a *transverse measure* μ , which assigns to any arc a in F that is transverse to \mathcal{F} a real number $\mu(a) \in \mathbb{R}_{\geq 0}$, where μ is required to satisfy:

No Holonomy: If a_0, a_1 are homotopic through arcs a_t transverse to \mathcal{F} , for $0 \leq t \leq 1$, keeping the endpoints of a_t on the same leaf for all t , then $\mu(a_0) = \mu(a_1)$;

σ -Additivity: If a is the serial concatenation of transverse arcs a_1, a_2, \dots , then $\mu(a) = \sum_{i \geq 1} \mu(a_i)$.

In other words, in the neighborhood of a non-singular point, there is a local chart $\phi : U \rightarrow \mathbb{R}^2 = \{(x, y) : x, y \in \mathbb{R}\}$ so that $\phi^{-1}(\{y = \text{constant}\})$ are the leaves of the foliation $\mathcal{F} \cap U$. If two charts U_i and U_j intersect, then the transition function ϕ_{ij} are of the form $\phi_{ij}(x, y) = (h_{ij}(x, y), c_{ij} \pm y)$, where c_{ij} is constant. In these coordinates, the transverse measure is $|dy|$. In case the transition functions can be chosen with constant sign $\phi_{ij}(x, y) = (h_{ij}(x, y), c + y)$, i.e., if the foliation is “transversely orientable”, then (away from the singular points) y is the primitive of a closed one-form on F .

Another canonical construction of a measured foliation on a Riemann surface is given by taking the leaves of the foliation to be the level sets of a harmonic function, where the transverse measure is given by integrating the conjugate differential along transverse arcs. Still another example is given by the homotopy class of a finite collection of disjointly embedded (weighted) curves, as we shall see.

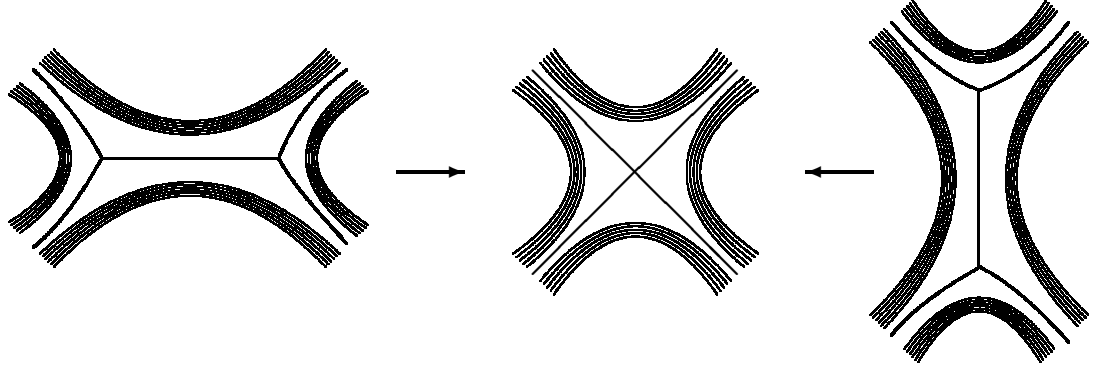


Figure 7-Whitehead collapses on foliations

There is an equivalence relation on measured foliations generated by isotopy and *Whitehead collapse* as illustrated in Figure 7, and the set of all equivalence classes (including the empty measured foliation \emptyset) is denoted $\mathcal{MF} = \mathcal{MF}(F)$, where the class of (\mathcal{F}, μ) is denoted $[\mathcal{F}, \mu]$. To naturally topologize \mathcal{MF} , we introduce the discrete set $\mathcal{S} = \mathcal{S}(F)$ consisting of all free homotopy classes $[c]$ of simple closed curves c in F which are neither null homotopic nor puncture-parallel. We shall also require the set $\mathcal{S}' = \mathcal{S}'(F)$ consisting of homotopy classes of all disjointly embedded families of curves in F , where each component of the family lies in \mathcal{S} and no two components are homotopic.

One can show [36] that for any $[c] \in \mathcal{S}$, there is a representative $c_{\mathcal{F}} \in [c]$ which minimizes the μ -transverse measure in its homotopy class; furthermore, given equivalent measured foliations (\mathcal{F}_i, μ_i) , for $i = 1, 2$, we have $\mu_1(c_{\mathcal{F}_1}) = \mu_2(c_{\mathcal{F}_2})$ [36], and hence there is a well-defined mapping

$$J : \mathcal{MF} \rightarrow \mathbb{R}_{\geq 0}^{\mathcal{S}}$$

$$(\mathcal{F}, \mu) \mapsto \left(i_{(\mathcal{F}, \mu)} : [c] \mapsto \mu(c_{\mathcal{F}}) \right),$$

where the empty measured foliation \emptyset is identified with $\vec{0} = \{0\}^{\mathcal{S}}$. This mapping J is an injection [36] and induces a topology on \mathcal{MF} (where a neighborhood of \emptyset is homeomorphic to a cone from \emptyset over $\mathcal{MF}/\mathbb{R}_{>0}$, with the natural action by homothety of $\mathbb{R}_{>0}$ on measures). The function $i_{(\mathcal{F}, \mu)}$ is called the *(geometric) intersection function* of the measured foliation (\mathcal{F}, μ) .

Given $[c] \in \mathcal{S}$, there is a corresponding measured foliation defined as follows. Choose a representative c of $[c]$ and collapse $F - c$ onto a spine (making further choices) to build a foliation \mathcal{F}_c of F , whose leaves either lie in the spine or are homotopic to c , and choose a transverse measure μ_c on \mathcal{F}_c that pulls back under the collapsing map the counting measure δ_c on c . It is a classical fact due to Whitehead [36] that the resulting Whitehead equivalence class $[\mathcal{F}_c, \mu_c]$ is well-defined independent of any choices. Taking the projective class of this foliation, we may thus regard

$$\mathcal{S} \subseteq \mathcal{PF}_0.$$

Furthermore by construction, $i_{[\mathcal{F}_c, \mu_c]}([d])$, for $[d] \in \mathcal{S}$, is just the geometric intersection number of $[c]$ and $[d]$, i.e., the total number of intersections of representatives c with d ,

where c and d intersect minimally. More generally, given a family of curves c_1, \dots, c_n representing a point of \mathcal{S}' , together with a collection $w_1, \dots, w_n \in \mathbb{R}_{>0}$ of “weights”, we may again collapse to a spine of $F - \cup\{c_i\}_1^n$ to produce a foliation \mathcal{F} and choose a measure μ on \mathcal{F} that pulls back the weighted sum $\sum_1^n w_i \delta_{c_i}$ to get a well-defined Whitehead equivalence class $[\mathcal{F}, \mu]$. As mentioned before, one may thus associate a measured foliation to a weighted curve family.

Of special interest is the subspace $\mathcal{MF}_0 = \mathcal{MF}_0(F)$ consisting of all measured foliations (\mathcal{F}, μ) of compact support, i.e., any leaf of \mathcal{F} with a transverse arc a so that $\mu(a) > 0$ must be disjoint from a neighborhood of the punctures and no such leaf is puncture parallel. There is a natural $\mathbb{R}_{>0}$ -action on $\mathcal{MF} - \{\emptyset\}$ and $\mathcal{MF}_0 - \{\emptyset\}$ given by scaling the transverse measure, and the corresponding quotients

$$\mathcal{PF} = \mathcal{PF}(F) = (\mathcal{MF}(F) - \{\emptyset\})/\mathbb{R}_{>0},$$

$$\mathcal{PF}_0 = \mathcal{PF}_0(F) = (\mathcal{MF}_0(F) - \{\emptyset\})/\mathbb{R}_{>0}$$

are the spaces of central interest in the sequel. The projective class of (\mathcal{F}, μ) and $[\mathcal{F}, \mu]$, respectively, will be denoted $(\mathcal{F}, \bar{\mu})$ and $[\mathcal{F}, \bar{\mu}]$.

A point of $\mathcal{T} = \mathcal{T}(F_g^s) = \mathcal{T}_g^s$ may be regarded as the class of a hyperbolic metric on F , i.e., a complete finite-area Riemannian metric on F of constant Gauss curvature -1 . We shall also require the “Yamabe space” $\mathcal{Y} = \mathcal{Y}(F)$ of all complete finite-area Riemannian metrics on F of constant Gauss curvature $-x^2$, for some $x \in \mathbb{R}_{>0}$. \mathcal{Y} is canonically homeomorphic to $\mathcal{T}_g^s \times \mathbb{R}_{>0}$, where (ρ, x) corresponds to the class of the metric $x\rho$, and we let $\pi : \mathcal{Y} \rightarrow \mathcal{T}$ denote the projection onto the first factor. Define the map

$$\begin{aligned} I : \mathcal{Y} &\rightarrow \mathbb{R}_{\geq 0}^s \\ \rho &\mapsto \ell_\rho(\cdot), \end{aligned}$$

where $\ell_\rho([c])$ is the ρ -length of the unique ρ -geodesic in the homotopy class $[c]$. Thus, if $\rho \in \mathcal{Y}$ corresponds to $(\pi(\rho), x)$, then $I(\rho) = I(\pi(\rho), x) = x I(\pi(\rho), 1)$.

The basic facts [36] are that $I : \mathcal{Y} \rightarrow \mathbb{R}_{\geq 0}^s$ and $J : \mathcal{MF}_0(F) \rightarrow \mathbb{R}_{\geq 0}^s$ are embeddings with disjoint images, and we may define a completion $\bar{\mathcal{Y}}$ of \mathcal{Y} in $\mathbb{R}_{\geq 0}^s$ by setting

$$\bar{\mathcal{Y}} = I(\mathcal{Y}) \cup J(\mathcal{MF}_0)$$

and identifying \mathcal{Y} with $I(\mathcal{Y})$. Passing to quotients under the homothetic actions of $\mathbb{R}_{>0}$ on $\mathbb{R}_{\geq 0}^s - \{\vec{0}\}$, on $\mathcal{Y} - \{\vec{0}\}$, and on $\mathcal{MF}_0 - \{\emptyset\}$, we obtain Thurston’s compactification

$$\bar{\mathcal{T}}_g^s = (\mathcal{T}_g^s \cup \mathcal{PF}_0) \approx (\bar{\mathcal{Y}} - \{\vec{0}\})/\mathbb{R}_{>0}$$

of $\mathcal{T} \approx (\mathcal{Y} - \{\vec{0}\})/\mathbb{R}_{>0}$ by $\mathcal{PF}_0 \approx (\mathcal{MF}_0 - \{\emptyset\})/\mathbb{R}_{>0}$.

Theorem 4.1 1. [15],[36],[32] $\mathcal{PF}_0(F_g^s)$ is naturally a piecewise linear sphere of dimension $6g - 7 + 2s$ which compactifies \mathcal{T}_g^s to produce a closed ball $\bar{\mathcal{T}}_g^s$.

2. [15],[8] The action of the mapping class group MC_g^s on \mathcal{T}_g^s extends continuously to an action on $\bar{\mathcal{T}}_g^s$, where the action on $\mathcal{PF}_0(F_g^s)$ is the natural one, and there are explicit piecewise linear formulas for the action of Dehn twist generators.

3. [15],[36] Suppose that a sequence of hyperbolic metrics ρ_i on F tends to a point $[\mathcal{F}, \bar{\mu}] \in \mathcal{PF}_0$. In the projectivization of $\mathbb{R}_{\geq 0}^S - \{\bar{0}\}$, the projectivized length functions $\bar{\ell}_{\rho_i}$ of ρ_i converge to the projectivized intersection function $\bar{i}_{(\mathcal{F}, \bar{\mu})}$ of $(\mathcal{F}, \bar{\mu})$.

4. [15],[17] The function $i_{(\mathcal{F}, \mu)} : \mathcal{S} \rightarrow \mathbb{R}_{\geq 0}$ extends continuously to the “geometric intersection pairing” $\mathcal{MF}_0 \times \mathcal{MF}_0 \rightarrow \mathbb{R}_{\geq 0}$, that vanishes on the diagonal and which is also invariant under MC_g^s .

5. [15],[34],[19] The Weil–Petersson Kähler two-form on \mathcal{T}_g^s continuously extends (in the appropriate sense on Yamabe space) to a non-degenerate symplectic form, called “Thurston’s symplectic form”, on $\mathcal{MF}_0(F_g^s) (\approx \bar{\mathcal{Y}} - \mathcal{Y})$, which is invariant under MC_g^s .

Though there is all this beautiful natural structure on Thurston’s boundary, the quotient $\mathcal{PF}_0(F_g^s)/MC_g^s$ is maximally non-Hausdorff (i.e., its largest Hausdorff quotient is a singleton) as we shall see, so there is no correspondingly nice Thurston compactification on the level of Riemann’s moduli space.

Torus Example Recall that for the once-punctured torus $F = F_1^1$, the Teichmüller space is $\mathcal{T}_1^1 \approx \{z \in \mathbb{C} : |z| < 1\}$, and the mapping class group is $MC_g^s \approx PSL_2(\mathbb{Z})$. Indeed, the right Dehn twists M and L on the meridian and longitude, respectively, generate MC_1^1 , and a complete list of relations between them is given by $\iota = MLM = LML$ and $\iota^2 = 1$.

A point of $\mathcal{PF}_0(F)$ is uniquely determined by its “slope”, defined as follows. Fix two disjointly embedded ideal arcs x, y asymptotic to the puncture p which decompose F into an ideal quadrilateral, where $x \cup \{p\}$ is homotopic to the meridian, and $y \cup \{p\}$ is homotopic to the longitude. Given $[\mathcal{F}, \mu] \in \mathcal{MF}_0(F_1^1) - \{\emptyset\}$, compact support guarantees that $i_{[\mathcal{F}, \mu]}(x)$ and $i_{[\mathcal{F}, \mu]}(y)$ are well-defined and finite, and the ratio $|\theta| = i_{[\mathcal{F}, \mu]}(y)/i_{[\mathcal{F}, \mu]}(x) \in [0, \infty]$ is therefore projectively well-defined; we further imbue θ with a sign (when it is finite and non-zero) in the natural way, where the sign is positive if one (in fact, any) leaf of \mathcal{F} immediately after meeting x then meets the copy of y in the frontier of the ideal quadrilateral which lies to the right (where the orientation of the ideal quadrilateral is inherited from that of F_1^1). It is easy to see that the slope θ is a well-defined and complete invariant of $[\mathcal{F}, \bar{\mu}] \in \mathcal{PF}_0(F_1^1)$, where we regard $\theta \in S^1$ in the natural way. Thus, $\mathcal{PF}_0(F_1^1) \approx S^1$, and $\bar{\mathcal{T}}_1^1 = \mathcal{T}_1^1 \cup \mathcal{PF}_0(F_1^1)$ is a closed ball (which you should *not* identify with the Poincaré disk together with its circle at infinity). The slope $\theta = p/q$ is rational if and only if the measured foliation corresponds to the simple closed curve wrapping p times around the meridian and q times around the longitude, where p and q are relatively prime integers. Geometrically, deforming hyperbolic structure to pinch this curve, it is clear from elementary considerations of hyperbolic geometry that the corresponding geodesic length functions converge projectively to the geometric intersection number with this curve. Furthermore, the geometric intersection number of curves with slopes $p/q, r/s$ written in least terms is given by $|ps - qr|$.

4.2 Train tracks

A *train track* $\tau \subseteq F$ is a graph (where vertices are called “switches” and edges are called “branches”) together with the following extra structure:

Smoothness: τ is C^1 away from its switches. Furthermore, for each switch v of τ , there is a tangent line ℓ to τ at v in the tangent plane to F at v so that for each half-branch whose closure contains v , the one-sided tangent at v lies in ℓ ;

Non-degeneracy: Vertices of τ are at least trivalent, and for any switch v of τ , there is an embedding $(0, 1) \rightarrow F$ with $f(\frac{1}{2}) = v$ which is C^1 as a map into F ;

Geometry: Suppose that C is a component of $F - \tau$, and let $D(C)$ denote the double of C along the C^1 frontier edges of C so the non-smooth points in the frontier of C give rise to punctures of $D(C)$. We demand that the Euler characteristic of $D(C)$ be negative.

The smoothness condition is synonymously called the structure of a “branched one-submanifold” and leads to the fundamental notion of a graph smoothly supporting a curve or another train track as we shall see. According to the non-degeneracy condition, the half-branches incident on a fixed switch decompose canonically into two non-empty sets of “incoming” and “outgoing” branches. The geometric condition rules out the following complementary regions: smooth disks (i.e., nullgons), monogons, bigons, smooth annuli, and once-punctured nullgons, and will be further explained below.

Let $B(\tau)$ denote the set of branches of τ . A function $\mu : B(\tau) \rightarrow \mathbb{R}_{\geq 0}$ induces $\mu : \{\text{half-branches of } \tau\} \rightarrow \mathbb{R}_{\geq 0}$ in the natural way (where $\mu(b_{\frac{1}{2}}) = \mu(b)$ if $b_{\frac{1}{2}} \subseteq b$) and satisfies the *switch conditions* provided that for each switch v of τ , we have

$$\sum_{\substack{\text{outgoing} \\ \text{half-branches } b}} \mu(b) = \sum_{\substack{\text{incoming} \\ \text{half-branches } b}} \mu(b).$$

Such a function satisfying the switch conditions is called a (*transverse*) *measure* on τ , and τ itself is said to be *recurrent* if it supports a *positive* measure μ with $\mu(b) > 0$ for each branch of τ . In the sequel, train tracks will tacitly be assumed to be recurrent.

Torus Example There is a unique combinatorial type of recurrent trivalent train track τ in the surface $F = F_1^1$, and two embeddings of it as spine are illustrated in Figure 8. $F - \tau$ consists of a single once-punctured bigon. There are two branches of τ so that μ is uniquely determined by its values on these branches, and the weight on the remaining branch of τ is given by their sum according to the switch condition. Notice that this train track is “orientable” in the sense that the graph underlying τ admits an orientation where incoming points toward outgoing at each vertex. Thus, fixing an orientation on τ , a measure μ on τ uniquely determines a homology class in $H_1(F_1^1, \mathbb{R})$. Equivalently, every measured foliation of compact support on F_1^1 is transversely orientable.

Construction 4.1 Given a train track τ and a positive measure μ on it, we may construct a measured foliation of a neighborhood of τ in the following way. For each branch b of

τ , take a rectangle of width $\mu(b)$ and length unity foliated by horizontal leaves. For each switch, place the rectangles of the incoming branches next to one another and likewise for the outgoing branches, and then finally glue the vertical edges of all the incoming to all the outgoing rectangles at each switch in the natural way preserving the transverse measure along the widths of the rectangles by the switch conditions. This produces from μ a measured foliation of a *tie neighborhood* of τ , where a vertical leaf in any rectangle is called a *tie*, and the *singular ties* arise from the vertical sides of the rectangles. As before by Whitehead's result, the Whitehead equivalence class of the resulting measured foliation is well-defined.

If a measured foliation arises in this way from a measure on a train track, then we say that the train track *carries* the measured foliation.

Let $U(\tau)$ denote the cone of all measures on τ , i.e., the subspace of $\mathbb{R}_{\geq 0}^{B(\tau)}$ determined by the switch conditions. There is again the natural $\mathbb{R}_{>0}$ -action on $U(\tau) - \{\vec{0}\}$ by homothety, and the quotient $V(\tau) = (U(\tau) - \{\vec{0}\})/\mathbb{R}_{>0}$ is the *polygon of projective measures* on τ . Construction 4.1 thus gives well-defined maps $U(\tau) \rightarrow \mathcal{MF}_0(F)$ and $V(\tau) \rightarrow \mathcal{PF}_0(F)$.

A recurrent train track is *maximal* if it is not a proper sub track of any recurrent train track. For general $F = F_g^s$, complementary regions to a maximal train track are either trigons or once-punctured monogons, but in the special case of the once-punctured torus, a maximal train track has a single complementary once-punctured bigon.

Theorem 4.2 [15],[32] *For any maximal recurrent train track τ in F , Construction 4.1 determines continuous embeddings*

$$U(\tau) \rightarrow \mathcal{MF}_0(F) \quad \text{and} \quad V(\tau) \rightarrow \mathcal{PF}_0(F)$$

onto open sets.

In fact, the geometric condition in the definition of train track precisely guarantees the injectivity in this theorem. In light of this result, one may regard a maximal train track in F as indexing a chart on the manifold \mathcal{PF}_0 , and we next study the transition functions of this putative manifold structure.

Torus Example For $F = F_1^1$, two embeddings of train tracks as spine are illustrated in Figure 8, and in fact, every foliation is carried by one of these two train tracks. The corresponding charts on the circle are also illustrated as well as the two points of intersection in the closures of these charts.

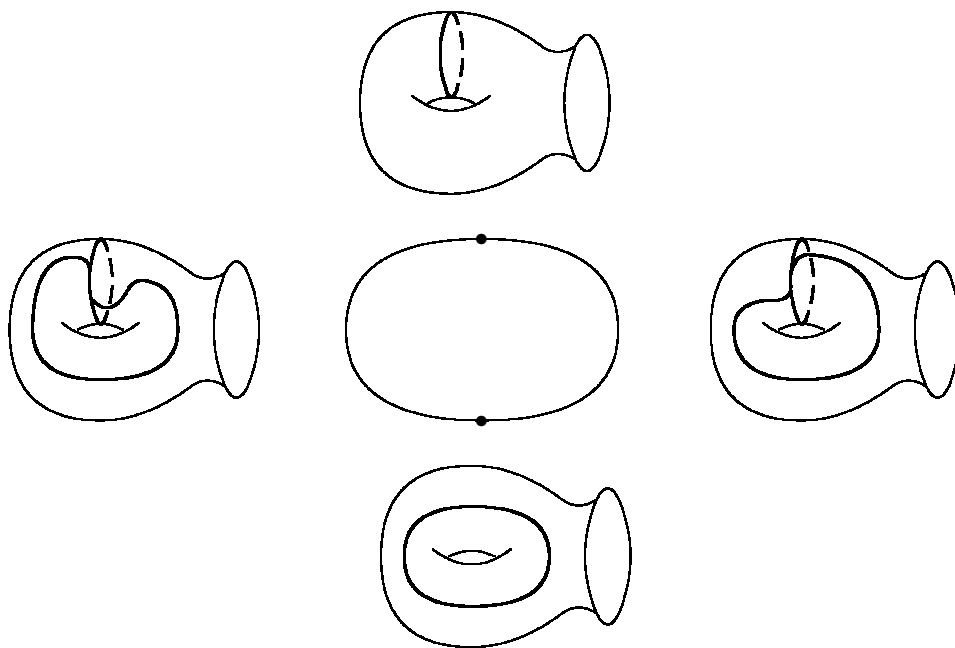


Figure 8-charts for torus

It is most convenient now to restrict to the “generic” case, where all switches of τ are trivalent. For each switch of τ , the decomposition of incident half-branches into incoming/outgoing thus consists of one singleton and one doubleton, and we say a branch of τ is *large* if it is a singleton at both its endpoints (which are then necessarily distinct) as illustrated with the branch labeled e in the left-hand side of Figure 9. Likewise, if a branch is a doubleton at both its endpoints, then it is called *small*, while a branch which is neither small nor large is called *half-large*.

Define the combinatorial *splitting* of a measured train track (τ, μ) along a large branch e as illustrated in Figure 9, where we identify an edge with its μ transverse measure $\mu(e)$ for convenience. One imagines separating bands of horizontal leaves in the rectangle associated to e by excavating along the two “singular leaves” beginning at the endpoints of the large branch, i.e., beginning at the singular ties. If the measure μ is so that (either of) the singular leaves starting at an endpoint of e turn left or right, then the respective split is called a *left* (case 1) or *right* (case 3) split, while if the two singular leaves coincide for e , then the split is called a *collision* (case 2).

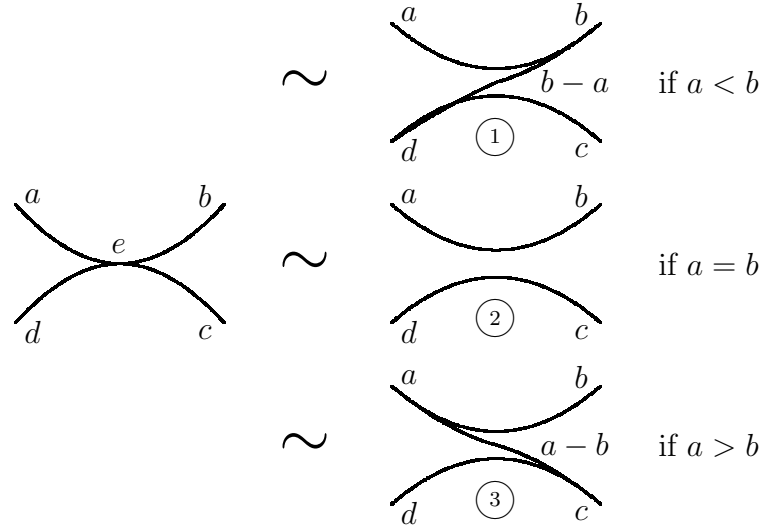


Figure 9-splitting

Splitting and smooth isotopy of measured train tracks generates an equivalence relation on the set of all measured train tracks in F , and we shall let $[\tau, \mu]$ denote the equivalence class of the measured train track (τ, μ) and $[\tau, \bar{\mu}]$ denote the equivalence class of the projectively measured train track $(\tau, \bar{\mu})$.

Theorem 4.3 [32] *If (τ_i, μ_i) are positively measured train tracks giving rise to corresponding measured foliations (\mathcal{F}_i, μ_i) via Construction 4.1, for $i = 1, 2$, then*

$$[\mathcal{F}_1, \mu_1] = [\mathcal{F}_2, \mu_2] \text{ if and only if } [\tau_1, \mu_1] = [\tau_2, \mu_2].$$

Thus, the space of all Whitehead equivalence classes of (projectivized) measured foliations is identified with the space of all splitting equivalence classes of (projectivized) measured train tracks up to isotopy.

There is another aspect to the splitting equivalence relation on the set of all measured train tracks. In addition to splitting, one considers also *shifting* along a half-large branch by pushing two confluent branches of a train track past one another as illustrated in Figure 10. Shifting plays a role in the later discussion, and a basic result in train track theory [32] is that if two train tracks are related by shifting, splitting, and smooth isotopy, then they are also related by splitting and smooth isotopy alone.

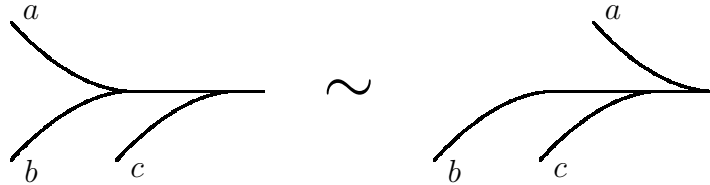


Figure 10-shifting

Let us finally give the idea of the proof that \mathcal{S} is dense in \mathcal{MF}_0 , as was mentioned before, by explaining density of \mathcal{S} in each chart $V(\tau) \subseteq \mathcal{PF}_0$, for some maximal train track $\tau \subseteq F$. We may approximate any $\mu \in V(\tau) \subseteq (\mathbb{R}_{\geq 0}^{B(\tau)} - \{\vec{0}\})/\mathbb{R}_{>0}$ by a rational measure $\mu' \in (\mathbb{Q}_{\geq 0}^{B(\tau)} - \{\vec{0}\})/\mathbb{R}_{>0}$ (satisfying the switch conditions). Furthermore clearing denominators in μ' , there are $N \in \mathbb{Z}_{>0}$ and $\nu \in (\mathbb{Z}_{\geq 0}^{B(\tau)} - \{\vec{0}\})/\mathbb{R}_{>0}$ so that $N\mu' = \nu$.

We may construct an embedded family of curves in F from ν by arranging $\nu(b) \geq 0$ tie-transverse strands parallel to b in a tie neighborhood of τ . By the switch conditions, there are at each vertex exactly as many incoming strands as outgoing, and there is a unique way to combine strands near vertices to produce a disjointly embedded family of curves. Let us give each component curve a weight $1/N$ and combine any parallel curves while adding their weights to produce our desired weighted family of disjointly embedded curves. Let $[\mathcal{F}, \mu_1]$ denote the corresponding measured foliation (discussed before); tracing through the constructions, one finds that $[\tau, \mu'] = 1/N[\tau, \nu]$ gives rise to $[\mathcal{F}, \mu_1]$. Letting $\mu' \rightarrow \mu$ and projectivizing, it follows easily that families of disjointly embedded curves are dense in $V(\tau)$. With a little more work [32], one can approximate (in the topology of $V(\tau)$) such disjointly embedded families with a single curve, and this gives the asserted density of \mathcal{S} itself.

Thus, Thurston's boundary $\mathcal{PF}_0(F)$ is a completion of the set \mathcal{S} . In fact, one can approximate with a single non-separating curve (provided $g \neq 0$); since any two such curves are equivalent under the action of MC_g^s , it follows that the action of MC_g^s on $\mathcal{PF}_0(F)$ has a dense orbit, and the maximal non-Hausdorffness of the quotient, which was mentioned before, is thereby established.

4.3 Laminations

Each basic formulation of the objects presented so far, namely, measured foliations and measured train tracks, requires passage to the quotient under an appropriate equivalence relation. Thurston has given a more ethereal, elemental, and elegant description of these objects as "measured geodesic laminations", where no passage to equivalence classes is necessary. Here we simply give the definition and a few basic properties referring the reader to [32] for instance for further details. A "lamination" \mathcal{L} in F is a foliation of a closed subset of F , and a "(transverse) measure" to \mathcal{L} is defined much as before as a σ -additive measure on arcs transverse to \mathcal{L} with the analogous condition of no-holonomy (where the homotopy is through arcs transverse to \mathcal{L} with endpoints disjoint from \mathcal{L}). \mathcal{L} is a "geodesic lamination" if its leaves are geodesic for some specified hyperbolic metric. The simplest case of a geodesic lamination is the geodesic representative of an element of $\mathcal{S}'(F)$. (In fact, for different choices of metric, the spaces of measured geodesic laminations are naturally identified via the circle at infinity in their universal covers, so we may speak of a geodesic lamination without the *a priori* specification of a metric.) A measured geodesic lamination has zero measure in F , and the intersection of a measured geodesic lamination \mathcal{L} with a transverse arc a in F is a Cantor set together with isolated points corresponding to intersections with simple geodesic curve components or arc components of \mathcal{L} , if any. There is a natural topology on the set of all measured geodesic laminations in F , which is induced by the weak topology on the set of all $\pi_1(F)$ -invariant measures supported on the Möbius band past infinity. $\mathcal{ML}(F)$ (and $\mathcal{ML}_0(F)$) is the corresponding space of measured geodesic laminations (and with compact support) and corresponding projectivization $\mathcal{PL}(F)$ (and $\mathcal{PL}_0(F)$). A basic result in Thurston theory is $\mathcal{ML}(F) \approx \mathcal{MF}(F)$, $\mathcal{ML}_0(F) \approx \mathcal{MF}_0(F)$, $\mathcal{PL}(F) \approx \mathcal{PF}(F)$, $\mathcal{PL}_0(F) \approx \mathcal{PF}_0(F)$, where train tracks give suitable charts on any of these piecewise linear manifolds. Furthermore,

the deformation theory due to Thurston, called “earthquaking” cf. [38], which we do not further discuss here, is most conveniently expressed in the context of laminations.

4.4 Dynamics on train tracks

In this section, we simply recall Thurston’s classification of surface automorphisms as well as recall several basic facts about “pseudo-Anosov” mappings. In the process, we develop further basic techniques which will be required in quantization. Since Thurston’s compactification produces a closed ball upon which the mapping class group acts continuously, one immediately is led to consider fixed points of this action.

Theorem 4.4 Thurston’s Classification [15],[36] *Any orientation-preserving homeomorphism $f : F \rightarrow F$ is homotopic to a diffeomorphism $f' : F \rightarrow F$ which satisfies one of the following conditions (and the only overlap is between 1. and 2.):*

1. f' fixes a unique point of \mathcal{T} and is of finite order;
2. f' is “reducible” in the sense that f' fixes an element of \mathcal{S}' ;
3. f' is “pseudo-Anosov” in the sense that there is some $\lambda > 1$ together with two measured foliations $(\mathcal{F}_\pm, \mu_\pm)$, which share singular points and are otherwise transverse, so that $f'(\mathcal{F}_\pm, \mu_\pm) = \lambda^{\pm 1} (\mathcal{F}_\pm, \mu_\pm)$. The projective classes $[\mathcal{F}_\pm, \bar{\mu}_\pm]$ are the unique fixed points of f on $\overline{\mathcal{T}}$. The invariant λ is called the dilatation of f or f' .

Notice the similarity with the trichotomy elliptic/parabolic/hyperbolic for fractional linear transformations. In the reducible case, one simplifies the dynamics by cutting F along a representative of the invariant element of \mathcal{S}' . A pseudo-Anosov mapping is the analogue of an Anosov map of the torus in the current context of surfaces with negative Euler characteristic.

In fact, train tracks provide a powerful tool for analyzing the dynamics of surface automorphisms owing to the fact that since a train track has a well-defined tangent line at each point, there is a coherent notion of a train track smoothly “carrying” a curve, another train track, or a lamination.

Suppose that κ is a smooth curve, a train track, or a measured geodesic lamination. We say that the train track τ carries κ and write $\kappa < \tau$, if there is a C^1 map $\phi : F \rightarrow F$ homotopic to the identity, called the supporting map, so that $\phi(\kappa) \subseteq \tau$, where the restriction of the differential $d\phi_p$ to the tangent line to κ at p is non-zero for every $p \in \kappa$.

We think of ϕ as squashing together nearly parallel strands of κ . For instance, any curve arising as before from an integral measure on τ is carried by τ , and more generally, any curve, train track or lamination κ which lies in a tie-neighborhood of τ and is transverse to the ties satisfies $\kappa < \tau$, where the supporting map collapses ties.

For example, if a train track σ arises from τ by splitting and shifting (but no collapsing), then $\sigma < \tau$, and we say that σ arises from τ by unzipping.

Suppose that the train track σ is transverse to a tie-neighborhood of τ , say with supporting map $\phi : F \rightarrow F$. Let us enumerate the branches b_j of τ , for $j = 1, \dots, n$, and a_i of σ , for $i = 1, \dots, m$, and choose $x_j \in b_j$ for each j . There is then an $m \times n$ -matrix

$A = (A_{ij})$ called the *incidence matrix*, where A_{ij} is the cardinality of $\phi^{-1}(x_j) \cap a_i$. It is clear that the incidence matrix $A : \mathbb{R}_{\geq 0}^n \rightarrow \mathbb{R}_{\geq 0}^n$ describes the inclusion $U(\sigma) \rightarrow U(\tau)$ in the train track coordinates.

We close this section with several basic results about pseudo-Anosov mappings.

Theorem 4.5 [15],[33] *A homeomorphism $f : F \rightarrow F$ is a pseudo-Anosov map if and only if there is a train track τ in F , with each component of $F - \tau$ an at most once punctured polygon, so that τ unzips to $f(\tau)$ with no collisions. Furthermore, the incidence matrix A of the carrying $f(\tau) < \tau$ is Perron–Frobenius, the eigenvector of A corresponding to the spectral radius λ gives the projective measure $\bar{\mu}_+$, and likewise the extreme eigenvector of the transpose of A gives $\bar{\mu}_-$.*

Given a measured train track (τ, μ) , consider the foliated neighborhood of τ determined by μ via Construction 4.1. Choose some enumeration of the switches of τ and serially follow the singular leaves from the switches until the first splitting (ignoring shifting), for the first switch, second switch, \dots , last switch, and then begin anew from the first switch. Suppose there are no collisions, and record the resulting sequence of right or left splits, so as to produce a semi-infinite word of rights and lefts.

Theorem 4.6 [33] *The right-left sequence is eventually periodic if and only if the corresponding measured foliation is fixed by some pseudo-Anosov mapping.*

An explicit and simple construction of pseudo-Anosov maps is given by the following result.

Theorem 4.7 [11] *Suppose that $\mathcal{C}, \mathcal{D} \in \mathcal{S}'$ admit representative arc families C, D intersecting minimally which satisfy the condition that each component of $F - \cup(C \cup D)$ is an at most once-punctured polygon. Take any composition w of Dehn twists to the right along elements of \mathcal{C} and to the left along elements of \mathcal{D} so that the Dehn twist along each element of \mathcal{C} or \mathcal{D} occurs at least once in w . Then w is pseudo-Anosov.*

Torus Example Consider a generic train track τ in F_1^1 , so τ has one large branch e and two small branches. The two small branches are canonically linearly ordered by first taking the branch a to the right and then the branch b to the left at either endpoint of e , and furthermore $U(\tau) \approx \mathbb{R}_{\geq 0}^{\{a,b\}}$, i.e., the measures of the small branches a, b are unconstrained and uniquely determine the measure on e as well. Given a measure $\mu \in U(\tau) - \{\vec{0}\}$, start unzipping (τ, μ) along either singular leaf, i.e., split along e , to produce another measured train track (τ_1, μ_1) ; of course, τ_1 is combinatorially equivalent to τ . For definiteness, suppose that $B = \mu(b) > \mu(a) = A$, so the split is a left split. The edge corresponding to b is the large edge of τ_1 , and the two small edges, in right/left order, have measures $(A, B - A)$. Continue unzipping, i.e., next split (τ_1, μ_1) along its large edge to produce (τ_2, μ_2) . Again suppose that $B > 2A$ for definiteness, so the second split is a left split as well, and the small branches of τ_2 have measures $(A, B - 2A)$. Continue unzipping (under the assumption that there are no collisions) until the first right split, say there are $a_1 = \lfloor \frac{B}{A} \rfloor > 1$ left splits before the first right split. Perform the right split along the large branch

of (τ_{a_1}, μ_{a_1}) , where the measures on the small branches are $(A, B_1) = (A, B - m_1 A)$, to produce a train track whose small edges have measures $(A - B_1, B_1)$. Continue unzipping and suppose there are no collisions, i.e., suppose A and B are not rationally related, to produce a semi-infinite sequence of symbols L (for left splits) and R (for right splits). Let a_1 denote the number of L 's that begin this sequence, a_2 denote the length of the next consecutive sequence of R 's, a_3 the length of the next consecutive sequence of L 's, and so on. It follows from the discussion above that the continued fraction expansion of B/A is given by

$$B/A = a_1 + \frac{1}{a_2 + \frac{1}{a_3 + \dots}}$$

Continued fractions occur in another related guise as well. The isomorphism $MC_1^1 \approx PSL_2(\mathbb{Z})$ is induced by $M \mapsto \begin{pmatrix} 1 & 1 \\ 0 & 1 \end{pmatrix}$ and $L \mapsto \begin{pmatrix} 1 & 0 \\ -1 & 1 \end{pmatrix}$, where M and L are the right Dehn twists on the meridian and longitude respectively. A mapping class in MC_1^1 is pseudo-Anosov, reducible, periodic if and only if the corresponding fractional linear transformation is hyperbolic, parabolic, elliptic respectively. Every hyperbolic element of $PSL_2(\mathbb{Z})$ is conjugate to a product

$$\begin{pmatrix} 1 & m_1 \\ 0 & 1 \end{pmatrix} \begin{pmatrix} 1 & 0 \\ n_1 & 1 \end{pmatrix} \cdots \begin{pmatrix} 1 & m_k \\ 0 & 1 \end{pmatrix} \begin{pmatrix} 1 & 0 \\ n_k & 1 \end{pmatrix},$$

where $m_i, n_i > 0$ are unique up to cyclic permutation. Furthermore, $m_1, n_1, \dots, m_k, n_k$ are the partial quotients of the periodic continued fraction expansion of the dilatation of the corresponding pseudo-Anosov map. It follows from this discussion that in MC_1^1 , all pseudo-Anosov mappings arise from the previous theorem. Indeed, the theorem gives the construction of two semi-groups corresponding to right/left or left/right twisting on meridian/longitude. For each semi-group, it is easy to construct a train track τ in F_1^1 so that the matrix representation above precisely describes the action of the corresponding semi-group on the measures of the linearly ordered small branches of τ ; indeed, these two train tracks are illustrated in Figure 8.

4.5 Decorated measured foliations and freeways

In this section, we recall material from [34] which is required for quantization. If $\Gamma \subseteq F$ is a cubic fatgraph spine of F , then we may blow-up each vertex of Γ into a little trigon as illustrated in Figure 11. The resulting object $\tau = \tau_\Gamma$ has both a natural branched one-submanifold structure and a fattening, and furthermore, components of $F - \tau$ are either little trigons or once-punctured nullgons. Thus, τ is not a train track, but it is almost a train track, and is called the *freeway* associated to Γ . Notice that each edge of Γ gives rise to a corresponding large branch of τ , and each vertex gives rise to three small

branches. It is easy to see that every measured lamination of compact support in F is carried by the freeway τ . The frontier of a once-punctured nullgon component of $F - \tau$ is a puncture-parallel curve called a *collar curve* of F . A small branch is contained in exactly one collar curve, while a large branch may be contained in either one or two collar curves.

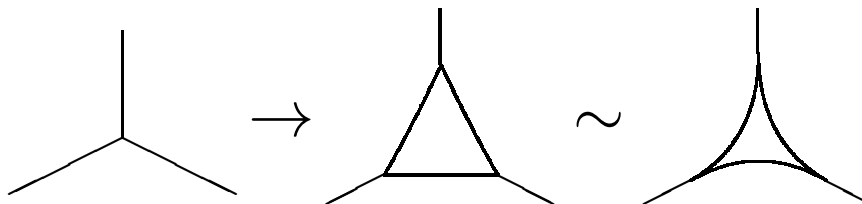


Figure 11—freeway from fatgraph

A *measure* on a freeway τ is a function $\mu \in \mathbb{R}^{B(\tau)}$ satisfying the switch conditions, where we wish to emphasize that the measure is not necessarily nonnegative (as it is for train tracks). Let $U(\tau)$ denote the vector space of all measures on τ . Notice that $\mu \in U(\tau)$ is uniquely determined by its values on the small branches alone, and the switch conditions are equivalent to the following “coupling equations”

$$\mu(a_1) + \mu(b_1) = \mu(e) = \mu(a_2) + \mu(b_2),$$

for any large branch e whose closure contains the switches $v_1 \neq v_2$, where a_i, b_i are the small branches incident on v_i for $i = 1, 2$. On the other hand, the values on the large branches alone also uniquely determine μ , and in fact, these values are unconstrained by the switch conditions. Indeed, letting a_i denote the large branches incident on a little trigon with opposite small branches α_i , for $i = 1, 2, 3$, we may uniquely solve for a measure μ on τ , where

$$\mu(\alpha_i) = \frac{1}{2}\{\mu(a_1) + \mu(a_2) + \mu(a_3) - 2\mu(a_i)\}, \text{ for } i = 1, 2, 3,$$

and so we identify $U(\tau) \approx \mathbb{R}^{LB(\tau)}$, where $LB(\tau)$ denotes the set of large branches of τ .

In particular, if μ is a nonnegative measure on τ , then the analogue of Construction 4.1 in the current context produces a well defined equivalence class of measured foliations in F , where this measured foliation will typically contain a collection of puncture-parallel annuli foliated by curves homotopic to collar curves. Deleting these foliated annuli produces a well-defined (but possibly empty) class in $\mathcal{MF}_0(F)$. Thus, a nonnegative measure on τ canonically determines a point of $\mathcal{MF}_0(F)$ together with a nonnegative “collar weight”, i.e., the transverse measure of a transverse arc connecting the boundary components of the corresponding foliated annulus.

In the general case that μ is not necessarily nonnegative, suppose that C is a collar curve of τ . The switches of τ decompose C into a collection of arcs, each of which inherits a corresponding real-valued weight from μ . Let $\{\gamma_i\}_1^n$ denote the collection of real numbers associated to the small branches of τ that occur in C . Define the *collar weight* of C for μ to be $\mu_C = \min\{\gamma_i\}_1^n$. Define a *collar weight* on F itself to be the assignment of such a weight to each puncture.

We may modify the original measure $\mu \in U(\tau)$ by defining $\mu'(b) = \mu(b) - \mu_C$ if b is contained in the collar curve C for any small branch b of τ . Thus, μ' is a nonnegative measure on μ with identically vanishing collar weights that determines a corresponding element of $\mathcal{MF}_0(F)$.

We are led to define the space $\widetilde{\mathcal{MF}}_0(F) = \mathcal{MF}_0(F) \times \mathbb{R}^s$ of *decorated measured foliations* and summarize the previous discussion:

Theorem 4.8 [34] *The space $U(\tau) \approx \mathbb{R}^{LB(\tau)}$ gives global coordinates on $\widetilde{\mathcal{MF}}_0$, and there is a canonical fiber bundle $\Pi : \widetilde{\mathcal{MF}}_0 \rightarrow \mathcal{MF}_0$, where the fiber over a point is the set \mathbb{R}^s of all collar weights on F .*

Remark 4.1 The natural action of MC_g^s is by bundle isomorphisms of Π . Furthermore, Π admits a natural MC_g^s -invariant section $\sigma : \mathcal{MF}_0 \rightarrow \widetilde{\mathcal{MF}}_0$ which is determined by the condition of identically vanishing collar weights. The restriction of σ to $\mathcal{MF}_0 \subseteq \widetilde{\mathcal{MF}}_0$ gives a piecewise-linear embedding of the piecewise-linear manifold \mathcal{MF}_0 into the linear manifold (vector space) $\widetilde{\mathcal{MF}}_0 \approx U(\tau) \approx \mathbb{R}^{LB(\tau)}$.

4.6 Shear coordinates for measured foliations

We now give an equivalent parametrization of measured foliations in terms of “Thurston’s shear coordinates” that are close analogues of Thurston’s shear coordinates Z_α on $\mathcal{T}_H(F)$. In fact, we have already encountered these quantities when describing the splitting procedure train tracks (see Figure 9). There, excavating along two different singular leaves, we have obtained the “new” edge, which can turn either left or right (for splittings) or be absent (for collisions).

We assign a corresponding signed quantity (positive for right, negative for left) as follows. Given a measure μ on the long branches of the freeway τ associated to the fatgraph spine $\Gamma \subseteq F$, define the (*Thurston’s foliation-*)*shear coordinate* of the edge indexed by α to be

$$\zeta_\alpha = \frac{1}{2}(\mu(A) - \mu(B) + \mu(C) - \mu(D)),$$

in the notation of Figure 1 for nearby branches. From the very definition, ζ_α is independent of collar weights. Again, Thurston’s foliation-shear coordinates are alternatively defined in terms of the signed transverse length of the arc between the singular leaves along Z_α , in analogy to the geometric interpretation given before of the shear coordinates on \mathcal{T}_H .

Note that the shear coordinates ζ_α are not independent. They are subject to the restrictions that

$$\sum_{\alpha \in I} \zeta_\alpha = 0 \tag{4.1}$$

for the sum over edges $\alpha \in I$ surrounding any given boundary component, and we shall refer to these conditions as the *face conditions* for shear coordinates. Thus, the space of foliation-shear coordinates is of dimension $LB(\tau) - n$, where we let n denote the number

of boundary components. One sees directly that for any assignment of shear coordinates, there is a well-defined point of \mathcal{MF}_0 realizing them, thereby establishing a homeomorphism between \mathcal{MF}_0 and this sub-vector space $\mathbb{R}^{LB(\tau)-n} \subseteq \mathbb{R}^{LB(\tau)}$ of shear coordinates on the long branches of τ .

To describe the action of the mapping class group on foliation-shear coordinates, we shall give the transformation under Whitehead moves, i.e., derive the analogue of formula (2.8) for measured foliations, which is an elementary calculation using the formulas for splitting as follows.

Lemma 4.9 *Under the Whitehead move in Figure 2, the corresponding foliation-shear coordinates of the edges A, B, C, D , and Z situated as in Figure 2 are transformed according to formula (2.8)*

$$M_Z : (\zeta_A, \zeta_B, \zeta_C, \zeta_D, \zeta_Z) \mapsto (\zeta_A + \phi_H(\zeta_Z), \zeta_B - \phi_H(-\zeta_Z), \zeta_C + \phi_H(\zeta_Z), \zeta_D - \phi_H(-\zeta_Z), -\zeta_Z)$$

with

$$\phi_H(\zeta_Z) = (\zeta_Z + |\zeta_Z|)/2, \tag{4.2}$$

i.e., $\phi_H(x) = x$, for $x > 0$, and zero otherwise. All other shear coordinates on the graph remain unchanged.

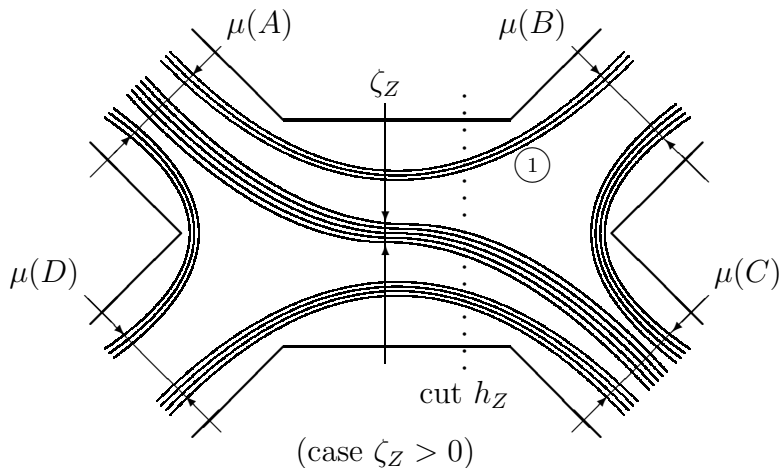


Figure 12-foliation-shear coordinates

Remark 4.2 Comparing expressions for the classical function $\phi(x) = \log(1 + e^x)$ and (4.2), one finds that the latter is a *projective limit* of the former:

$$\phi_H(x) = \lim_{\lambda \rightarrow +\infty} \frac{1}{\lambda} \phi(\lambda x) = \lim_{\lambda \rightarrow +\infty} \frac{1}{\lambda} \phi^h(\lambda x), \tag{4.3}$$

that is, all three transformations coincide asymptotically in the domain of large absolute values (or large eigenvalues for the corresponding operators) of Teichmüller space coordinates $\{Z_\alpha\}$. We shall actively use this property in Section 5.3.2 when proving the existence of the quantization of Thurston's boundary for the punctured torus.

5 On quantizing Thurston theory

5.1 Proper length of geodesics

Definition 5.1 The *proper length* $\text{p.l.}(\gamma)$ of a closed curve γ in the classical or quantum case is constructed from the quantum ordered operator P_γ associated to a closed oriented edge-path with basepoint (to begin the linearly ordered word P_γ) as

$$\text{p.l.}(\gamma) = \lim_{n \rightarrow \infty} \frac{1}{n} \text{tr} \log 2T_n(P_\gamma/2), \quad (5.1)$$

where we take the principal branch of the logarithm and T_n are Chebyshev's polynomials (cf. (3.20)). Since $T_n(\cosh \frac{t}{2}) = \cosh \frac{nt}{2}$, it follows that $\text{p.l.}(\gamma)$ agrees with half the hyperbolic length of γ in the Poincaré metric in the classical case.

More explicitly in the operatorial case, we can determine $\text{p.l.}(\gamma)$ explicitly in terms of the spectral expansion of the operator G_γ , which is known exactly. Namely, the basis of eigenfunctions of G_γ is “doubly reduced” in the sense that each eigenvalue (except 2, which is singular) with corresponding eigenfunction α_S , has the form $e^{S/2} + e^{-S/2}$, where S ranges over the entire real axis, and α_S has the same eigenvalue as α_{-S} . In fact, these functions coincide, so there is actually a representation on the positive real axis, which is nevertheless complete, and is singular at infinity and zero. We may define the proper length operator to be the one with the same eigenfunctions α_S for S positive (which constitute a basis in the function space) and with eigenvalues to be $|S/2|$. This operator $\text{p.l.}(\gamma)$ is then a well-defined operator on any compactum in function space.

The *proper length* of a QMC or GMC \hat{C} , again denoted $\text{p.l.}(\hat{C})$, is the sum of the proper lengths of the constituent geodesic length operators (or the sum of half geodesic lengths calculated in the Poincaré metric in the classical case) weighted by the number of appearances in the multiset.

5.2 Approximating laminations and the main theorem

Fix once and for all a spine Γ of F with corresponding freeway τ . A measure μ on τ gives rise to a (possibly empty) measured foliation in F together with a collar weight on the boundary components of F . Erasing collars yields an underlying measure $\mu_1 \geq 0$ on τ whose support is a sub-train track $\tau_1 \subseteq \tau$, and the measured train track (τ_1, μ_1) determines a (possibly empty) measured foliation. Via the canonical embedding of \mathcal{MF}_0 into $\widetilde{\mathcal{MF}}_0$ with vanishing collars, we may thus uniquely determine a point of \mathcal{MF}_0 by specifying foliation-shear coordinates on the long branches of τ satisfying the face conditions 4.1, i.e., \mathcal{MF}_0 is naturally identified with a codimension n subspace of $\mathbb{R}^{LB(\tau)}$. Passing to projective foliations, a point of \mathcal{PF}_0 is given by the projectivization $P\vec{\zeta}$ of a vector of foliation-shear coordinates $\vec{\zeta} = (\zeta_i)$, where $\vec{\zeta} \in \mathbb{R}^{LB(\tau)} - \{\vec{0}\}$, and i indexes the long branches of τ , i.e., the edges of Γ .

Definition 5.2 A sequence $\vec{n}^\beta = (n_i^\beta)$, for $\beta \geq 1$, of integer-valued n_i , for $i = 1, \dots, LB(\tau)$, on τ is an *approximating sequence* for the projectivized measured foliation $P\vec{\zeta}$ if the face conditions 4.1 hold on \vec{n}^β and if $\lim_{\beta \rightarrow \infty} n_i^\beta / n_j^\beta = \zeta_i / \zeta_j$ for all i, j with $\zeta_j \neq 0$.

Constructed from \vec{n} as an integral measure on τ is a GMC \hat{C} with integral collar weights. Just as with decorated measured foliations, components of \hat{C} which are puncture- or boundary-parallel can be erased to produce a corresponding multicurve to be denoted $\hat{C}_{\vec{n}}$. $\hat{C}_{\vec{n}}$ is carried by a sub-train track of τ , and it traverses the long branch of τ indexed by i some number, say, $m_i \geq 0$ of times, so m_i is the standard train track coordinate of integral transverse measure. In the usual notation as in Figure 12, one sees directly that $n_Z = \frac{1}{2}(m_A - m_B + m_C - m_D)$. We may also sometimes write $\hat{C}_{\vec{m}}$ for $\hat{C}_{\vec{n}}$

Definition 5.3 A *graph length* function with respect to the spine Γ is any linear function

$$\text{g.l.}_{\Gamma}^{\vec{a}}(\hat{C}_{\vec{n}}) = \text{g.l.}_{\Gamma}^{\vec{a}}(\hat{C}_{\vec{m}}) = \sum_i a_i m_i. \quad (5.2)$$

In particular, when all a_i are unity, the graph length is just the combinatorial length of $\hat{C}_{\vec{m}}$, i.e., the total number of edges of Γ traversed (with multiplicities) by all the component curves of $\hat{C}_{\vec{m}}$. When the spine Γ and \vec{a} are fixed or unimportant, then we shall write simply $\text{g.l.}(\hat{C}_{\vec{n}})$ or $\text{g.l.}(\hat{C}_{\vec{m}})$ for the graph length.

Any graph length function is evidently additive over disjoint unions of multicurves, and more generally, is a linear function of \vec{m} .

We next describe the bordered or punctured torus case in detail. Each multicurve on the torus is uniquely determined by three nonnegative integers (m_X, m_Y, m_Z) that satisfy one of the three triangle equalities $m_i = m_j + m_k$, where $\{i, j, k\} = \{X, Y, Z\}$. Projectivization allows us to re-scale so that m_j and m_k are relatively prime using this degree of freedom, so that the corresponding multicurve has just one component.

As in Figure 8, the space $\mathcal{PF}_0(F_1^1)$ of projectivized measured foliations with compact support is a piecewise-linear circle for $r+s=1$, and an alternative family of charts on this circle is given in Figure 13. The relation \sim in Figure 13 denotes the equivalence between different boundary cases between two different charts, and arrows represent one-simplices in $\mathcal{PF}(F_1^1)$.

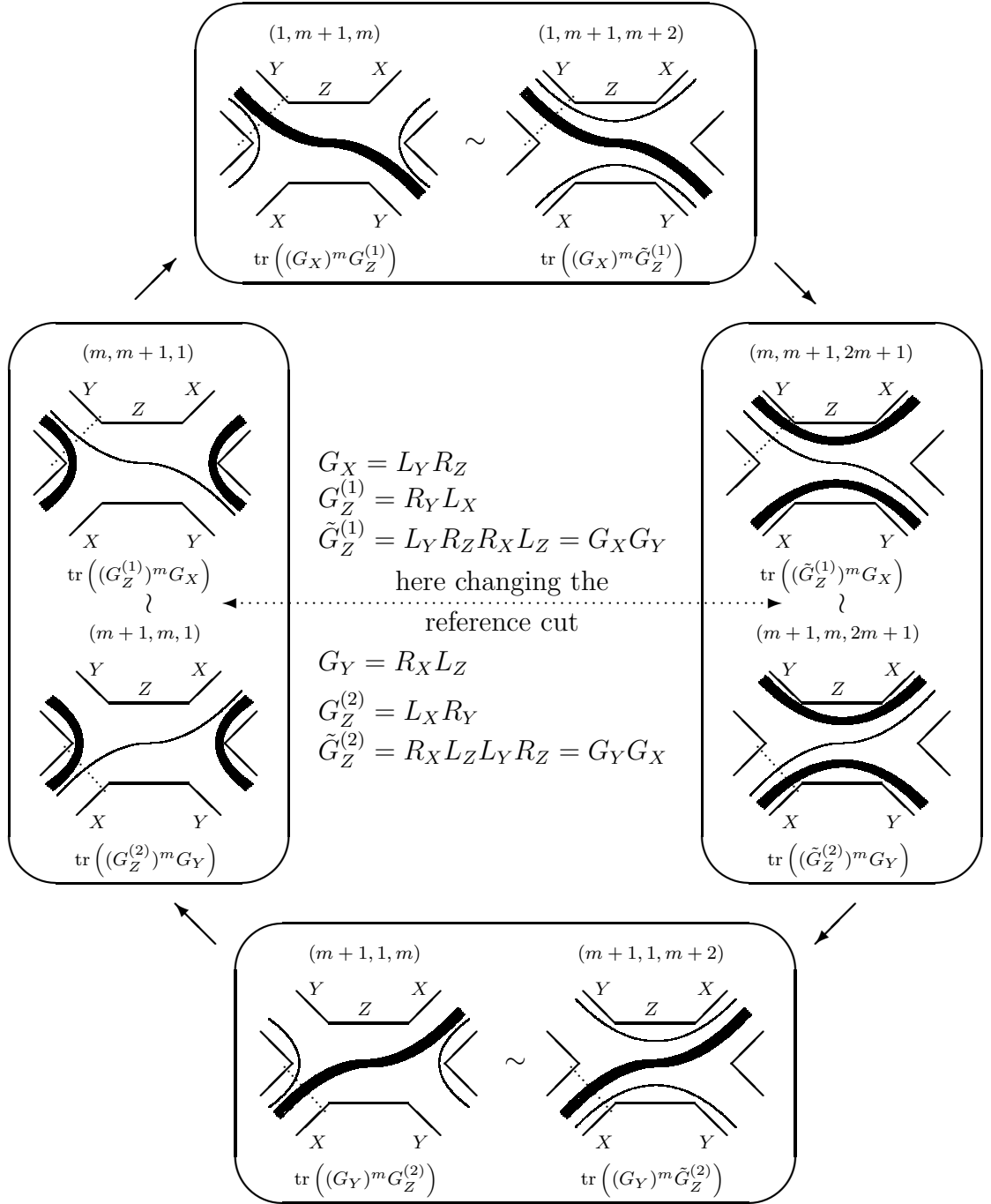


Figure 13—the circle $\mathcal{P}\mathcal{L}_0(F_1^1)$

In Figure 13, we use the previous notation G_X , etc. (see (2.15)) but in a slightly different sense. Now, these quantities are (2×2) -matrices, not just geodesic functions, i.e., we do not evaluate traces in the corresponding formulas. There is thus an ambiguity in choosing the place in the graph where the matrix products begin. We indicate this place by drawing the reference cut (the dotted line). Changing the reference cut when moving along the circle corresponds to passing from one chart to another in the chart covering of the circle. Of course, choosing the reference cut does not affect the quantum

trace operation.

In order to have a good transition in the boundary cases, for instance, in the upper case in Figure 13 (and the other cases are similar and omitted), we must ensure that the corresponding functions for the quantities $G_X^m G_Z^{(1)}$ and $G_X^m \tilde{G}_Z^{(1)}$ must coincide in the limit $m \rightarrow \infty$ with each other and with the corresponding quantity calculated merely for the “short” geodesic function G_X . To prove this, given two (2×2) -matrices G_X and G_Z corresponding to geodesic curves, we can conjugate them by respective unitary transformations U_X and U_Z to diagonal form with real eigenvalues $e^{\pm l_X/2}$ and $e^{\pm l_Z/2}$ since G_X, G_Z are hyperbolic. We then have

$$\text{tr } G_X^m G_Z = \text{tr} \begin{pmatrix} e^{ml_X/2} & 0 \\ 0 & e^{-ml_X/2} \end{pmatrix} V \begin{pmatrix} e^{l_Z/2} & 0 \\ 0 & e^{-l_Z/2} \end{pmatrix} V^{-1}, \quad V = U_X^{-1} U_Z \quad (5.3)$$

and the proper length (5.1) is $ml_X/2 + O(1)$.² In order to have a well-defined projective limit, we shall “kill” the factor m in a consistent way, and this can be achieved by dividing the result by any graph length function of the curve since $\text{g.l.}(G_X^m G_Z) = m \cdot \text{g.l.}(G_X) + \text{g.l.}(G_Z)$.

In the quantum case, however, the situation is much more involved. Indeed, let us consider an example of the product, which is of form $U^m V$, as in (5.3), where $U = e^{X/2}$, $V = e^{Y/2}$, and $[X, Y] = 4\pi i \hbar$. Thus, $(U^m)V = e^{mX/2 + Y/2 + m\pi i \hbar/2}$ while $V(U^m) = e^{mX/2 + Y/2 - m\pi i \hbar/2}$, and the corresponding logarithms do not coincide as $m \rightarrow \infty$. Moreover, even the Hermiticity condition does not often suffice to determine the proper length. For instance, given operators $U = e^{\alpha X^2}$ and $V = e^{i\beta \partial_x}$, we may calculate that $V(U^m)V = e^{m\alpha X^2 + 2i\beta \partial_x + m\alpha \beta/3}$, i.e., the proper length in this case is $\alpha X^2 + \alpha \beta/3$ and depends on the parameter β (of course, this correction is purely quantum). This illustrates that proving continuity for the boundary transitions in the quantum case requires more subtle estimates, which we perform in the next section after deriving recurrence relations for the operators of quantum approximating multicurves.

We may now formulate our main result on quantizing Thurston theory:

Theorem 5.1 *Fix a spine Γ of F_1^1 with corresponding freeway τ . Fix any projectivized vector $P\vec{\zeta}$ of foliation-shear coordinates on τ and any graph length function g.l. . For any approximating sequence \vec{n}^β to $P\vec{\zeta}$, the limit*

$$\lim_{\beta \rightarrow \infty} \frac{\text{p.l.}(\hat{C}_{\vec{n}^\beta})}{\text{g.l.}(\hat{C}_{\vec{n}^\beta})} \quad (5.4)$$

exists both in the classical case as a real number and in the quantum case as a weak operatorial limit.

²Unless the matrix $U_X^{-1} G_Z U_X$ has the form $\begin{pmatrix} 0 & -r^{-1} \\ r & \phi \end{pmatrix}$. For this matrix to determine a hyperbolic element, the quantity ϕ must be real greater than two. Multiplying this matrix by the diagonal matrix above, we obtain $\begin{pmatrix} 0 & -r^{-1} e^{ml_X/2} \\ r e^{-ml_X/2} & \phi e^{-ml_X/2} \end{pmatrix}$, so for sufficiently large m , the resulting product ceases to be hyperbolic, which is absurd.

Because both the numerator and denominator in the limit are additive, this limit is projectively invariant and defines a continuous function (in the classical case) or a weakly continuous family of operators (in the quantum case) on the circle $\mathcal{P}\mathcal{L}_0(F_{1,r}^s)$, for $r+s=1$.

The proof of the previous theorem occupies the remainder of this section. The continued fraction structure intrinsic to the torus case is used extensively, and various analogous operatorial recursions are derived and studied. There is a second essentially combinatorial proof of this result, however, only in the classical case since we have no means to control the quantum ordering of the procedure. Nevertheless, the structures discovered are interesting, and we present this second proof in Appendix A, which depends upon the recursion (5.8) derived later in Lemma 5.2. Indeed, this basic recursion arises from “Rauzy–Veech–Zorich induction” [35] in the special case of the torus, which is derived from first principles in the next section.

5.3 Elements of the proof

5.3.1 Continued fraction expansion

In each one-simplex in $\mathcal{P}\mathcal{L}_0(F)$, illustrated as arrows in Figure 13, the approximating multicurve is determined by two nonnegative integers, m_1 and m_2 , where we assume that $m_1 > m_2$ with m_1 and m_2 relatively prime. It is convenient to represent the ratio m_2/m_1 as a simple continued fraction:

$$m_2/m_1 = \frac{1}{a_1 + \frac{1}{a_2 + \frac{1}{\ddots + \frac{1}{a_{n-1} + \frac{1}{a_n}}}}}. \tag{5.5}$$

We concentrate on the case $m_X = m_2$, $m_Y = m_1$, $m_Z = m_X + m_Y$, with the other cases following by symmetry, and describe the recurrence procedure for constructing the corresponding approximating multicurves (i.e., approximating geodesics, since any multicurve in the torus is just a multiple of a single geodesic).

Referring to Figure 13, it is convenient to visualize this case by drawing a line

$$\begin{array}{cccccccccccccccc}
 \textcircled{2} & \textcircled{1} \\
 \bullet & \bullet & \dots & \bullet & \bullet & \circ & \dots & \circ & \dots & \circ & \dots & \circ & \dots & \circ & \dots & \circ & \dots & \circ & \dots & \circ & \dots & \circ \\
 1 & 2 & & m_1 - 1 & m_1 & m_1 + 1 & & m_1 + m_2 - 1 & m_1 + m_2 & & & & & & & & & & & & & &
 \end{array} \tag{5.6}$$

which represents (the right side of) the cut over the edge Z (homotopic to the cut h_Z in Figure 12). The geodesic function is constructed as follows. Considering the multicurve in a neighborhood of the edge Z , we start from the lowest thread that goes from the edge Z to the edge X (labelled by the circled number one in Figure 12 and in (5.6)) and moves to the right (this corresponds to the leftmost \circ in (5.6)). We have the matrix G_Y corresponding to passing consecutively through edges Z and X and come back to the line

(5.6), which must be periodically continued, at the point that is situated to the right by m_2 points (in this case, just the leftmost \bullet in (5.6) marked there by a circled number two). Each time passing the bullet sign, we must set the matrix G_X and passing the \circ sign we must set the matrix G_Y .

We thus move along the periodically continued line of circles and bullet signs in (5.6), at each step jumping m_2 points to the right and setting the corresponding matrices G_X or G_Y . We describe a recurrence procedure that produces from the continued fraction expansion (5.5) the correct sequence of operators, i.e., the correct ordered sequence of branches traversed by the corresponding curve. We shall split the construction procedure into stages. Let us consider the trajectory of the starting thread (the point $m_1 + 1$ in (5.6)). Each stage terminates as soon as we come closer to the starting thread 1 than the distance to it at the beginning of the stage (approaching it from the opposite side compared to the beginning of the stage, see (5.7) below). We shall let L_i denote the string of matrices for the first i stages, where by convention we arrange matrices from right to left. We terminate the first stage at the thread that is closer than m_2 to the left of the starting point, i.e., $L_1 = (G_X)^{a_1} G_Y$.

Define $\tilde{L}_0 \equiv G_X$ and introduce \tilde{L}_i , for $i \geq 1$, which is the matrix L_i (composed from the elementary matrices G_X and G_Y) in which the first two symbols of elementary matrices must be interchanged: if the first symbol of L_i is G_Y and the second is G_X , then the first symbol of \tilde{L}_i is G_X and the second is G_Y ; all other elementary matrices retain their forms. We illustrate this procedure in Figure 14.³

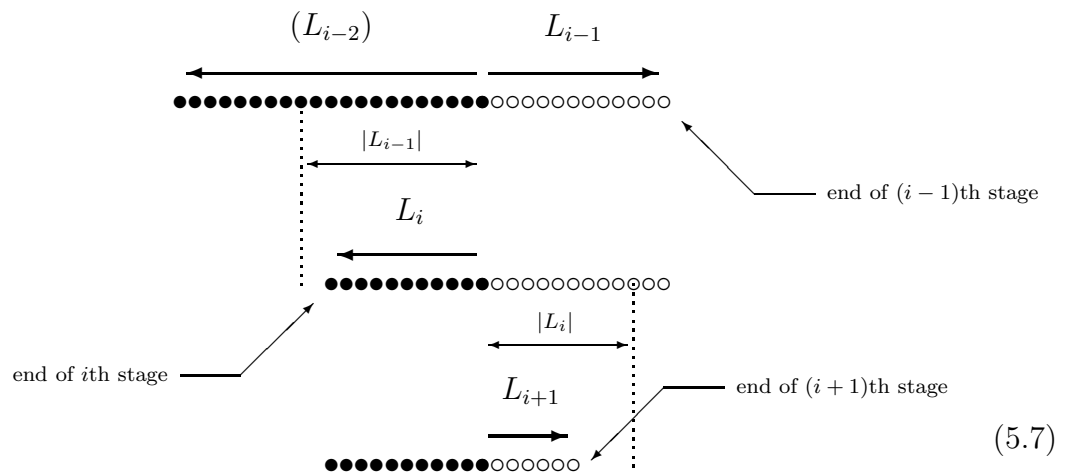


Figure 14—threads a curve

³Note that we terminate a stage whenever we come closer to the starting thread; this occurs at each stage on the opposite side from the previous stage, just as for continued fractions. The appearance of tilded quantities is explained as follow: each time during the recursion when we start a string “parallel” to some L_k from the right to the starting thread (in the circled domain), we must follow the same string of branches because, by definition, there are no threads in the string L_k except the very first thread that appears at a distance closer than $|L_k|$ to the starting thread. On the other hand, if we start from the left of the starting thread, then we must interchange exactly the first two appearances of matrices in the resulting string.

One thus sees directly that

$$\begin{aligned}
L_2 &= (L_1)^{a_2-1} \tilde{L}_0 L_1 \\
L_3 &= (\tilde{L}_2)^{a_3-1} L_1 L_2 \\
L_4 &= (L_3)^{a_4-1} \tilde{L}_2 L_3 \\
L_5 &= (\tilde{L}_4)^{a_5-1} L_3 L_4 \\
&\vdots
\end{aligned}$$

and this leads to the following recurrence relation.

Lemma 5.2 *Given the simple continued fraction expansion (5.5) of m_2/m_1 , the sequence of matrices L_n associated to the corresponding geodesic is given by the following recursion*

$$\begin{aligned}
L_{2i} &= (L_{2i-1})^{a_{2i}-1} \tilde{L}_{2i-2} L_{2i-1} \\
L_{2i+1} &= (\tilde{L}_{2i})^{a_{2i+1}-1} L_{2i-1} L_{2i}
\end{aligned}
\quad \text{for } i \geq 1, \quad \tilde{L}_0 = G_X, \quad L_1 = (G_X)^{a_1} G_Y. \quad (5.8)$$

Turning to the quantum case, we first show that the proper length operator (5.1) $\text{p.l.}(\times L_{2i} \times) / \text{g.l.}(L_{2i})$ must agree with $\text{p.l.}(\times L_{2i-1} \times) / \text{g.l.}(L_{2i-1})$ for $a_{2i} \rightarrow \infty$, that is, the operators corresponding to continued fractions of form (5.5) with large coefficient a_n must converge to the operator corresponding to the continued fraction terminated at the $(n-1)$ st step. To this end, we must analyze the structure of matrix products and corresponding operators. Indeed, the operators L_i and \tilde{L}_i enjoy elegant commutation relations as we shall next see.

Notice that for every stage i we have a geodesic corresponding to the matrix L_i (because we can close the corresponding geodesic line without self-intersections), and we can therefore define the corresponding QMC

$$\mathcal{L}_i \equiv \times \text{tr } L_i \times.$$

The first observation pertains to L_i and \tilde{L}_i : One of the corresponding curves can be obtained from the other by a parallel shift along the cut h_Z illustrated in Figure 12. Thus, the curves are disjoint and hence are homotopic on the torus, and so $\text{tr } L_i = \text{tr } \tilde{L}_i$, i.e.,

$$\mathcal{L}_i = \tilde{\mathcal{L}}_i, \quad \text{for } i \geq 1. \quad (5.9)$$

Furthermore, the curves L_i and L_{i+1} can be perturbed to have exactly one intersection as one sees by considering how the corresponding geodesic curves pass through the cut h_Z .⁴ In the case where $i = 2k$, we obtain (in the notation of (3.24))

$$[\mathcal{L}_{2k}, \mathcal{L}_{2k+1}]_q = \xi \times \text{tr } L_{2k} L_{2k+1} \times, \quad \text{and} \quad [\mathcal{L}_{2k+1}, \mathcal{L}_{2k}]_q = \xi \times \text{tr } L_{2k-1} (\tilde{L}_{2k})^{a_{2k+1}-1} \times, \quad (5.10)$$

⁴One of these curves necessarily has odd subscript $2k+1$, and we can make a small shift of all threads of this curve to the right from the threads of the second curve L_{2k} (or L_{2k+2} , depending on the situation). We find that there are no intersections of threads outside the region between terminating points of L_{2k+1} and L_{2k} (or L_{2k+2}), and in this domain, when closing the curves, there is produced exactly one intersection point.

where the proper quantum ordering is assumed for the terms in the right-hand sides.

Formulas (5.10) are crucial when proving the continuity. Letting

$$I_m \equiv \underset{\times}{\text{tr}} (L_{2i-1})^{m-1} \tilde{L}_{2i-2} L_{2i-1} \underset{\times}{},$$

$$\mathcal{L}_{2i-1} \equiv e^{\ell_X/2} + e^{-\ell_X/2},$$

we find

$$I_{m-1} \mathcal{L}_{2i-1} = q^{1/2} I_m + q^{-1/2} I_{m-2}, \quad (5.11)$$

$$\mathcal{L}_{2i-1} I_{m-1} = q^{-1/2} I_m + q^{1/2} I_{m-2}, \quad (5.12)$$

where the basis of the recursion is given by $I_0 \equiv e^{\ell_Y/2} + e^{-\ell_Y/2}$ and $I_{-1} \equiv e^{\ell_Z/2} + e^{-\ell_Z/2}$. From (5.11), we have the exact equalities

$$I_m = q^{-m/2} I_0 (e^{m\ell_X/2} + e^{-m\ell_X/2}) - q^{-m/2-1/2} I_{-1} (e^{(m-1)\ell_X/2} + e^{-(m-1)\ell_X/2}), \quad (5.13)$$

or, equivalently,

$$I_m = q^{m/2} (e^{m\ell_X/2} + e^{-m\ell_X/2}) I_0 - q^{m/2+1/2} (e^{(m-1)\ell_X/2} + e^{-(m-1)\ell_X/2}) I_{-1}. \quad (5.14)$$

We wish to present the expression (5.13) or (5.14) in the form $e^{mH_1+H_0}$, where H_1, H_0 are Hermitian operators independent of m , so the proper length is then just H_1 (while H_0 introduces quantum corrections that do not affect the proper length limit but are important for ensuring the proper commutation relations).

Let us choose a compact domain \mathcal{F} in the function space $L^2(\mathbb{R})$ such that norms of all the operators in play are bounded for functions from this domain. Notice that neither term on the right-hand side in (5.13) is self-adjoint, but if one of these terms prevails (and it can be only the first term since we have an expression with coefficients that are all positive in the classical limit of the right-hand side, and hence we must have a positive left-hand side as well), then we can replace the total sum by this prevailing term and obtain an approximate equality

$$q^{-m/2} I_0 (e^{m\ell_X/2} + e^{-m\ell_X/2}) \sim q^{m/2} (e^{m\ell_X/2} + e^{-m\ell_X/2}) I_0$$

in this limit. By considering the spectral expansion with respect to the eigenfunctions of the operator ℓ_X , we immediately conclude that $I_0 \sim e^{-2\pi i \hbar \partial / \partial |\ell_X|}$ in this limit, and then

$$H_1 = |\ell_X|/2, \quad (5.15)$$

where the modulus has to be understood in terms of the spectral expansion: having a QMC operator \mathcal{L}_X which admits a spectral decomposition (see formulas (5.24)–(5.26) below) in functions $|\alpha_S\rangle$, we define the operator $|\ell_X|$ by its action on these functions: $|\ell_X| |\alpha_S\rangle = |S| |\alpha_S\rangle$.

A potentially problematic situation is when neither of the terms prevails and their difference remains finite as $m \rightarrow \infty$. This would correspond, as in the classical case discussed before, to a situation where the corresponding element fails to be hyperbolic. As we next show, we must obtain “long” curves when m goes to infinity, so this is also

impossible in the quantum case; that is, for G_X , G_Y , G_Z , and \tilde{G}_Z from (2.15), (3.22) and representing $G_X = e^{\ell_X/2} + e^{-\ell_X/2}$, we must prove the operatorial inequality

$$G_Y e^{|\ell_X|/2} > q^{1/2} \tilde{G}_Z. \quad (5.16)$$

To prove this, first express $e^{\ell_X/2}$ through G_X . Taking the positive branch of the square root, we find from the left-hand side of (5.16) the expression

$$G_Y \left(\frac{G_X}{2} + \sqrt{\frac{G_X^2}{4} - 1} \right),$$

and since $G_Y G_X = q^{1/2} \tilde{G}_Z + q^{-1/2} G_Z$, we must compare two expressions $G_Y \sqrt{\frac{G_X^2}{4} - 1}$ and $(q^{1/2} \tilde{G}_Z - q^{-1/2} G_Z)/2$. Multiplying by the Hermitian conjugate on the right in both expressions, we eliminate the square root and arrive at Laurent polynomial expressions. After some simple algebra, we come to the inequality to be proved:

$$\frac{1}{2}(q \tilde{G}_Z G_Z + q^{-1} G_Z \tilde{G}_Z) > G_Y^2.$$

To see this, we expand the left-hand side

$$\begin{aligned} & (e^{-X-Z} + e^{X-Z} + e^{X+Z} + (q + q^{-1}) e^X) \\ & + \frac{q + q^{-1}}{2} (e^{-X-Y-Z} + e^{X+Y+Z} + e^Z + 2e^{-Z} + (q + q^{-1})) \\ & + \frac{q^2 + q^{-2}}{2} (e^{Y+Z} + e^{-Y-Z} + e^{-Y+Z} + (q + q^{-1}) e^{-Y}) + \frac{q^3 + q^{-3}}{2} e^Z, \end{aligned}$$

while the right-hand side is expressed as

$$G_Y^2 = e^{-X-Z} + e^{X-Z} + e^{X+Z} + 2 + (q + q^{-1})(e^X + e^{-Z}).$$

Subtracting this expression from the previous one, we obtain that this difference is

$$\frac{q^2 + q^{-2}}{2} G_X^2 + \frac{q + q^{-1}}{2} [e^{X+Y+Z} + e^{-X-Y-Z} - q - q^{-1}], \quad (5.17)$$

and both these terms are positive definite for $|q| = 1$.

The operatorial inequality (5.16) has therefore been established. This proves that the limit (5.4) exists and is well defined at rational points of the continued fraction expansion, and we next turn to the case of infinite continued fraction expansions, i.e., infinite sequences of elementary operators.

5.3.2 Mapping class group transformations and the unzipping procedure

We consider now an infinite continued fraction expansion $a_1, a_2, \dots, a_n, a_{n+1}, \dots$ extending the notation of (5.5). As we shall see, there is a corresponding sequence of unzippings of the freeway τ associated to a spine Γ of F as in Section 4.5 as well as an associated

sequence of mapping class group elements, expressed as Dehn twists, which reduce an approximating multicurve to one of two possible graph simple curves.

Given the recursive representation (5.8) for the operator of a geodesic curve determined by a continued fraction expansion (5.5) and applying two (unitary) operators D_X and D_Y of the modular transformations of the form (3.12) that correspond to the respective Dehn twists along the corresponding closed curves γ_X and γ_Y (with the respective geodesic functions G_X and G_Y), we shall construct the sequence of zipping or unzipping transformations.

Definition 5.4 An approximating multicurve is determined by two nonnegative integers m_1 and m_2 . As in Figure 13, enumerate such a pair as a triple $(m_1, m_2, m_1 + m_2)$. If $m_1 > m_2$, the action of the Dehn twist D_Y^{-1} along γ_Y (an *unzipping* transformation—the Dehn twist in the opposite direction) is

$$D_Y^{-1} : (m_1, m_2, m_1 + m_2) \mapsto (m_1 - m_2, m_2, m_1)$$

while if $m_1 < m_2$, we apply the unzipping transformation along the curve γ_X , which gives

$$D_X^{-1} : (m_1, m_2, m_1 + m_2) \mapsto (m_1, m_2 - m_1, m_2).^5$$

Given a continued fraction expansion (5.5), we construct the sequence of unzipping transformations

$$D_{(X \text{ or } Y)}^{-a_n} D_{(Y \text{ or } X)}^{-a_{n-1}} \cdots D_Y^{-a_3} D_X^{-a_2} D_Y^{-a_1}, \quad (5.18)$$

which, when applied to the approximating multicurve $(m_1, m_2, m_1 + m_2)$, reduces it either to $(1, 0, 1) \equiv \gamma_Y$ for n even or to $(0, 1, 1) \equiv \gamma_X$ for n odd.

Definition 5.5 Equivalently, we can consider the *zipping* procedure, that is, given a sequence of Dehn twists $D_Y^{a_1} D_X^{a_2} D_Y^{a_3} \cdots D_Y^{a_{n-1}} D_X^{a_n}$ applied to the curve γ_Y , we obtain the curve $(m_1, m_2, m_1 + m_2)$.

Considering the sequence (5.18) of quantum Dehn twist operators (3.12) and exploiting the quantum invariance from Lemma 3.9, we come to the main observation that having an involved expression for the proper limit (5.1) of a QMC operator constructed by the rules described in Lemmas 3.9 and 5.2 in terms of the elementary operators X, Y, Z , we may perform the sequence (5.18) of unzipping quantum modular transformations, which reduces this operator to a standard form of the quantum operator G_Y or G_X expressed through the new operators $X^{(n)}, Y^{(n)}, Z^{(n)}$ related to the initial operators by this sequence of quantum modular transformations. This is the operatorial statement of naturality of lengths under the mapping class group action.

It is intuitively natural to imagine that as the geodesic lengths must diverge as m_1, m_2 tend to infinity, we must eventually come to an asymptotic regime where all quantities $X^{(n)}, Y^{(n)}$ are large in the literal or operatorial sense for all sufficiently large n . The inexorability of the approach to this asymptotic regime is not obvious and is described in the next section.

⁵In terms of the symbolic dynamics of elementary operators G_X and G_Y , we can present this action as follows: $D_X^{-1}(G_X) = G_X$, $D_X^{-1}(G_X G_Y) = G_Y$ and $D_Y^{-1}(G_X G_Y) = G_X$, $D_Y^{-1}(G_Y) = G_Y$.

5.3.3 Asymptotic regime

Let us recall the modular transformations for X , Y , and Z variables:

$$D_X^{-1}(X, Y, Z) \mapsto (X + 2\phi^{\hbar}(Z), -Z, Y - 2\phi^{\hbar}(-Z)) \quad (5.19)$$

and

$$D_Y^{-1}(X, Y, Z) \mapsto (-Z, Y - 2\phi^{\hbar}(-Z), X + 2\phi^{\hbar}(Z)). \quad (5.20)$$

In terms of the quantities $U \equiv e^{X/2}$ and $V \equiv e^{-Y/2}$ in the case where $X + Y + Z = 0$, we have

$$D_X^{-1} \begin{pmatrix} U \\ V \end{pmatrix} D_X = \begin{pmatrix} e^{X/2} + e^{-X/2-Y} \\ e^{-Y/2+X/2} \end{pmatrix} \equiv \begin{pmatrix} U + VU^{-1}V \\ q^{1/2}U^{-1}V \end{pmatrix}, \quad (5.21)$$

$$D_Y^{-1} \begin{pmatrix} U \\ V \end{pmatrix} D_Y = \begin{pmatrix} e^{X/2+Y/2} \\ e^{-Y/2} + e^{Y/2+X} \end{pmatrix} \equiv \begin{pmatrix} q^{1/2}UV^{-1} \\ V + UV^{-1}U \end{pmatrix}. \quad (5.22)$$

Worth mentioning is that since each operator Z_α is Hermitian, each exponential is positive definite, so we can always write, for instance, that $U + VU^{-1}V > U$ in the sense of spectral expansion: $\langle f|U + VU^{-1}V|f \rangle > \langle f|U|f \rangle$ for any function $f \in L^2(\mathbb{R})$.

Using now an alternating sequence of transformations (5.21), (5.22), we shall subsequently show that we attain the asymptotic regime of large positive X (large U) and large in absolute value negative Y (large V) starting from every pair of X and Y lying in a compact domain of the (X, Y) -plane in the classical case or acting within a compactum of test functions with bounded derivatives in the function space in the quantum operatorial case.

In this section, we verify that the asymptotic regime is attained for the distinguished sequence of modular transformations corresponding to the Fibonacci number sequence (golden mean), namely, for alternating D_X^{-1} and D_Y^{-1} . The proof in the general case is analogous although the structure is more involved, as described in the next section.

Given the sequence of transformations $D_X^{-1}D_Y^{-1} \cdots D_X^{-1}D_Y^{-1} = (D_X^{-1}D_Y^{-1})^n$, we obtain

$$\begin{aligned} D_X^{-1}D_Y^{-1} \begin{pmatrix} U \\ V \end{pmatrix} &= \\ &= \begin{pmatrix} UV^{-1}U + V \\ V^{1/2}(V^{-1}Uq^{-1/2} + U^{-1}Vq^{1/2})U(V^{-1}Uq^{-1/2} + U^{-1}Vq^{1/2})V^{1/2} + V^{1/2}U^{-1}V^{1/2} \end{pmatrix}. \end{aligned} \quad (5.23)$$

In the classical case, the asymptotics is already clear from this formula; for the first entry in (5.23), we have $UV^{-1}U + V = U(V^{-1}U + U^{-1}V) > 2U$ as the expression in the parentheses has the form $e^S + e^{-S} \geq 2$ for any real S . The same logic applies to the second entry in (5.23), and we deduce that the classical part $V(U + U^{-1})$ has the same property.

The proof given below in the quantum case is more subtle as it needs a thorough operatorial analysis. Nevertheless, the estimates turn out to be close to those in the classical case, which we briefly discuss here: we must prove that a lower bound on the

operatorial spectrum on a compactum in the function space diverges with n . This is a routine procedure, which uses that the action of operators X and Y in the basis of, say, normalized Hermitian functions h_n has the form

$$\begin{aligned} X|h_n\rangle &= \sqrt{4\pi\hbar}(\sqrt{n+1}|h_{n+1}\rangle + \sqrt{n}|h_{n-1}\rangle) \\ Y|h_n\rangle &= \sqrt{4\pi\hbar}\frac{i}{2}(\sqrt{n+1}|h_{n+1}\rangle - \sqrt{n}|h_{n-1}\rangle). \end{aligned}$$

These operators “almost” commute in the domain of large n , which allows the combinatorics to be analyzed semiclassically.

In the quantum case, we recall the construction of quantum Dehn twists and their eigenfunctions from [28]. The generator of the Dehn twist D_X has the form

$$D_X = e^{q_1^2/2\pi i\hbar} F^\hbar(q_1 + p_1), \quad q_1 = X/2, \quad p_1 = 2\pi i\hbar\partial_X \quad (5.24)$$

and because it commutes with the geodesic length operator G_X , they share the common set of eigenfunctions

$$|\alpha_S\rangle = e^{-X^2/16\pi i\hbar} F^\hbar(S+X) F^\hbar(-S+X) \quad (5.25)$$

with the eigenvalues

$$G_X|\alpha_S\rangle = 2 \cosh(S/2)|\alpha_S\rangle; \quad D_X|\alpha_S\rangle = e^{S^2/2\pi i\hbar}|\alpha_S\rangle. \quad (5.26)$$

The functions $|\alpha_S\rangle$ constitute a complete set of functions in the sense that

$$\langle\alpha_T|\alpha_S\rangle = \delta(S-T)\nu^{-1}(S), \quad \nu(S) = 4 \sinh(\pi S) \sinh(\pi\hbar S)$$

and

$$\int_0^\infty \nu(S) dS |\alpha_S\rangle\langle\alpha_S| = \text{Id}$$

We now split the plane of the variables $(X, Y) = (X^{(0)}, Y^{(0)})$ into four sub-domains and consider the action of the Dehn twists D_X^{-1} and D_Y^{-1} in each sub-domain.

Domain I. $\{X^{(0)} > 0, Y^{(0)} > 0\} \cup \{X^{(0)} > 0, Y^{(0)} < 0 \text{ and } |X^{(0)}| > |Y^{(0)}|\}$.

$$\begin{aligned} D_X^{-1}(X^{(0)}, Y^{(0)}) &= (X^{(1)}, Y^{(1)}) = (X^{(0)}, X^{(0)} + Y^{(0)}) \in \text{Domain I}; \\ D_Y^{-1}(X^{(0)}, Y^{(0)}) &= (X^{(1)}, Y^{(1)}) = (X^{(0)} + Y^{(0)}, -2X^{(0)} - Y^{(0)}) \in \text{Domain II}; \end{aligned}$$

Domain II. $\{X^{(0)} > 0, Y^{(0)} < 0 \text{ and } |X^{(0)}| < |Y^{(0)}|\} \cup \{X^{(0)} < 0, Y^{(0)} < 0\}$.

$$\begin{aligned} D_X^{-1}(X^{(0)}, Y^{(0)}) &= (X^{(1)}, Y^{(1)}) = (-X^{(0)} - 2Y^{(0)}, X^{(0)} + Y^{(0)}) \in \text{Domain I}; \\ D_Y^{-1}(X^{(0)}, Y^{(0)}) &= (X^{(1)}, Y^{(1)}) = (X^{(0)} + Y^{(0)}, Y^{(0)}) \in \text{Domain II}; \end{aligned}$$

Domain IIIa. $\{X^{(0)} < 0, Y^{(0)} > 0 \text{ and } |X^{(0)}| < |Y^{(0)}|\}$.

$$\begin{aligned} D_X^{-1}(X^{(0)}, Y^{(0)}) &= (X^{(1)}, Y^{(1)}) = (X^{(0)}, X^{(0)} + Y^{(0)}) \in \text{Domain IIIa or IIIb}; \\ D_Y^{-1}(X^{(0)}, Y^{(0)}) &= (X^{(1)}, Y^{(1)}) = (X^{(0)} + Y^{(0)}, -2X^{(0)} - Y^{(0)}) \in \text{Domain I or II}; \end{aligned}$$

Domain IIIb. $\{X^{(0)} < 0, Y^{(0)} > 0 \text{ and } |X^{(0)}| > |Y^{(0)}|\}$.

$$D_X^{-1}(X^{(0)}, Y^{(0)}) = (X^{(1)}, Y^{(1)}) = (-X^{(0)} - 2Y^{(0)}, X^{(0)} + Y^{(0)}) \in \text{Domain I or II};$$

$$D_Y^{-1}(X^{(0)}, Y^{(0)}) = (X^{(1)}, Y^{(1)}) = (X^{(0)} + Y^{(0)}, Y^{(0)}) \in \text{Domain IIIa or IIIb}.$$

We see that only Domain III is potentially problematic. This regime is however unstable: absolute values of X and Y variables decrease in this regime and they eventually leave the asymptotic regime as soon as we *remain* in Domain III; immediately upon leaving this domain, we come to domains I and II and will never leave this three quarters of the (X, Y) -plane. The above considerations of U, V just demonstrate that even if we were initially in Domain III, we come to the nonasymptotic domain of bounded X and Y and then will leave this compactum moving toward asymptotic expansions in domains I and II.

The asymptotic dynamics always takes place in the first three quarters of the (X, Y) -plane. Nevertheless, even this dynamics is rather involved. The stable regime corresponds to the case where we are in Domain II before applying one or several operators D_X^{-1} . The application of the first of these operators brings us to Domain I, and upon subsequent applications of the operators D_X^{-1} we remain in Domain I. Next, if we were in Domain I, then the very first application of the operator D_Y^{-1} brings us to Domain II, and we then remain in Domain II upon subsequent applications of D_Y^{-1} .

We turn now to actual geodesic lengths of curves or proper lengths of operators. If a sequence of unzipping transformations terminates, this means that we have a graph simple geodesic, which is either G_X if the last transformation was D_Y^{-1} or G_Y if the last transformation was D_X^{-1} . Considering the corresponding geodesic or proper lengths, we find that up to exponentially small corrections, the leading contributions in the above domains are

$$\text{p.l.}(\gamma_Y) = X + Y/2 \quad \text{in domain I,} \quad (5.27)$$

$$\text{p.l.}(\gamma_X) = -Y - X/2 \quad \text{in domain II} \quad (5.28)$$

(see expressions (2.15)).

Thus, although the transformation laws for the variables X, Y themselves do not possess the property of linearity with respect to the parameters a_i, a_j , when applying sequences of transformations $(D_X^{-1})_i^{a_i} \equiv D_X^{-a_i}$ or $(D_Y^{-1})_j^{a_j} \equiv D_Y^{-a_j}$, the proper lengths do possess this property! Namely, starting with variables $(X^{(0)}, Y^{(0)})$ lying in the corresponding domains and applying the sequences of transformations $D_X^{-a_i}$ or $D_Y^{-a_j}$, we obtain for the resulting proper lengths the following expressions:

$$\text{p.l.}(\gamma_{Y^{(i)}}) = -\frac{Y^{(0)}}{2} + a_i \left(-Y^{(0)} - \frac{X^{(0)}}{2} \right) \quad \text{for } X^{(0)}, Y^{(0)} \in \text{domain II} \quad (5.29)$$

$$\text{p.l.}(\gamma_{X^{(j)}}) = \frac{X^{(0)}}{2} + a_j \left(X^{(0)} + \frac{Y^{(0)}}{2} \right) \quad \text{for } X^{(0)}, Y^{(0)} \in \text{domain I} \quad (5.30)$$

Let us now explore the asymptotic formulas (5.27), (5.28) and (5.29), (5.30) first in the classical case to close this section, relegating the discussion of the quantum case to the next section.

Assume that we start from the variables $(X^{(0)}, Y^{(0)})$ in domain I and have the corresponding initial length p.l. $(\gamma_{Y^{(0)}})$ from (5.27). Applying the transformation $D_Y^{-a_j}$, we obtain new variables $(X^{(j)}, Y^{(j)})$ and the new proper length p.l. $(\gamma_{X^{(j)}})$ (5.30) having form (5.28) in these new variables, which must now lie in domain II. Note that explicitly

$$(X^{(j)}, Y^{(j)}) = (X^{(0)} + Y^{(0)} + (a_j - 1)(-2X^{(0)} - Y^{(0)}), -2X^{(0)} - Y^{(0)}).$$

We then apply the transformation $D_X^{-a_i}$ to obtain variables $(X^{(j,i)}, Y^{(j,i)})$, and the proper length p.l. $(\gamma_{Y^{(j,i)}})$ is expressed as in (5.29), where the term multiplied by a_i is none other than p.l. $(\gamma_{X^{(j)}})$ and the term $-\frac{Y^{(j)}}{2}$ is exactly p.l. $(\gamma_{Y^{(0)}})$. We thus find in the asymptotic regime that the corresponding lengths are related by *exactly the same* recurrence relation as for a graph length (the latter of which follows immediately from (5.8)):

$$\text{p.l.}(\gamma_{Y^{(j,i)}}) = a_i \text{p.l.}(\gamma_{X^{(j)}}) + \text{p.l.}(\gamma_{Y^{(0)}}), \quad (5.31)$$

$$\text{g.l.}(\gamma_{Y^{(j,i)}}) = a_i \text{g.l.}(\gamma_{X^{(j)}}) + \text{g.l.}(\gamma_{Y^{(0)}}). \quad (5.32)$$

It is then easy to conclude that the ratio of these two quantities has a definite limit as $i \rightarrow \infty$ for any sequence of numbers a_i . It is a standard estimate: given two numerical sequences (5.31) and (5.32) and denoting the relative error of their ratio as ε_i , i.e., at the i th step, the ratio is $S(1 + \varepsilon_i)$, where S is constant, for $a_{i+1} > 1$ at the $(i + 1)$ th step, we obtain $\varepsilon_{i+1} < \varepsilon_i / (a_{i+1} - 1/2)$, or if we have two coefficients $a_{i+1} = a_i = 1$, then $\varepsilon_{i+1} < \varepsilon_{i-1} / 1.5$. In general, for ε_i small enough, we always have $\varepsilon_{i+1} < \varepsilon_i$. This shows that the relative error decreases exponentially with the index i .

5.3.4 Quantum continued fraction expansion

Let us turn again to the sequence (5.18) of unzipping transformations. In order to obtain operatorial expressions, we consider the unitary operators D_X , D_Y and explicitly indicate the variables in which these operators are expressed, i.e., we write $D_{X^{(j)}} \equiv D_X(X^{(j)}, Y^{(j)})$ for the Dehn twist along γ_X at the $(j + 1)$ th step. Thus,

$$(X^{(n)}, Y^{(n)}) = D_{X^{(n-1)}}^{-a_n} D_{Y^{(n-2)}}^{-a_{n-1}} \cdots D_{X^{(1)}}^{-a_2} D_{Y^{(0)}}^{-a_1} (X^{(0)}, Y^{(0)}) D_{Y^{(0)}}^{a_1} D_{X^{(1)}}^{a_2} \cdots D_{Y^{(n-2)}}^{a_{n-1}} D_{X^{(n-1)}}^{a_n}, \quad (5.33)$$

In order to represent such long strings of operators in terms of the original operators $(X^{(0)}, Y^{(0)})$, we invert the dependence, i.e., we remember that, for instance,

$$D_{X^{(1)}}^{-a_2} = D_{Y^{(0)}}^{-a_1} D_{X^{(0)}}^{-a_2} D_{Y^{(0)}}^{a_1},$$

etc., which gives

$$(X^{(n)}, Y^{(n)}) = D_{Y^{(0)}}^{-a_1} D_{X^{(0)}}^{-a_2} \cdots D_{Y^{(0)}}^{-a_{n-1}} D_{X^{(0)}}^{-a_n} (X^{(0)}, Y^{(0)}) D_{X^{(0)}}^{a_n} D_{Y^{(0)}}^{a_{n-1}} \cdots D_{X^{(0)}}^{a_2} D_{Y^{(0)}}^{a_1} \quad (5.34)$$

We shall compute with bases of functions that are convenient in the asymptotic regime. Let

$$|f_{\mu,s}\rangle \equiv e^{i\mu(x-s)^2/2} \quad \mu, s \in \mathbb{R}. \quad (5.35)$$

These functions constitute a basis at each μ :

$$\langle f_{\mu,t} | f_{\mu,s} \rangle = \frac{2\pi}{\mu} \delta(s - t), \quad \int_{-\infty}^{\infty} ds |f_{\mu,s}\rangle \langle f_{\mu,s}| = \frac{2\pi}{\mu} \text{Id}. \quad (5.36)$$

For two arbitrary real numbers w and γ , we have

$$e^{iw x^2/2} |f_{\mu,s}\rangle = e^{i\mu w s^2/2} \left| f_{\mu+w, \frac{s}{1+w/\mu}} \right\rangle, \quad (5.37)$$

$$e^{i\gamma \partial_x^2/2} |f_{\mu,s}\rangle = \frac{1}{\sqrt{1+\gamma\mu}} \left| f_{\frac{1}{\gamma+1/\mu}, s} \right\rangle, \quad (5.38)$$

and

$$\langle f_{\mu,s} | x | f_{\mu,t} \rangle = \frac{2\pi}{i\mu^2} \delta'(s-t) + \frac{2\pi}{\mu} s \delta(s-t), \quad (5.39)$$

$$\langle f_{\mu,s} | \frac{1}{i} \partial_x | f_{\mu,t} \rangle = \frac{2\pi}{i\mu} \delta'(s-t). \quad (5.40)$$

We now define the dimensionless variable x and set

$$X |f_{\mu,s}\rangle = \sqrt{4\pi\hbar} x \cdot |f_{\mu,s}\rangle; \quad Y |f_{\mu,s}\rangle = \sqrt{4\pi\hbar} \frac{1}{i} \frac{\partial}{\partial x} \cdot |f_{\mu,s}\rangle. \quad (5.41)$$

The explicit formulas for the operators D_X and D_Y acting on $|f_{\mu,s}\rangle$ in the asymptotic regime are

$$D_X^{a_i} |f_{\mu,s}\rangle = e^{i(a_i-1)x^2/2} e^{-i\partial_x^2} e^{ix^2/2} |f_{\mu,s}\rangle, \quad (5.42)$$

$$D_Y^{a_j} |f_{\mu,s}\rangle = e^{i(a_j-1)\partial_x^2/2} e^{-ix^2} e^{i\partial_x^2/2} |f_{\mu,s}\rangle. \quad (5.43)$$

In order to establish the required recurrence relation, we must compare matrix elements of the three consecutive length operators in the corresponding operatorial decompositions:

$$\begin{aligned} A_{st}^{(0)} &= \langle f_{\mu,s} | X + \frac{Y}{2} | f_{\mu,t} \rangle, \\ A_{st}^{(j)} &= \langle f_{\mu,s} | D_Y^{-a_j} | -Y - \frac{X}{2} | D_Y^{a_j} f_{\mu,t} \rangle, \\ A_{st}^{(j,i)} &= \langle f_{\mu,s} | D_Y^{-a_j} D_X^{-a_i} | X + \frac{Y}{2} | D_X^{a_i} D_Y^{a_j} f_{\mu,t} \rangle. \end{aligned}$$

Now, using formulas (5.37)–(5.43), it is straightforward to show that

$$A_{st}^{(j,i)} = A_{st}^{(0)} + a_i A_{st}^{(j)}, \quad (5.44)$$

for all s, t , i.e., we again attain the recurrence relation (5.31) in the asymptotic regime, but now for the matrix elements of the operators of the quantum proper lengths. Estimates show that the corrections due to both the (operatorial) deviations from the asymptotic regime and the error parameters ε_i (as for (5.31), (5.32)) decrease exponentially with the index i , so the limit (5.4) exists in a weak operatorial sense. We conclude that ratios (5.4) define a weakly continuous family of operators parameterized by projective transverse measures on the freeway associated to a spine of the once-punctured torus. This completes the proof of Theorem 5.1.

6 Conclusion

We hope to have added to the mathematical foundation and general understanding of the quantization of Teichmüller space and its geometric underpinnings in the first several sections of this paper. We also hope that the survey given here of train tracks and their extensions might be useful.

The quantization of Thurston’s boundary in general seems to be a substantial project, which we have only just begun here with the quantization of continued fractions. First of all, one would like a better understanding of the operators we have constructed, for instance, an intrinsic characterization or an explicit calculational framework for them. At the same time, our current constructions depend upon a choice of spine, and there would seem to be a more invariant version of the theory, where the choice of spine is dictated by the combinatorics of the cell decomposition of Teichmüller space; the calculations in this paper apply to each such spine (since there is a combinatorially unique cubic one) for the once-punctured torus.

Second of all, the quantization of Thurston’s boundary for higher-genus or multiply-punctured surfaces may be approachable using the improved quantum ordering. Namely, in any fixed spine of the surface, there is a fixed finite family of “edge-simple” closed edge-paths which by definition never twice traverse the same oriented edge. It is elementary to see that any closed edge-path on Γ may be written non-uniquely as a concatenation of edge-simple paths, where the particular concatenation depends upon a starting point. (Edge-simple paths were studied as “canonical curves” on train tracks in [8]; they contain the extreme points of the polyhedron of projective measures on the track.) It follows that an arbitrary leaf of a measured foliation carried by a freeway can be written as a concatenation of paths from this finite collection of edge-simple paths. The corresponding quantum operatorial statement results from the improved quantum ordering described here. Thus, whereas the quantization of the once-punctured torus devolved, in effect, to an analysis of two-letter words, the quantization of Thurston’s boundary sphere in general may depend upon an analysis of words comprised of letters which are edge-simple paths.

One appealing long-term goal would be to discover the Thurston classification already on the operatorial level, for instance, with the dilatation in the pseudo-Anosov case explicitly computable from the MCG operator or from the invariant projective foliation operator.

Another intriguing aspect involves generalizations of graph length functions insofar as the proof of Theorem 5.1 holds taking as graph length any continuous positive definite function which is homogeneous of degree one. A natural choice of such a function is induced by the geodesic length of the corresponding geodesic curve taken for a fixed basepoint in Teichmüller space on its fixed spine, for instance, vanishing shear coordinates on the usual spine in the once-punctured torus. What sort of regularity (e.g., piecewise smoothness) is achieved in the operators corresponding to points of Thurston’s boundary under such “gauge fixing”?

Also worth mentioning are very recent advances in the description of quantum $sl(n, \mathbb{R})$ connections [40], where one finds an improved quantum ordering in a more complicated higher-dimensional setting.

Appendix A Combinatorial proof of Theorem 5.1

In this appendix, we give a complementary, combinatorial proof of the classical Theorem 5.1 using the recurrence relation (5.8). At the present state of understanding, the proof applies only to the classical case as we cannot control the quantum ordering.

Let us recall the structure of the matrix product (2.5). It is a sequence of matrices L_Z, R_Z with different Z . It can be always segregated into clusters of matrices

$$L_{\bar{Z}} \equiv L_{Z_{i+s}} L_{Z_{i+s-1}} \cdots L_{Z_i}$$

and

$$R_{\bar{Z}} \equiv R_{Z_{j+k}} L_{Z_{j+k-1}} \cdots L_{Z_j}.$$

The periodic extension of expression (5.8) is always an alternating sequence of matrices $L_{\bar{Z}}$ and $R_{\bar{Z}}$:

$$P_{Z_1, \dots, Z_n} = \cdots (L_{\bar{Z}_s} R_{\bar{Z}_{s-1}}) \cdots (L_{\bar{Z}_1} R_{\bar{Z}_2}) \cdots .$$

First note that it is impossible to have arbitrarily long sequences of only left or right matrices for a given graph: the maximum length is restricted to be less or equal the maximum graph length of geodesics around holes. This means that the length of a single cluster for a given graph is always bounded once the topology is fixed.

One can directly calculate the product $(L_{\bar{Z}_1} R_{\bar{Z}_2})$ for $L_{\bar{Z}_1} = L_{Z_1} \cdots L_{Z_m}$ and $R_{\bar{Z}_2} = R_{Z_{m+1}} \cdots R_{Z_{m+k}}$:

$$\begin{aligned} (L_{\bar{Z}_1} R_{\bar{Z}_2}) &= A s_1^+ s_2^+ + B (s_1^- s_2^- + S_1 s_2^- + S_1 S_2) \\ &\quad + D (s_1^+ s_2^- + s_1^+ S_2) + P S_1 s_2^+, \end{aligned} \quad (\text{A.1})$$

where S_j, s_j^\pm , for $j = 1, 2$, are the following coefficient functions:

$$\begin{aligned} s_1^\pm &= e^{\pm \sum_{i=1}^m Z_i/2}, & s_2^\pm &= e^{\pm \sum_{j=m+1}^{m+k} Z_j/2} \\ S_1 &= \sum_{q=2}^m e^{+\sum_{r=1}^{q-1} Z_r/2 - \sum_{r=q}^m Z_r/2}, & S_2 &= \sum_{q=m+2}^{m+k} e^{-\sum_{r=m+1}^{q-1} Z_r/2 + \sum_{r=q}^{m+k} Z_r/2}, \end{aligned}$$

and A, B, D, P are the special (2×2) -matrices (“letters”):

$$\begin{aligned} A &= \begin{pmatrix} +1 & 0 \\ -1 & 0 \end{pmatrix}, & B &= \begin{pmatrix} 0 & 0 \\ 0 & +1 \end{pmatrix} \\ D &= \begin{pmatrix} 0 & -1 \\ 0 & +1 \end{pmatrix}, & P &= \begin{pmatrix} 0 & 0 \\ -1 & 0 \end{pmatrix}. \end{aligned} \quad (\text{A.2})$$

These letters possess interesting multiplication properties which are summarized in the next lemma, whose proof is a routine calculation.

Lemma A.1 The alphabet lemma. *The multiplication table of letters (A.2) reads:*

$$\begin{array}{c|cccc}
 & A & B & D & P \\
 \hline
 A & A & 0 & D & 0 \\
 B & P & B & B & P \\
 D & A & D & D & A \\
 P & P & 0 & B & 0
 \end{array} , \tag{A.3}$$

so the trace of any product of these matrices is either unity or zero. In the product of t matrices of form (A.1), the only monomials that survive are

$$[(A + D)^{i_\alpha} D] B^{j_\beta} (B + P) \cdots [(A + D)^{i_\rho} D] B^{j_\omega} (B + P) \text{ and } (A + D)^t, B^t. \tag{A.4}$$

The main point is that almost all cancellations of letters in long words are due to the local multiplication rules (A.3). This means that, having a long sequence of letters, say, L_{I+N} from Lemma 5.2, we can split it into pieces depending on sequences of letters L_I , L_{I-1} , \tilde{L}_I , and \tilde{L}_{I-1} , where the index I is also assumed to be big enough. That is, let $L_{I+N} = L_I L_{I-1} \tilde{L}_I L_I \dots L_I$ comprise p_N entries L_I and \tilde{L}_I and q_N entries L_{I-1} and \tilde{L}_{I-1} . We have then the following estimate:⁶

$$|\log \text{tr } L_{I+N} - p_N \log \text{tr } L_I - q_N \log \text{tr } L_{I-1}| < C (q_N + p_N), \tag{A.5}$$

where the constant C depends only on the Teichmüller space coordinates Z_α and on the genus and the number of holes of the Riemann surface, and we have also used (5.9). The ratio of the coefficients is given by the continued fraction

$$\begin{aligned}
 q_N/p_N = & \frac{1}{a_{I+1} + \frac{1}{a_{I+2} + \dots + \frac{1}{a_{I+N-1} + \frac{1}{a_{I+N}}}}} , \tag{A.6}
 \end{aligned}$$

and also has a definite limit as $N \rightarrow \infty$. Now the estimate follows: up to exponential corrections, $\text{p.l.}(L)$ coincides with the $\log \text{tr } L$, so for any $\varepsilon > 0$, let us choose the index I such that $\varepsilon \text{p.l.}(L_{I-1})/2 > C$ and $\varepsilon \text{p.l.}(L_I)/2 > C$. Thus,

$$\frac{\text{p.l.}(L)(L_{I+N})}{\text{g.l.}(L_{I+N})} = (1 + O(\varepsilon/2)) \frac{p_N \text{p.l.}(L)(L_I) + q_N \text{p.l.}(L)(L_{I-1})}{p_N \text{g.l.}(L_I) + q_N \text{g.l.}(L_{I-1})}, \tag{A.7}$$

and because the ratio q_N/p_N has a definite limit as $N \rightarrow \infty$, there exists N_0 such that the relative error of this ratio times the sum of ratios of proper and graph lengths of L_I and L_{I-1} will not exceed $\varepsilon/2$. Thus, the collective relative error for such fixed I and for all $N > N_0$ is less than ε , proving the theorem.

⁶This estimate also follows from the properties of long geodesic lines in hyperbolic geometry: for two lines of large lengths L_1 and L_2 intersecting at angle α , the length L_3 of the third side of the resulting triangle is $L_1 + L_2 + \log((1 - \cos \alpha)/2) + O(1/L)$. This also shows that our estimate is very rough.

Appendix B Degeneracy of the Poisson structure

We shall explicitly calculate the degeneracy of the Poisson brackets (2.9) for a special graph and choose the graph whose “building blocks” are depicted in Figure 15. Namely, we have a line tree subgraph comprising edges X_i with attached subgraphs as in Figure 15a and 15b. Attaching a subgraph of type a corresponds to adding a handle (increasing g by unity) while a subgraph of type b corresponds to adding a hole (increasing s by unity). We shall assume that $2g + 2s > 5$ to avoid the once-punctured torus, which is already handled separately in Section 3.

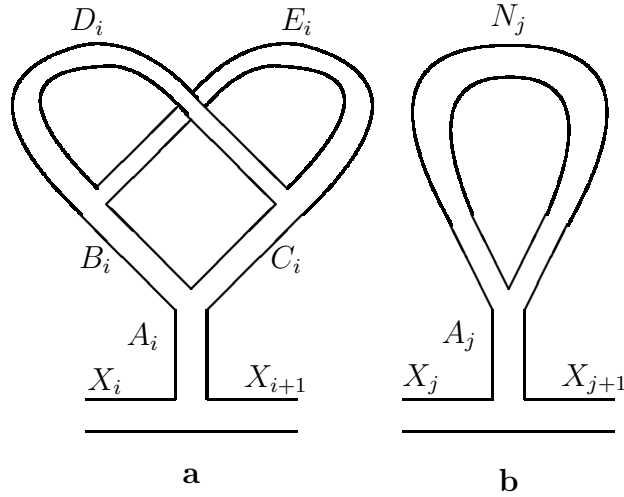


Figure 15-building blocks

For the variables A, B, C, D, E in Figure 15a, we have the Poisson bracket (sub)matrix

$$\begin{array}{c|ccccc}
 & A_i & B_i & C_i & D_i & E_i \\
 \hline
 A_i & 0 & 1 & -1 & 0 & 0 \\
 \hline
 B_i & -1 & 0 & 1 & 1 & -1 \\
 C_i & 1 & -1 & 0 & 1 & -1 \\
 D_i & 0 & -1 & -1 & 0 & 2 \\
 E_i & 0 & 1 & 1 & -2 & 0 \\
 \hline
 \end{array},$$

where the entries are the Poisson brackets between the corresponding variables. Adding the last row to the next-to-the-last row as well as adding the last column to the next-to-the-last column, then adding the third row to the second row as well as the third column to the second column, we obtain the matrix

$$\begin{pmatrix}
 0 & 0 & -1 & 0 & 0 \\
 0 & 0 & 1 & 0 & -2 \\
 1 & -1 & 0 & 0 & -1 \\
 0 & 0 & 0 & 0 & 2 \\
 0 & 2 & 1 & -2 & 0
 \end{pmatrix},$$

which obviously has rank four and can be further reduced (without adding the first column or row to any other) to the form

$$\begin{pmatrix} 0 & 0 & 0 & 0 & 0 \\ 0 & 0 & +1 & 0 & 0 \\ 0 & -1 & 0 & 0 & 0 \\ 0 & 0 & 0 & 0 & +2 \\ 0 & 0 & 0 & -2 & 0 \end{pmatrix}.$$

Thus, erasing all columns and rows corresponding to the variables B_i , C_i , D_i , and E_i leaves invariant the rank of the Poisson bracket matrix.

Adjoining the subgraph in Figure 15b creates exactly one degeneracy as the variable N_j Poisson commutes with everything (as it must be when adding a hole).

It remains only to calculate the rank of the matrix corresponding to a tree graph with edges X_i and A_i remaining after erasing all B -, C -, D -, E -, and N -variable rows and columns. The corresponding Poisson bracket matrix has dimension $2g + 2s - 5 > 0$ and the simple block-diagonal form

0	1	-1	0	0	.	.	.
-1	0	1	0	0			
1	-1	0	1	-1			
	0	-1	0	1	0	0	
	0	1	-1	0	1	-1	
			0	-1	0	1	
			0	1	-1	0	⋱
					⋱	⋱	⋱

Adding each even-index row to its predecessor as well as adding each even-index column to its predecessor, this reduces to the matrix whose only nonzero elements are +1 on the main super-diagonal and -1 on the main sub-diagonal. Since this matrix has full rank, the discussion is complete.

References

- [1] E. Verlinde and H. Verlinde, *Conformal field theory and geometric quantization*, Proc. Superstrings 1989 (Trieste, 1989), World Scientific, River Edge, NJ, 1990, 422–449.
- [2] V. V. Fock and A. A. Rosly, *Poisson structures on moduli of flat connections on Riemann surfaces and r-matrices*, Preprint ITEP 72–92 (1992)// *Amer. Math. Soc. Transl.*, Ser. 2, 1999, Vol. 191, 67–86.
- [3] V. V. Fock and A. A. Rosly, *Flat connections and Polyubles*, *Theor. Math. Phys.*, **95**, (1993), 526–535.

- [4] L. Chekhov and V. Fock, talk on May, 25 at *St. Petersburg Meeting on Selected Topics in Mathematical Physics*, LOMI, 26–29 May, 1997; *A quantum Teichmüller space*, *Theor. Math. Phys.*, **120** (1999) 1245–1259; *Quantum mapping class group, pentagon relation, and geodesics* *Proc. Steklov Math. Inst.* **226** (1999) 149–163.
- [5] R. M. Kashaev, *Quantization of Teichmüller spaces and the quantum dilogarithm*, *Lett. Math. Phys.*, **43**, No. 2, (1998), 105–115; q-alg/9705021.
- [6] J. Teschner, *From Liouville theory to the quantum geometry of Riemann surfaces*, hep-th/0308031; the contribution to: *Proc. Intl. Congress Math.*, Lisbon, 2003. World. Sci. Publ., to appear
- [7] R. C. Penner, *The decorated Teichmüller space of Riemann surfaces*, *Commun. Math. Phys.*, **113**, (1988), 299–339.
- [8] —, “The action of the mapping class group on isotopy classes of curves and arcs in surfaces”, thesis, Massachusetts Institute of Technology (1982), 180 pages.
- [9] —, “Weil-Petersson volumes”, *Journal of Differential Geometry* **35** (1992), 559-608.
- [10] —, “Universal constructions in Teichmüller theory”, *Advances in Mathematics* **98** (1993), 143-215.
- [11] —, “A construction of pseudo-Anosov homeomorphisms”, *Proceedings of the American Math Society* **104** (1988), 1-19.
- [12] M. Kontsevich, *Intersection theory on the moduli space of curves and the matrix Airy function*, *Commun. Math. Phys.*, **147**, (1992), 1–23.
- [13] L. D. Faddeev, *Discrete Heisenberg–Weyl group and modular group*, *Lett. Math. Phys.*, **34**, (1995), 249–254.
- [14] R. M. Kashaev, *Liouville central charge in quantum Teichmüller theory*, *Proc. Steklov Math. Inst.* **226** (1999) 62–70.
- [15] W. P. Thurston, *On the geometry and dynamics of diffeomorphisms of surfaces*, *Bull. Amer. Math. Soc.*, **19** (1988) 417–431.
- [16] —, *Minimal stretch maps between hyperbolic surfaces*, preprint (1984), math.GT/9801039.
- [17] F. Bonahon *Bouts des variétés hyperboliques de dimension 3*, *Annals of Math* **124** (1986), 441-479.
- [18] —, *Shearing hyperbolic surfaces, bending pleated surfaces and Thurston’s symplectic form*, *Ann. Fac. Sci. Toulouse Math* **6 5** (1996), 233-297.
- [19] F. Bonahon, Y. Sözen, *The Weil-Petersson and Thurston symplectic forms*, *Duke Math Jour* **108** (2001), 581-597.
- [20] O.Ya. Viro, *Lectures on combinatorial presentations of manifolds*. Differential Geometry and Topology (Alghero, 1992), 244–264, World Sci. Publishing, River Edge, NJ, 1993.
- [21] K. Strebel, *Quadratic Differentials* (Ergeb. Math. Grenzgeb. (3), Vol. 5), Springer, Berlin–Heidelberg–New York 1984.
- [22] V. V. Fock, *Combinatorial description of the moduli space of projective structures*, hep-th/9312193.

- [23] W. M. Goldman, *Invariant functions on Lie groups and Hamiltonian flows of surface group representations*, *Invent. Math.*, **85**, (1986), 263–302.
- [24] J. E. Nelson and T. Regge, *Homotopy groups and (2+1)-dimensional quantum gravity*, *Nucl. Phys.* **B328**, (1989), 190–199;
J. E. Nelson, T. Regge, and F. Zertuche, *Homotopy groups and (2 + 1)-dimensional quantum de Sitter gravity*, *Nucl. Phys.* **B339**, (1990) 516–532.
- [25] M. Havlíček, A. V. Klimyk, and S. Pošta, *Representations of the cyclically symmetric q -deformed algebra $so_q(3)$* , *J. Math. Phys.*, **40**, No. 4, (1999) 2135–2161; math.qa/9805048.
- [26] M. Ugaglia: *On a Poisson structure on the space of Stokes matrices*, *Int. Math. Res. Not.*, **1999**, No. 9, (1999), 473–493; math.ag/9902045.
- [27] A. Bondal, *A symplectic groupoid of triangular bilinear forms and the braid groups*, preprint IHES/M/00/02 (Jan. 2000).
- [28] R. M. Kashaev, *On the spectrum of Dehn twists in quantum Teichmüller theory*, in: *Physics and Combinatorics*, (Nagoya 2000). River Edge, NJ, World Sci. Publ., 2001, 63–81; math.QA/0008148.
- [29] V. G. Turaev, *Skein quantization of Poisson algebras of loops on surfaces*, *Ann. Scient. Éc. Norm. Sup.*, Ser. 4, **24**, (1991), 635–704.
- [30] D. Bullock and J. H. Przytycki, *Multiplicative structure of Kauffman bracket skein module quantizations*, *Proc. Am. Math. Soc.*, **128**, No. 3, (2000), 923–931; math.QA/9902117.
- [31] J. E. Nelson and T. Regge, *2+1 quantum gravity*, *Phys. Lett.* **B272**, (1991), 213–216;
J. E. Nelson and T. Regge, *Invariants of 2 + 1 gravity*, *Commun. Math. Phys.* **155**, (1993) 561–568.
- [32] R. C. Penner with J. L. Harer, *Combinatorics of Train Tracks*, *Annals of Mathematical Studies*, **125**, Princeton Univ. Press, Princeton, NJ 1992.
- [33] A. Papadopoulos and R. C. Penner, “Enumerating pseudo-Anosov conjugacy classes”, *Pacific Journal of Math* **142** (1990), 159-173.
- [34] —, “The Weil-Petersson symplectic structure at Thurston’s boundary”, *Transactions of the American Math Society* **335** (1993), 891-904.
- [35] G. Rauzy, *Echanges d’intervalles et transformations induites*, *Acta Arith.* **34** (1979), 325-328.
- [36] A. Fathi, F. Laudenbach, V. Poenaru, *Travaux de Thurston sur les Surfaces*, *Asterisque* **66-67**, Soc. Math. de France, Paris (1979).
- [37] S. Wolpert *On the symplectic geometry of deformations of a hyperbolic surface*, *Ann. Math* **117** (1983), 207-234.
- [38] D. B. A. Epstein, A. Marden, *Convex hulls in hyperbolic space, a theorem of Sullivan, and measured pleated surfaces*. Analytical and geometric aspects of hyperbolic space (Coventry/Durham, 1984), 113–253, London Math. Soc. Lecture Note Ser., 111, Cambridge Univ. Press, Cambridge, 1987.
- [39] M. Reed, B. Simon, *Methods of modern mathematical physics. I. Functional analysis*. Second edition. Academic Press, Inc. [Harcourt Brace Jovanovich, Publishers], New York, 1980.

- [40] V. V. Fock and A. B. Goncharov, *Moduli spaces of local systems and higher Teichmüller theory*, math.AG/0311149; *Cluster ensembles, quantization and dilogarithm*, math.AG/0311245.